

# Investigation of anisotropic charge transport in conjugated polymer based organic FETs by controlling the molecular orientation in large area ribbon-shaped floating films

著者	Tripathi Atul Shankar Mani
その他のタイトル	大面積リボン状浮遊膜の分子配向制御による共役高分子系有機FETにおける異方性電荷輸送の検討
学位授与年度	平成30年度
学位授与番号	17104甲生工第335号
URL	<a href="http://hdl.handle.net/10228/00007404">http://hdl.handle.net/10228/00007404</a>



**Investigation of anisotropic charge transport in conjugated polymer based organic FETs by controlling the molecular orientation in large area ribbon-shaped floating films**

*DISSERTATION*  
*FOR THE DEGREE OF*  
***DOCTOR OF PHILOSOPHY***

**ATUL SHANKAR MANI TRIPATHI**

Supervisor: SHYAM S. PANDEY

**Division of Green Electronics**  
**Graduate School of Life Sciences and Systems Engineering**  
**Kyushu Institute of Technology, Japan**

**2019**

*Dedicated*

*To*

*My Parents*

## Abstract

Conjugated polymers (CPs) have emerged as one of the potential candidates as active semiconducting elements in organic electronics owing to their low cost device fabrication in the area of organic field effect transistors, organic light emitting diodes and solar cells etc. The main feature of this class material lies in the preparation of the thin film via facile solution processing. CPs are susceptible to anisotropic charge transport owing to their inherent one-dimensional nature. In order to delineate optical anisotropy and anisotropic charge transport various techniques for molecular alignment of CPs have been attempted in the recent past. Existing problems like mechanical damage, solubility of under-layer and difficulty in multilayer film fabrication during molecular alignments needs the development of suitable methods. To circumvent these issues, floating film transfer method (FTM) having capability of anisotropic thin film fabrication have been proposed in the recent past. Although in the proposed FTM oriented films could be easily obtained, most commonly observed circular orientation hinders further upscaling of this method for the large area applications. In this thesis, a new improvisation for unidirectional film spreading during FTM have been made by implementing a newly designed PTFE slider leading to ribbon-shaped floating films and named as Ribbon-shaped FTM.

A number of most widely used CPs such as PQT-C12, F8T2, non-regiocontrolled (NR) P3HT, PBTTT-C14, PTB7 and regioregular (RR) P3ATs etc. have been successfully oriented using ribbon-shaped FTM. These oriented films have been characterized by a number of techniques like polarized electronic absorption spectroscopy, atomic force microscopy, X-ray diffraction. Parametric optimization for film casting conditions such as viscosity/temperature of the liquid substrate, temperature and concentration polymer solution were amicably carried out. Influence of these casting conditions on the nature of ribbon-shaped FTM in terms of extent of macroscopic

film formation, variation on the optical anisotropy and film thickness were investigated in detail. Amongst several CPs used for investigation, PQT-C12 exhibited not only the optical anisotropy but also the pronounced anisotropic charge transport with highest charge carrier mobility for OFETs based on oriented CPs.

PQT-C12 was utilized for in-depth investigation pertaining to the implication molecular weight and its distribution on the optoelectronic anisotropies by synthesizing polymers with different molecular weight and polydispersity index (PDI). It has been found too high or low molecular weights or not favorable for promoting molecular orientation and relatively smaller PDI promotes the facile anisotropic charge transport. One of the batch of synthesized PQT-C12 and large area thin film by ribbon-shape FTM exhibited remarkably high optical anisotropy ( $DR > 22$ ) under at optimized casting condition. Microstructural investigation of these highly oriented films as probed by in plane GIXD exhibited edge-on orientation for the films fabricated under ambient conditions. A clear dependence of extent of molecular orientation on charge carrier mobility and anisotropic charge transport was demonstrated.

Intractability of polythiophene led to development of RR-poly(3-alkylthiophene) derivatives but drastic decrease (4-5 orders) in mobility as function increasing alkyl chain length and enforced maximum research on hexyl substituted derivative (P3HT). Efforts were directed to prepare large area oriented thin films of RR-P3ATs by ribbon shaped FTM and influence of molecular orientation on alkyl chain length was investigated. A decrease in DR with increasing alkyl chain length substitution was explained by increasing extent of interdigitating alkyl chains as confirmed by XRD results. Moreover, drastic hampering of charge carrier mobility as function of alkyl chain was not observed for FTM oriented films, which was explained by edge-on orientation as evidenced by in-plane GIXD investigations.

# Table of Contents

<b>Chapter-1 Introduction .....</b>	<b>1</b>
1.1 Background.....	1
1.2 Semiconductor.....	4
1.2.1 Inorganic Semiconductor .....	4
1.2.1.1 Conductor, metals and Insulators.....	5
1.2.1.2 Charge carriers and energy bands.....	6
1.2.1.3 Charge carriers transport .....	9
1.2.2 Organic semiconductor .....	11
1.2.2.1 Conjugated polymer .....	12
1.2.2.2 Carrier charge in conjugated polymer .....	12
1.2.2.3 Charge carriers transport in conjugated polymer .....	13
1.3 Thin film fabrication and molecular orientation.....	15
1.4 Organic field effect transistors .....	16
1.4.1 Device configuration.....	17
1.4.2 Working principle .....	18
1.4.3 Electrical characterizations .....	19
1.5 Research motivation .....	21
1.6 Thesis organization .....	23
1.7 References .....	25
<b>Chapter-2 Experimental .....</b>	<b>28</b>
2.1 Materials.....	28

2.2 Deposition methods .....	29
2.2.1 Spin coating .....	29
2.2.2 Dynamic floating film transfer method .....	30
2.2.3 Thermal evaporation .....	32
2.3 Thin films characterization .....	34
2.3.1 Ultraviolet-visible spectroscopy .....	34
2.3.2 Interference microscopy .....	35
2.3.3 2D Positional mapping .....	36
2.3.4 X-ray diffraction .....	36
2.3.5 Atomic force microscopic .....	37
2.3.7 Gel permeation chromatography .....	38
2.4 Device fabrication .....	39
2.4.1 Surface treatment .....	39
2.4.2 Deposition of semiconductor layers and electrodes .....	40
2.4.3 Electrical characterization .....	41
2.5 References .....	43

## **Chapter-3 Ribbon-shaped FTM: parametric optimizations.....45**

3.1 Introduction .....	45
3.2 Experimental work .....	46
3.3 Results and discussion .....	48
3.3.1 Casting of floating film.....	48
3.3.2 Controlling the casting parameter.....	50
3.3.2.1 Casting temperature .....	50
3.3.2.2 Polymer concentration.....	51
3.3.2.3 Liquid substrate viscosity .....	54
3.4 Conclusion .....	55

3.5 References .....	56
----------------------	----

**Chapter-4 Charge transport in poly(quarterthiophene): Implication of optical anisotropy and molecular weight ..... 58**

4.1 Introduction .....	58
4.2 Experimental work .....	59
4.3 Results and discussion.....	61
4.3.1 Molecular orientation .....	61
4.3.2 Probing orientation by XRD .....	67
4.3.3 Electrical characterizations .....	68
4.4 Conclusion .....	74
4.4 References .....	76

**Chapter-5 Optoelectronic properties of conjugated polymers prepared by ribbon-shaped FTM .....79**

5.1 Introduction .....	79
5.2 Experimental work .....	81
5.3 Results and discussion .....	83
5.3.1 Non-polarized absorption spectra .....	86
5.3.2 Polarized absorption spectra .....	88
5.3.2 Anisotropic charge transport .....	92
5.4 Conclusion .....	97
5.5 References .....	99

**Chapter-6 Orientation and anomalous charge transport in regioregular poly(3-alkylthiophenes).....103**



6.1 Introduction .....	103
6.2 Experimental work .....	104
6.3 Results and discussion.....	106
6.3.1 Fabrication of oriented thin films .....	106
6.3.2 Polarized and non-polarized electronic absorption spectra.....	108
6.3.3 XRD analysis.....	110
6.3.4 Anisotropic charge transport .....	112
6.4 Conclusion .....	116
6.5 References .....	117
<b>Chapter-7 General conclusion and future work .....</b>	<b>120</b>
<b>Achievements .....</b>	<b>123</b>
Publications .....	123
Presentations .....	124
<b>Acknowledgement .....</b>	<b>127</b>

## ***Chapter 1: Introduction***

### **1.1 Background**

Currently, increasing the demand of consumer electronics in day-to-day life became the basic need for the modern human life. To fulfill the demand of modern society in better ways, further development was done by miniaturization in microelectronics in order to change the circuit for high speed electronic devices. Since 19<sup>th</sup> century great effort have been done for the development of the inorganic semiconductor in which Si was the most interesting material because of the unique feature. Although it have unique feature in terms of high efficiency but in order to purification of Si wafer at the level of such high efficiency need very sophisticated and energy consuming instrument which is very costly for the production. Apart from this high class clean room was also one of the requirement for fabrication as well as device characterization. Finally in addition to all these production facilities make more costly. To avoid these processing cost one alternative semiconductor was emerged now days, named as organic semiconductor. Organic electronics is a branch of modern electronics where this organic semiconductor material such as polymer or small molecule was used as an active layer. This technology is based on carbon, similar to molecules in living things. Normally we consider about organic material properties we may not feel this material as an electrical conductor. In 1970 three scientists named as Heeger, MacDiarmid, and Shirakawa was discovered the first conductive polymer by certain modification in polymer named polyacetylene which is conductive in nature. [1,2] After the discovery of first conductive polymer still 10 years there is no involved of electronics application. In mid of 1980 interest was increased in the field of applied physics and engineering and first organic solid state field effect transistor was fabricated by Van Slyke [3] where polythiophene was the active layer. At the end of 1980

some group member presented the organic ices by using organic small molecules or say oligomer. Although oligomer were deposited by thermal evaporator rather than solution processibility because of the poor solubility. Now days various types of organic devices fabricated by using organic material with solution processibility such as organic solar cell, organic field effect transistor, organic light emitting diode and organic photodiode, etc. The main feature of this technology of solution processable in order to make flexible, ease of handling, colorful and economic too. At present increasing the performance of the OFET make more interesting to design the complex circuit for the application in different area. Someya et al. reported large area pressure sensor made with OFET for the application of electronics artificial skin [4]. Subramanian et al. reported mobility  $10^{-1} \text{ cm}^2/\text{Vs}$  by inkjet printer for the deposition of semiconductor, dielectric insulator and metal contact. This achieved OFET performance sufficient for 135 KHz RFID technology [5]. Klauk et al. [6] also reported integrated organic circuit operated with very low power supply in range of 1.5-3V and power consumption 1nW per logic gate. Apart from this Jung at al. reported roll to roll transfer antenna, rectifiers and ring oscillator on flexible substrate for the application of RFID tag work on 13.5 MHz. [7]

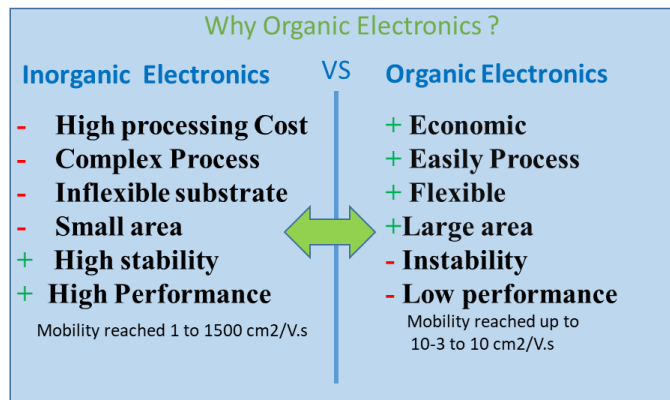


**Figure: 1.1** Importance and drawbacks of organic electronics as compared to inorganic electronics.

At present development of organic devices are very fast by utilization of solution processable organic material specially conjugated polymer. Now conjugated material reached the mobility up to  $1\text{cm}^2/\text{Vs}$  which is sufficient for low frequencies devices like RFID and display devices. It is very important to note that the main aim of organic electronics not to replace the high mobility crystalline Si but we can replace amorphous Si at least having similar mobility. Now days in organic electronics conjugated polymer was utilizing the most interesting material having unique properties such as solution processable and mechanical flexibility for high performance devices fabrication. Although the device performance depends on many factors such as molecular weight, dielectric interface and other processing condition [8,9]. Recently high performance device was fabricated by align the film morphology of conjugated polymer by applying external force [10]. The oriented film having many advantage over the non-oriented film prepared by some method such as spin coat and doctor blad coating and drop casting etc. In this article we utilized the large scale oriented thin film fabrication technique named as ribbon shaped FTM [11]. The main advantage of this technique over the other orientation method to resolve the exiting problem such as mechanical damage, static charge accumulation, solubility in interatrial layer and bottleneck of multilayer casting.

According to Organic Electronics Market Report, published by Allied Market Research, [12] forecasts that the global market is expected to \$79.6 million by 2020, registering a CAGR of 29.5% during the period 2014-2020. In organic electronics market Organic displays are one of the largest revenue source for covering to nearly  $2/3^{\text{rd}}$  of the market. The main application of OLED displays, in laptops, tablets and TV sets, hold lions share in the global organic electronics displays market. In global market Asia Pacific generates about 63.5% of the revenue which is almost  $3/4^{\text{th}}$  of the

global electronics manufacturing industry, which is the primary application area for organic electronics.

## **1.2 Semiconductor:**

Semiconductor is a class of crystalline solid which having intermediate electrical conductivity below the conductor and above the insulator. Semiconductors are basically utilized for the fabrication of various types of electronics devices such as diode, transistor and integrated circuit. It is having the capability to control wide range current and voltage and important for fabrication of complex microelectronics circuits. In periodic table elements are arranged according to their properties. In group four of periodic table there are some elements such as C, Si, Ge, Sn and Pb in which there are four valence electrons available for covalent bonding. Si is the second most abundant element in the world but ranks first in its application in semiconductor technology. However the cost of processing it demands high energy consuming instrument and clean room for device fabrication as well as for characterization. So an alternative way to minimize such high cost is substituting the Si with organic materials which demand no such high cost of processing. The elements Si, Ge, Sn, Pb contribute to the inorganic semiconductor.

### **1.2.1 Inorganic Semiconductor:**

A class of material made from non-carbon based material like Si, Ge, gallium or arsenide utilized for the fabrication of all logic circuit and memory chip contrary to organic semiconductor. In spite of having different physics in both of them, abutment inorganic semiconductor cannot be expelled from organic semiconductor research, especially when discuss about transistor based devices. From the first day of integrated circuit and recent 2018 announced 10 nm CMOS technology based microprocessor chips [13]. For this Si is the one of the most top position for evaluation of

semiconductor technology. In this section we will be discuss the basic fundamental of inorganic semiconductor and also specially focused on Si properties. In following section we will discuss the contrast in organic semiconductor.

### 1.2.1.1 Conductor, Metal and Insulator

Although it is already define the solid state materials are classified according to their conductivity ( $\sigma$ ) is the main criterion. Materials with conductivity in the range of  $10^{-6}$  to  $10^{-18} \Omega^{-1} \text{ m}^{-1}$  belongs to classified as an insulator and at the other extreme, the conductivity in the range of  $10^4$  to  $10^8$  classified as conductors. But the intermediate range of conductivity  $10^{-3}$  to  $10^{-6} \Omega^{-1} \text{ m}^{-1}$  which is below the conductor and above the insulator classified as Semiconductor. Figure 1.2 shown the classification of material according to their conductivity.

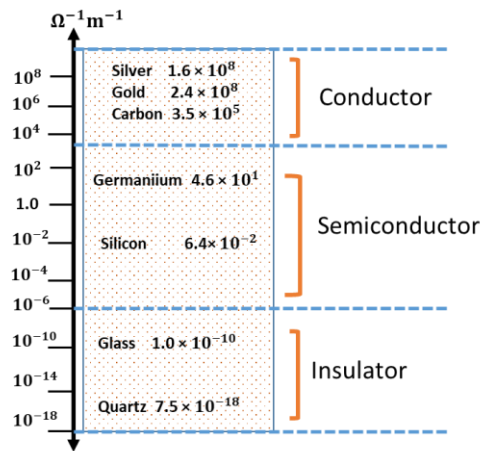


**Figure: 1.2** shown the range of conductivity in conductor semiconductor and insulator.

In figure the conductor having a properties to pass a various types of energy. In metals conductivity is based on the free electrons due the internal bonding. In all metals gold and silver are best but costly so rarely used. In chip the gold is using for contact. An alternative metals such as aluminum, copper are using for wiring from one component to another in microchip.

Insulator passes no current in any substance because of no free electron to serve as charge carriers so it is non-conductive in nature. Due to the nature of non-conductive basically used for packaging as well as isolation from one layer to other. In insulator belongs to some best insulating materials such as glass, paper and Teflon which have very high resistivity.

In semiconductor the conductivity is function of temperature and increase by increment in temperature. Semiconductor having the very good properties to alter the conductivity by adding some impurities in crystal structure. In semiconductor Si and Ge are the best semiconducting material but Si is most preferred in semiconductor technology. Their conductivity is increased by adding some amount of impurities such as pentavalent (antimony, phosphorus, or arsenic) or trivalent (boron, gallium or indium) impurities and this process is called doping and resultant semiconductor named extrinsic semiconductor.

Semiconductor based device having useful properties like easily current passing in one direction than other, showing variable resistance and sensitivity to light or heat. The electrical properties of semiconductor can be optimized by doping or by electric fields or light, and can be used for amplifying, switching and energy conversion.

### **1.2.1.2 Charge Carriers and Energy Bands**

According to band theory, at absolute zero the four valence electrons occupy in 3s subshell of their respective states and another 3p subshell is unoccupied. At this extreme condition there is no charge conduction via crystal because occupied 3s subshell does not allow to unoccupied empty subshell 3p. The highest occupied band 3s is called valance band and the lowest occupied band is called conduction band. In conduction band the lowest energy level is denoted by  $E_C$  while  $E_V$  is denoted the highest energy level of valance band. The energy gap between  $E_C$  and  $E_V$  is called

energy band gap and denoted by  $E_G$ . This energy gap difference decide the nature of the material to be semiconductor, conductor or insulator. The filled electron in conduction band need some amount of energy to excite the electron from valance band to conduction band [14,15]. These excited electron are called free electron and electron deficiencies in valance band create holes. These electrons and holes are the charge carriers in semiconductor. In case of metals, there is an overlapping in conduction and the valance band ( $E_G = 0$ ) due to this the electrons in the CB become electrically conductive. In energy momentum relation the dependence of  $E_c$  and  $E_v$  on momentum (K) define the direct band semiconductor or indirect band semiconductor. In direct band semiconductor for example GaAs, the minimum  $E_c$  occurs for the same K and maximum  $E_v$  while in indirect band gap semiconductor for example Si, the level maximum and minimum appears at different K respectively. The direct band gap semiconductor having the great importance for optoelectronics application because their band structure facilitates absorption and emission of photon and show higher quantum yields as compared to Si. Having this type of properties play importance role for high efficient devices, such as LED. In crystal lattice structure, the charge carries move over the size of unit cell the momentum differ as per expected value and simplified by the concept of effective mass of electron ( $m_e^*$ ) as well as hole ( $m_h^*$ ). In equation 1 mention the effective mass depends on energy momentum relation [16]

$$m_e = \frac{\hbar k^2}{2(E(k) - E_0)} \quad (1)$$

Where  $E(k)$  energy of the electron in band,  $E_0$  is the edge energy of the band,  $k$  is the momentum and  $\hbar$  is the Planck constant ( $6.582 \times 10^{-16}$  eV.s)



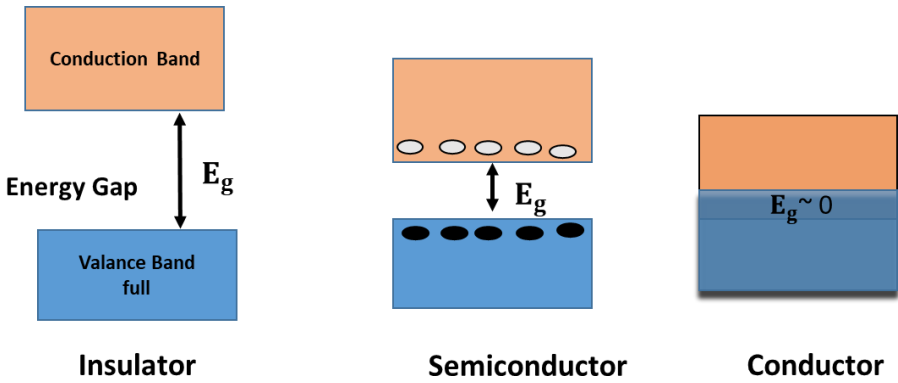


**Figure: 1.3** Energy band gap of insulator semiconductor and conductor

Without any external excitation, after given non-zero temperature for thermal activation only the mechanism to induce the electron-hole pair generation. The semiconductor is classified two types intrinsic and extrinsic based on impurities. In intrinsic, the concentration of small impurities in semiconductor crystal as compared to thermally generated carrier pairs while adding doping impurities of other group such as group III to V in semiconductor crystal due to this introduce new energy levels called as extrinsic. The electron density per unit volume can be calculated by taking the integral of density of state and probability function  $F(E)$  which is also known by fermi distribution function. When  $F(E) = 1/2$  called fermi energy. In intrinsic semiconductor the position of the fermi energy in the middle of the band gap. The electron and hole density positioned bottom of the conduction band and top of the valance band which is denoted by  $n$  and  $p$  respectively. The important case in intrinsic semiconductor,  $n=p = n_i$  here  $n_i$  stand for intrinsic carrier density. In extrinsic semiconductor in case of electron donation the density is denoted by  $N_D$  while in case of acceptor density is denoted by  $N_A$ . These are affected the position of the fermi level and calculated by this equation:

$$E_C - E_F = kT \ln \left( \frac{N_C}{N_D} \right) \quad (2)$$

$$E_F - E_V = kT \ln \left( \frac{N_V}{N_A} \right) \quad (3)$$

Where  $k$  is Boltzmann's constant,  $T$  is absolute temperature,  $N_C, N_V$  are effective density state in conduction as well as valance band and  $N_D, N_A$  are donor and acceptor density. The equation for charge carrier density in intrinsic semiconductor

$$n = n_i \exp \frac{E_F - E_i}{KT} \quad (4)$$

$$p = n_i \exp \frac{E_i - E_F}{KT} \quad (5)$$

Where  $E_i$  is intrinsic fermi level.

In this case the product of  $n$  and  $p$  are equal to  $n_i^2$  at thermal equilibrium and also called mass action law.

$$np = n_i^2 \quad (6)$$

According to this law the carriers having highest concentration called as majority carriers while in minority called minority carriers. In extrinsic semiconductor when electron are majority carriers called n-type while hole is majority carriers called p-type semiconductor.

### 1.2.1.3 Charge Carrier Transport

The charge carrier transport is an important topic for discussion because the movement of free carriers lead current flow in any semiconductor devices [17]. Carrier movement caused electric field because of applied the external voltage. We will assign this charge transport mechanism as a carrier drift since the charge carriers are charge particle. Apart from this, carriers also move a region where the carrier density is high to the region of low carrier density. This charge transport mechanism is because of thermal energy and associated to the random motion of the carriers,

referred to as carrier diffusion. The addition of carrier drift and carrier diffusion is total current in semiconductor and these two factors are important for electrical conduction in any semiconductor.

Some other phenomena such as electron-hole pair generation and recombination, quantum tunneling, avalanche multiplication and thermionic emission also play important contribution to the current conduction of the semiconductor.

In semiconductor after applied the bias, an electrostatic force is exerted on the partially occupied electrons along the applied field lines. Due to electric field, velocity component induced and known as drift velocity that is calculated as

$$v_n = - \frac{qt_c}{m_n^*} \epsilon \quad (7)$$

Where  $q$  is the elementary charge,  $\epsilon$  is electric field and  $v_n$  is drift velocity of electron.

According to equation, the  $\frac{qt_c}{m_n^*}$  known as electron mobility and denoted by  $\mu_n$ . Likewise,  $\mu_p$  as a hole mobility. Charge carrier mobility is very important parameter for both inorganic as well as organic semiconductor and used for the evaluations of electrical performance.

$$\mu = \frac{qt_c}{m^*} \quad (8)$$

Where  $m^*$  is the effective mass of the charge carriers.

The total current in a semiconductor induced by an applied electric field is called drift current  $I_{drift}$  and equals the sum of electron and hole drift currents. The conductivity  $\sigma$  of the semiconductor equals

$$\sigma = q (\mu_n + p\mu_p) \quad (9)$$

Where  $n$  is the electron density,  $p$  is the hole density,  $\mu_n$  is the electron mobility and  $\mu_p$  is the hole mobility.

The drift current density  $J_{drift}$  is the drift current per unit area which flows through a semiconductor of a cross-sectional area  $A$  under the effect of an applied field  $\epsilon$  and it can be expressed by Ohm's law:

$$J_{drift} = \frac{I_{drift}}{A} = \sigma \epsilon \quad (10)$$

In this case, the induced current is called diffusion current  $I_{diff}$  and has two components; the electron diffusion current and the hole diffusion current. Its density  $J_{diff}$  in a semiconductor of cross-sectional area  $A$  is defined as:

$$J_{diff} = \frac{I_{diff}}{A} = q \left( D_n \frac{dn}{dx} - D_p \frac{dp}{dx} \right) \quad (11)$$

where  $D_n$  and  $D_p$  are the diffusion coefficients, constants or diffusivities of electrons and holes, respectively, and  $\frac{dn}{dx}$  and  $\frac{dp}{dx}$  are the spatial derivatives of electron density and hole density, respectively.

The total current density  $J_{total}$  is the sum of drift and diffusion current densities for both electrons and holes;

$$J_{total} = J_{drift} + J_{diffusion} = q \left( n \mu_n \epsilon + D_n \frac{dn}{dx} + p \mu_p \epsilon - D_p \frac{dp}{dx} \right) \quad (12)$$

## 1.2.2 Organic Semiconductor

Recently in last 20 years tremendous development has been done by using the organic semiconductor in electronics devices. Organic semiconductor emerges new class of material that

provide interesting electronic properties and many other benefits as compared to inorganic semiconductor. Since the organic materials specially polymer having the features such as low molecular weight, ease of processing for thin film fabrication, low temperature and low cost production. In next section we will discuss about the conjugated polymer which is very interesting research topic in organic semiconductor.

### 1.2.2.1 Conjugated Polymer

In organic semiconductor conjugated material are most important class of material and classified in two groups [18] such as conjugated polymers and conjugated oligomers. In polymer many identical units bonded together in a long chain for example polythiophene, while only a few units bonded in oligomer. In these materials, due to delocalized  $\pi$ - electron formed the  $\pi$ -conjugated system [19,20]. Apart from this some other  $\pi$ - conjugated organic semiconductor such as pentacene fullerenes and etc. having of semiconducting properties. In figure shown some conjugated polymers chemical structure.

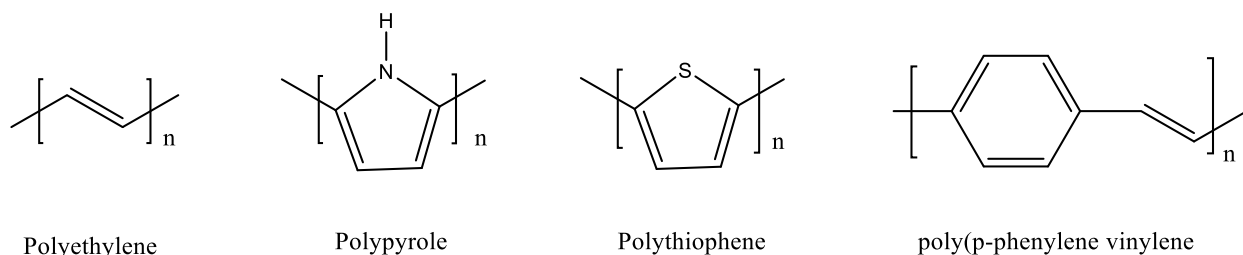


**Figure: 1.4** Chemical structure of some of the widely studied conjugated polymers.

### 1.2.2.2 Charge Carriers in Conjugated Polymer

In conjugated polymers the charge carriers was created by partial oxidation or by partial reduction and understand by p-type doping and n-type doping, due to this charge defects induces named as polaron, bipolaron and soliton [21]. In organic semiconductor, according to molecular orbital

theory, the conduction band can be understood by lowest unoccupied molecular orbital (LUMO) while highest occupied molecular orbital (HOMO) known as valence band. These HOMO and LUMO are also called frontier orbitals of molecule. The energetic difference between HOMO and LUMO levels known as band gap. In organic semiconductor the band gap is also small (1eV-4eV) due to this thermal excitation of electrons from HOMO to LUMO states is possible. In organic semiconductor the energy band gap depends upon the conjugation of molecule. When molecules conjugation increases delocalization in  $\pi$ -electron become more and decrease the energy gap between subsequent discrete energy states.

### 1.2.2.2 Charge Carriers Transport in Conjugated Polymer

As discussed already in inorganic semiconductor band transport theory unlike in organic molecule. In this section we will discuss the charge transport theory in organic semiconductor. In organic semiconductor the charge transport depends on many factors and explained by polaron model, effect of disorder, effect of space charge and effect of charge carrier traps. In polaron model, the band transport in organic semiconductor first reported by Karl et al. in pure crystals of oligoacenes, [22] where author explained mobility dependence on temperature.

$$\mu \propto T^{-n} \quad (13)$$

Another better received theory based on drift velocity as discussed in inorganic semiconductor.

$$v = \mu \epsilon \quad (14)$$

Total mobility of carriers by polaron model

$$\mu = \mu_{coherent} + \mu_{hopping} \quad (15)$$

Where  $\mu_{coherent}$  is stand for band like transport mechanism and  $\mu_{hopping}$  is incoherent transport mechanism.

In disorder effect of diagonal and off diagonal, the distribution of effective conjugation length and other effect of electrostatic nature [23] belongs to diagonal disorder while off diagonal based on molecular packing and the morphology of a semiconducting thin-film.

The space charge effect can be understand in intrinsic semiconductor (un-doped), the injection of charge carriers from metal electrode into bulk of semiconductor introduces space charge along the conduction path. These charges affect the externally applied field, due to this there is a reduction in resulting current and known as space charge limited current (SCLC) and its current density is described by

$$J_{SCLC} = \frac{9}{8} \epsilon_r \epsilon_0 \mu \frac{V^2}{L^3} \quad (16)$$

Where  $\epsilon_r$  is the static permittivity of the semiconductor,  $\epsilon_0$  is the vacuum permittivity ( $\sim 8.854 \times 10^{-12}$  F/m),  $\mu$  is the mobility of charge carriers, V is the externally applied voltage and L is the length of the conduction path.

The effect of charge carrier traps is unavoidable in organic semiconductor devices. The charge traps either electron traps, when the electron affinity ( $E_a$ ) of the semiconductor is somewhat lower than their energy state, or hole traps, when their ionization potential ( $I_p$ ) is somewhat higher than their energy state. Charge carriers are effectively trapped by these energy sites due to the aforementioned energy differences.

### 1.3 Thin Film Fabrication and Molecular Orientation

In organic electronics thin film fabrication was deposited by either thermal evaporation for small molecules, or solution processable for the polymers. Recently in solution processable, there are many methods such as spin coating, dip coating and doctor blading used for thin film fabrication in which spin coating is most preferred method. Although these methods make the thin film well which is isotropic in nature. Recently some orientation techniques such as mechanical rubbing, friction transfer, strain alignment, roll transfer and solution flow etc. have been used to align the polymer chain. The main advantage of orienting film of its single dimensionality which show optical as well as electrical anisotropy. The large scale orientation in conjugated polymers can be explain by two way, first the preferred alignment in main chain of conjugated polymer from the substrate and in second preferential alignment at the length scale. The preferential alignment of polymeric backbone can be understood by three different way such as edge-on, face-on and end-on. First, in edge-on orientation, the axis of conjugated backbone and  $\pi$ -stacking lie in the plain of substrate. Where as in second, face-on orientation, the conjugation and alkyl stacking axis parallel to the substrate and  $\pi$ -stacking normal to the substrate. It is documented and believed that along the conjugation direction and  $\pi$ -stacking direction, high carrier transport occurs, while lower in alkyl stacking direction [24]. It is also well known that edge –on orientation is preferred for the OFET, which need high in plain transport, while the face-on orientation is suitable for solar cell because out-of-plane is desirable [25]. In third, end-of orientation, there are few report where polymer backbone direction in normal to the substrate direction, [26] which show high out-off-plane transport that is promising geometry for solar cell [27].

The orientation can be understood on the basis of quantitative characterization of thin film conjugated polymer, for that polarized absorption spectroscopic and polarized emission



spectroscopic were used. Some other orientation investigation can be understood by polarized Fourier transform infrared spectroscopy and polarized Raman spectroscopy. However, for detailed orientation of the crystallite in their thin films involve sophisticated characterization such as grazing incidence X-ray diffraction and electron diffraction measurements.

#### 1.4 Organic Field Effect Transistor:

Transistors are backbone of in modern circuitry and used for signal amplifier or on/off switches. This work on the basis of field effect phenomenon where the conductivity of a semiconductor changes by applying the electric field normal to its surface [28]. When applying the electric field it act as parallel plate capacitor in which one plate consider as metal and another as semiconductor, isolated by insulator. The FET consist of having three terminals such as source drain and gate work as electrode shown in figure

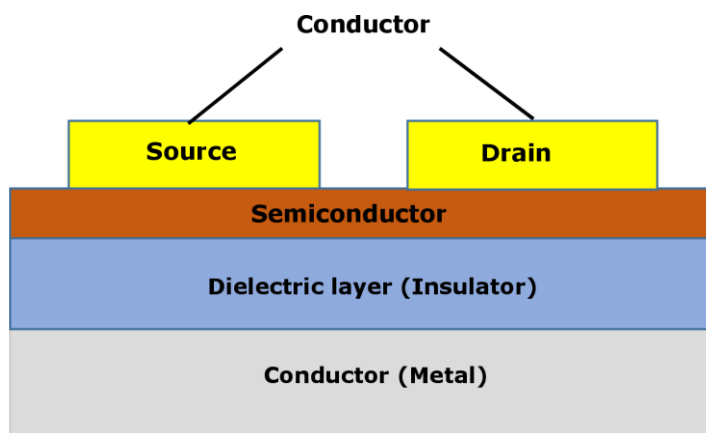


**Figure: 1.5** shown the bottom gate top contact (BGTC) OFETs configuration having three terminal source, drain and gate.

The dielectric can be made of a variety of dielectric materials, through SiO<sub>2</sub> grown on doped silicon. In figure source and drain are two separate electrode physically connected to the semiconductor layer with separation, and the gap between two electrodes called channel. In this

configuration channel is important parameter that is understood by channel length (L) separation between electrodes while the width of electrode is channel width (W).

### 1.4.1 Device Configuration

The configuration of OFETs varies according to fabrication method but in principle there are four types of configuration available in trend shown in figure 1.6 which is basically based on above discussed requirements. Amongst four configuration the bottom gated configuration is mostly preferred. This configuration are usually common where  $\text{SiO}_2$  is grown on doped silicon wafers, which is easily purchase by the researcher for study the preliminary evaluation of semiconductor material performance.

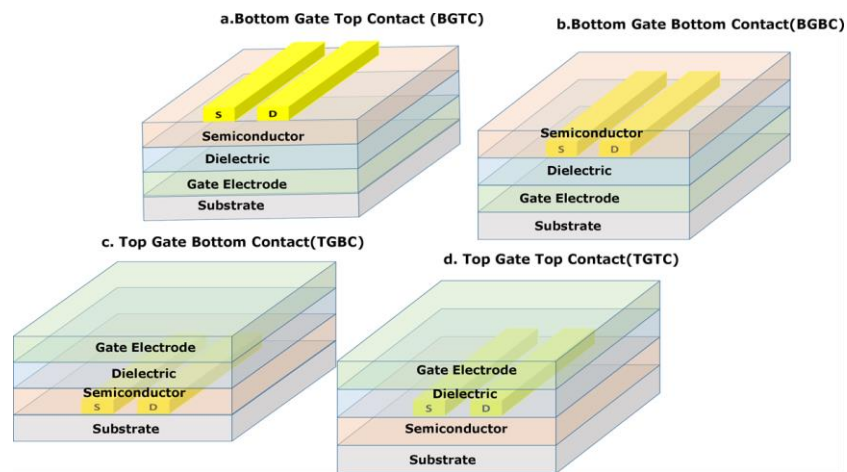


**Figure: 1.6** shown the possible four types of typical configuration of OFETs (a) BGTC (b) BGBC (c) TGBC and (d) TGTC

The gate dielectric layer play an important role since its capacitance, which is actually determined by its thickness permittivity, influence the number of charge carrier to be generated in the semiconductor, concomitantly the operating voltage of the device. To satisfy the need of low voltage operating gate dielectric which can be solution processed, transparent and can be utilized as flexible substrate as well, a number of new organic gate dielectric has been developed

in the recent past, simultaneously. The advantage of organic dielectric is that it can be solution processed in order to fabricate top gated devices without harming the metal electrodes and semiconductor layer unlikely to other inorganic dielectrics which needed to be deposited using sputtering and thermal evaporation.

### 1.4.2 Working Principle

The main difference between OFET and MOSFET is that OFETs usually operate in accumulation mode but they also known for operate in depletion and inversion mode [29-31]. In accumulation mode the  $V_G$  is biased and source will be grounded in this mode charge carriers accumulate at semiconductor /dielectric interface. This accumulated charge of few nanometer thickness [32] formed in layer, called transistor channel. The channel length,  $L$  and width,  $W$ , can be optimized by spatial arrangement of the source and drain electrode. The areal charge density of accumulated charge in the channel,  $Q_{channel}$ , and when applying the gate voltage it works as a parallel plate capacitor model.

$$Q_{channel} = C_i \times V_G \quad (17)$$

When applied gate to source voltage  $V_{GS}$  the free electron/hole accumulated in the HOMO/LUMO at the channel, second bias drain to source voltage is also applied which is known as drain voltage  $V_D$ . After applying the second bias  $V_D$  and with addition to  $V_G$  generate a current in the channel known as drain current  $I_D$ . There are three main case for the current flow in channel. If  $V_D = 0$ , in this case there is no changing in accumulated layer at semiconductor / dielectric interface, called cut –off , where drain current  $I_D = 0A$ . In second case when a little increase in drain current,  $0V < V_D < V_G$ , the charges will start to inject from source to attract the drain, in this case constant resistance across the channel, and carrier concentration vary linearly due to this drain

current increases linearly. This region is known as linear regime. In third case when  $V_D \geq V_G > 0V$ , the more depleted charge carriers having high resistance started to inject next to the drain electrode. This high resistance resultant non-linear conductivity across the channel and called as saturation regime.

### 1.4.3 Electrical Characterization:

By applying the  $V_D$  across the channel the voltage varies gradually and employed a gradual-channel approximation model. This model is basically used in case of MOSFET but it has been utilized in OFETs by slightly modification [33]. According to this model, discuss the current flow across the channel. As previously discussed available trap need to be filled before the mobile carriers induce at semiconductor/insulator interface. The required voltage to fill this trap and produce mobile charges known as threshold voltage,  $V_{th}$ . From equation the density of mobile charges in channel  $Q_{mob}$

$$Q_{mob} = C_i (V_G - V_{th}) \quad (18)$$

As the charge carrier density depends on the position in the channel,  $V(x)$ ,

$$Q_{mob} = C_i [V_G - V_{th} - V(x)] \quad (19)$$

Assuming that, under the external field  $V_D$ , drift current dominates the channel, then diffusion and gate leakage can be neglected (i.e. only consider the movement of charge carriers due to the applied field). The current through the channel,  $I_D$ , is then proportional to the width of the channel,  $W$ , the density of mobile charges,  $Q_{mob}$ , the electric field  $V$  at position  $x$ ,  $F(x)$ , and the speed of the charge carriers due to the applied electric field,  $\mu$ :

$$I_D = W \mu Q_{mob} F(x) \quad (20)$$

Where  $F(x) = \frac{dV}{dx}$  (21)

$$\mu = \frac{V}{E} \quad (22)$$

where  $\mu$  is the mobility, which is defined as the drift velocity,  $V$ , of the charge carriers in cm/s per applied electric field,  $E$ , in V/cm.

Substituting Equation (19) and (21) into Equation (20) resultant:

$$I_D dx = W \mu C_i [V_G - V_{th} - V(x)] dV \quad (23)$$

and integrating over the potential difference range between the source and the drain, i.e. the channel length,  $L$ , gives

$$\int_0^L I_D dx = W \mu \int_0^{V_D} C_i [V_G - V_{th} - V(x)] dV \quad (24)$$

$$I_D = \frac{W}{L} C_i \mu \left[ (V_G - V_{th}) \times V_D - \frac{V_D^2}{2} \right] \quad (25)$$

By approximating  $V_D \ll V_G$  in Equation (25), the current between the source and drain during linear regime operation is given by the following

$$I_D = \frac{W}{L} C_i \mu [(V_G - V_{th}) \times V_D] \quad (26)$$

To find the current in the saturation regime,  $V_D = (V_G - V_{th})$  can be substituted into the gradual channel approximation in Equation (25), as when  $V_D$  is greater than  $(V_G - V_{th})$ , there is no noticeable increase in  $I_D$

$$I_{D,sat} = \frac{W}{2L} C_i \mu (V_G - V_{th})^2 \quad (27)$$

From here, the saturation mobility,  $\mu_{sat}$ , can be found either from the second derivative of Equation (28) with respect to  $V_G$ .

$$\mu_{sat} = \frac{2L}{WC_i} \left( \frac{\partial \sqrt{I_D}}{\partial V_G} \right)^2 \quad (28)$$

## 1.5 Motivation for the Research

Now days, organic electronics is growing field for the development of the electronic devices such as organic field effect transistor, solar cell, organic light emitting diode and photodetector etc. Fast growth if this technology is associated with the features such as low cost, flexibility and ease of processing. The main advantage of this technology is solution processability due to this it can be cast on variety of substrate such as plastic, cloths and glass etc. at large area to make the functional devices. Devices performances are evaluated on the basis of mobility, for that conjugated polymers with solution processable, will be the promising material for the development of the next generation electronics. Currently in conjugated polymer the mobility stand up to 10 cm<sup>2</sup>/V.s [34].

Mobility was improved by adopting a number of approaches like molecular design, processing conditions, making composites and blends but controlling the film morphology of conjugated polymer owing to their inherent single-dimensionality plays a dominant role. Currently mobility is also controlled by aligning the conjugated polymer in 3-D space, and inducing crystallinity in 3-D resultant  $\pi$ - $\pi$  stacking increase due to reduction of inter-chain resistance. There is exiting problem in solution processed conjugated polymer during the casting of the multilayer without affecting the underlying layers. Recently one orientation method was developed, which basically protects the damage of underlying layers during the multilayer casting named as floating film transfer method [35, 36]. In this method film was fabricated on liquid substrate by dropping a 20  $\mu$ l of polymer solution. The polymer solution was spread on liquid substrate and make a floating oriented solid film on liquid substrate that is easily transferred on desired substrate. The film thickness and orientation was easily controlled by controlling the casting temperature, polymer

concentration and viscosity of liquid substrate [37]. In order to circumvent issues like non-uniformity and multi-directional film spreading, we have recently reported an improvisation in our conventional floating film transfer method [38]. Utilization of a custom-made slider during film spreading for providing directionality to the spreading film in FTM led to the large area (14-20 cm) and highly oriented films formation named as Ribbon- shaped FTM [11]. This oriented film was transferred on desired substrate for the application in electronics device with improved device performance. This method is different to spin coating and other solution based method needs orthogonal solvent to avoid the existing problem such as morphological and compositional damages during the multilayer deposition [39]. FTM shows unidirectional orientation of liquid crystalline conjugated polymer having the tendency to align the backbone structures in preferred direction at a certain optimized temperature [36]. Subsequently this method was applied for many conjugated polymers to form oriented film at large area and later applied to electronic devices showing anisotropy in OFET and organic light emitting diodes [40-41]. In order to have large area implementation of organic electronics, having following features are highly desired;

1. Solution based procedure
2. Capable of fabricating large area oriented films
3. Minimum material wastage
4. No need of sophisticated instrument
5. Ease of handling
6. Thickness of the film can be easily controlled

After consideration of above features, there are a needs to develop this method further in order to implement this large area for the fabrication of electronic devices while maintaining the high performance. This method should be applicable for various types of conjugated polymer having different in polymeric backbone structure by controlling the casting factor control in orientation that improved the device performance. Therefore, the motivation lies to carry out the development of this method and to demonstrate the various features of this procedures and the same has been conveyed in the subsequent chapters.

## **1.6 Thesis Organization**

This thesis has been organized in to seven chapters by summarizing the research work carried and research results as follows;

First chapter provides a brief introduction to the concerns related to the present state-of-art in organic electronics over the conventional electronics, background problems related to thin film fabrication techniques for conjugated polymers and aim of this present work. Theory related to the basic knowledge of inorganic and organic semiconductor specially conjugated polymers, their charge carriers, energy band as well as charge carrier transport, with existing thin film fabrication techniques and working principle of organic field effect transistor.

Second chapter presents brief outline of the conjugated polymers utilized in the present thesis, their film processing with especial emphasis on the introduction to the orientation technique with emphasis on developed floating film transfer method, various characterization procedures for oriented film, device fabrication and analysis.

Third chapter focuses on the further improvisation of conventional floating film transfer method by introducing the assisting slider and making the large area oriented film in ribbon shaped. This



chapter also discusses the controlling factors for ribbon shaped FTM utilizing non regiocontrolled poly(3-hexylthiophene) as one of the representative conjugated polymer.

Fourth chapter of the thesis presents optoelectronic characterization of large area oriented films of PQT-C12 conjugated polymer prepared by ribbon-shaped FTM. Implication of molecular weight and its distribution on molecular orientation and anisotropic charge transport has been systematically carried out.

Fifth chapter deals with molecular orientation and charge transport anisotropy in various type of conjugated polymers prepared by ribbon shaped FTM. The main aim of the work carried out in this chapter to delineate the nature of polymeric backbone upon extent of molecular orientation and the resulting anisotropic charge transport after fabricating OFETs by stamping the oriented films in the parallel and perpendicular to the channel.

Sixth chapter of this thesis discusses about the orientation, electrical characteristics and anisotropic charge transport in the large area regioregular poly(3-alkylthiophene) thin films by fabricating OFETs. Thanks to the edge-on oriented thin films fabricated by ribbon-shaped FTM, demonstrated in this work, there was very little influence of alkyl chain length on charge transport, which is one of most serious problems in spin-coated thin films reported previously by many research groups.

Finally, the seventh and last chapter of this thesis presents the overall conclusion of the whole work summarizing the main results along with future work and their perspectives.

## References:

- [1] C.K. Chiang, C.R. Fincher, Y.W. Park, A.J. Heeger, H. Shirakawa, E.J. Louis, Electrical conductivity in doped polyacetylene. *Phys Rev Lett* 1977, 39(17):1098-101.
- [2] H. Shirakawa, E.J. Louis, A.G. MacDiarmid, C.K. Chiang, A.J. Heeger, Synthesis of Electrically Conducting Organic Polymers, *Polymer (Guildf)*. 36 (1977) 578–580. doi:10.1039/C39770000578.
- [3] C.W. Tang, S.A. Vanslyke, Organic electroluminescent diodes, *Appl. Phys. Lett.* 51 (1987) 913–915. doi:10.1063/1.98799.
- [4] T. Someya, Y. Kato, T. Sekitani, S. Iba, Y. Noguchi, Y. Murase, H. Kawaguchi, T. Sakurai, G.M. Whitesides, T. Someya, Y. Kato, T. Sekitani, S. Iba, Y. Noguchi, Y. Murase, Conformable, flexible, large-area networks of pressure and thermal sensors with organic transistor active matrixes, *Proc. Natl Acad Sci U S A*. 102(35) (2005) 12321-5.
- [5] V. Subramanian, P.C. Chang, J.B. Lee, S.E. Molesa, S.K. Volkman, Printed organic transistors for ultra-low-cost RFID applications, *IEEE Trans. Components Packag. Technol.* 28 (2005) 742–747. doi:10.1109/TCAPT.2005.859672.
- [6] H. Klauk, U. Zschieschang, J. Pfau, M. Halik, Ultralow-power organic complementary circuits, *Nature*. 445 (2007) 745–748. doi:10.1038/nature05533.
- [7] M. Jung, J. Kim, J. Noh, N. Lim, C. Lim, G. Lee, J. Kim, H. Kang, K. Jung, A.D. Leonard, J.M. Tour, G. Cho, All-Printed and Roll-to-Roll-Printable Tag on Plastic Foils, *IEEE Trans. Electron Devices*. 57 (2010) 571–580. doi:10.1109/TED.2009.2039541.
- [8] P. Pingel, A. Zen, D. Neher, I. Lieberwirth, G. Wegner, S. Allard, U. Scherf, Unexpectedly high field-effect mobility of a soluble, low molecular weight oligoquaterthiophene fraction with low polydispersity, *Appl. Phys. A Mater. Sci. Process.* 95 (2009) 67–72.
- [9] H. Sirringhaus, Device physics of solution-processed organic field-effect transistors, *Adv. Mater.* 17 (2005) 2411–2425.
- [10] M. Brinkmann, L. Hartmann, L. Biniek, K. Tremel, N. Kayunkid, Orienting semi-conducting pi-conjugated polymers, *Macromol. Rapid Commun.* 35 (2014) 9–26.
- [11] A.S.M. Tripathi, M. Pandey, S. Sadakata, S. Nagamatsu, Anisotropic charge transport in highly oriented films of semiconducting polymer prepared by ribbon-shaped floating film, *Appl. Phys. Lett.* (2018) **112**, 123301 (n.d.).
- [12] <https://www.alliedmarketresearch.com/press-release/organic-electronics-market-is-expected-to-reach-79-6-billion-global-by-2020-allied-market-research.html>.
- [13] <https://newsroom.intel.com/newsroom/wp-content/uploads/sites/11/2017/03/Mark-Bohr->

2017-Moores-Law.pdf.

- [14] D. Liming, *Intelligent Macromolecules for Smart Devices. Structure* (2004)
- [15] J.E. Carlé, <http://plasticphotovoltaics.org>.
- [16] Antonis Dragoneas , Organic Semiconductor Devices: Fabrication, Characterisation and Sensing Applications, [http://theses.whiterose.ac.uk/5763/1/Dragoneas%20PhD%20Thesis%20\(Library\).pdf](http://theses.whiterose.ac.uk/5763/1/Dragoneas%20PhD%20Thesis%20(Library).pdf).
- [17] Charge carrier intro [https://ecee.colorado.edu/~bart/book/book/chapter2/ch2\\_7.htm](https://ecee.colorado.edu/~bart/book/book/chapter2/ch2_7.htm)
- [18] F. Garnier, “Scope and limits of organic-based thin-film transistors,” *Phil. Trans.*, 1997 vol. 355, pp. 815–827.
- [19] C. D. Dimitrakopoulos and D. J. Mascaro, “Organic thin-film transistors, a review of recent advances, 2001 *IBM J. Res. Dev.*, vol. 45, pp. 11–27.
- [20] E. Cantatore, “Organic materials: A new chance for electronics?,” *Proc. of the SAFE/IEEE workshop*, vol. workshop 2000,27, pp. 27–31.
- [21] D. Liming, *Intelligent Macromolecules for Smart Devices. Structure* (2004).
- [22] N. Karl, J. Marktanner, R. Stehle, and W. Warta, “High-Field Saturation of Charge Carrier Drift Velocities in Ultrapurified Organic Photoconductors,” *Synthetic Metals*, 1991, vol. 42, no. 3, pp. 2473-2481.
- [23] V. Coropceanu, J. Cornil, D. A. da Silva, Y. Olivier *et al.*, “Charge transport in organic semiconductors,” *Chemical Reviews*, vol. 107, no. 4, pp. 926-952, Apr, 2007.
- [24] Jimison, L. H., Toney, M. F., McCulloch, I., Heeney, M. & Salleo, A. Charge-Transport Anisotropy Due to Grain Boundaries in Directionally Crystallized Thin Films of Regioregular Poly(3-hexylthiophene). *Adv. Mater.* **21**, 1568–1572 (2009).
- [25] H. Sirringhaus, Two-dimensional charge transport in self-organized, high-mobility conjugated polymers. *Nature* (1999), **401**, 685–688.
- [26] M. Aryal, K. Trivedi, W. Hu, Nano-Confinement Induced Chain Alignment in Ordered P3HT Nanostructures Defined by Nanoimprint Lithography, *ACS Nano*, (2009) **3**, 3085– 3090.
- [27] J. Ma, K. Hashimoto, T. Koganezawa, K. Tajima, Enhanced vertical carrier mobility in poly ( 3- alkylthiophene ) thin films sandwiched between self-assembled monolayers and surface- segregated layers. *Chem. Commun.* **50**, 3627 (2014).
- [28] R.F. Pierret, G.W. Neudeck, *Advanced Semiconductor Fundamentals*, Pearson Educ. Inc. 6 (1987) 17–18. doi:10.1017/CBO9781107415324.004.
- [29] G. Horowitz, R. Hajlaoui, H. Bouchriha, R. Bourguiga, M. Hajlaoui, Concept of

- 'threshold voltage' in organic field-effect transistors, *Adv. Mater.* 10 (1998) 923–927. doi:10.1002/(SICI)1521-4095(199808)10:12<923::AID-ADMA923>3.0.CO;2-W.
- [30] M. Zhu, G. Liang, T. Cui, K. Varshneyan, Depletion-mode n-channel organic field-effect transistors based on NTCDA, *Solid. State. Electron.* 47 (2003) 1855–1858. doi:10.1016/S0038-1101(03)00141-2.
- [31] B. Lüssem, M.L. Tietze, H. Kleemann, C. Hoßbach, J.W. Bartha, A. Zakhidov, K. Leo, Doped organic transistors operating in the inversion and depletion regime, *Nat. Commun.* 4 (2013) 1–6. doi:10.1038/ncomms3775.
- [32] A. Salleo, Charge transport in polymeric transistors, *Mater. Today.* 10 (2007) 38–45. doi:10.1016/S1369-7021(07)70018-4.
- [33] S.D. Brotherton, *Introduction to Thin Film Transistors: Physics and Technology of TFTs.* Switzerland: Springer; 2013.
- [34] Y. Yamashita, F. Hinkel, T. Marszalek, W. Zajaczkowski, W. Pisula, M. Baumgarten, H. Matsui, K. Müllen, J. Takeya, Mobility Exceeding 10 cm<sup>2</sup>/(V·s) in Donor-Acceptor Polymer Transistors with Band-like Charge Transport, *Chem. Mater.* 28 (2016) 420–424. doi:10.1021/acs.chemmater.5b04567.
- [35] T. Morita, V. Singh, S. Nagamatsu, S. Oku, W. Takashima, K. Kaneto, Enhancement of transport characteristics in poly(3-hexylthiophene) films deposited with floating film transfer method, *Appl. Phys. Express.* 2 (2009) 1–4. doi:10.1143/APEX.2.111502.
- [36] D. Arnaud, R.K. Pandey, S. Miyajima, S. Nagamatsu, R. Prakash, W. Takashima, S. Hayase, K. Kaneto, Fabrication of large-scale drop-cast films of  $\pi$ -conjugated polymers with floating-film transfer method., *Trans. Mater. Res. Soc. Japan.* 38 (2013) 305–308. doi:10.14723/tmrj.38.305.
- [37] M. Pandey, S.S. Pandey, S. Nagamatsu, S. Hayase, W. Takashima, Controlling Factors for Orientation of Conjugated Polymer Films in Dynamic Floating-Film Transfer Method, *J. Nanosci. Nanotechnol.* 17 (2017) 1915–1922. doi:10.1166/jnn.2017.12816.
- [38] A. Tripathi, M. Pandey, S. Nagamatsu, S.S. Pandey, S. Hayase, W. Takashima, Casting Control of Floating-films into Ribbon-shape Structure by modified Dynamic FTM, *J. Phys. Conf. Ser.* 924 (2017). doi:10.1088/1742-6596/924/1/012014.
- [39] T. Morita, V. Singh, S. Oku, S. Nagamatsu, W. Takashima, S. Hayase, K. Kaneto, Ambipolar transport in bilayer organic field-effect transistor based on poly(3-hexylthiophene) and fullerene derivatives, *Jpn. J. Appl. Phys.* 49 (2010) 0416011–0416015. doi:10.1143/JJAP.49.041601.
- [40] A. Dauendorffer, S. Nagamatsu, W. Takashima, K. Kaneto, Optical and transport anisotropy in poly(9,9-dioctyl-fluorene-alt- bithiophene) films prepared by floating film transfer method, *Jpn. J. Appl. Phys.* 51 (2012). doi:10.1143/JJAP.51.055802.
- [41] A. Dauendorffer, S. Miyajima, S. Nagamatsu, W. Takashima, S. Hayase, K. Kaneto, One-step deposition of self-oriented  $\beta$ -phase polyfluorene thin films for polarized polymer light-emitting diodes, *Appl. Phys. Express.* 5 (2012). doi:10.1143/APEX.5.092101.

## *Chapter 2: Experimental*

### **2.1 Materials**

Chemicals like methanol, ethylene glycol, glycerol, methanol, ferric chloride and super dehydrated chloroform etc. were purchased from Wako Chemicals Japan. Starting materials like 3-alkylthiophenes were purchased from TCI-chemicals Japan while, 3,3''-didodecyl-quarterthiophene and conjugated polymer poly[2,5-bis(3-tetradecylthiophene-2-yl)thieno[3,2-b]thiophene] (PBT-TT-C14) were purchased from Sigma-Aldrich and used as received without any further purification. Conjugated polymers non-regiocontrolled poly(3-hexylthiophene) (NR-P3HT) and poly(3,3''-didodecylquarterthiophene) (PQT-C12) were synthesized as per the reported literature procedure [1-3]. The synthesized conjugated polymers were further purified by Soxhlet extraction as already reported in our previous work [4-5]. NR-P3HT was synthesized by FeCl<sub>3</sub> catalyzed chemical polymerization, where it was having 80% of moderate regioregularity. Regioregularity of this polymer was confirmed by <sup>1</sup>H-NMR considering fraction of  $\alpha$ -methylene proton [6]. PQT-C12 was chemically synthesized from its monomer 3,3''-didodecyl-quarterthiophene) by FeCl<sub>3</sub> catalyzed oxidative polymerization followed by purification by Soxhlet extraction. It is a p-type liquid crystalline conjugated polymer having larger stability for oxygen doping as compared to most commonly used P3HT [7]. Poly(9,9-dioctylfluorene-alt-bithiophene) (F8T2) is an alternating copolymer synthesized by Suzuki coupling as per the literature procedures [9-10]. Regioregular poly(3-alkylthiophenes) (P3ATs) with varying chain length from four (C<sub>4</sub>H<sub>9</sub>) to eighteen (C<sub>18</sub>H<sub>37</sub>) were purchased from Sigma Aldrich. Poly[4,8-bis[(2-ethylhexyl)oxy]benzo[1,2-b:4,5-b']dithiophene-2,6-diyl][3-fluoro-2-[(2-ethylhexyl)carbonyl]thieno[3,4-b]thiophenediyl] (PTB7) was purchased from 1-material. Molecular structure of various conjugated polymers used have been shown in the figure 2.1

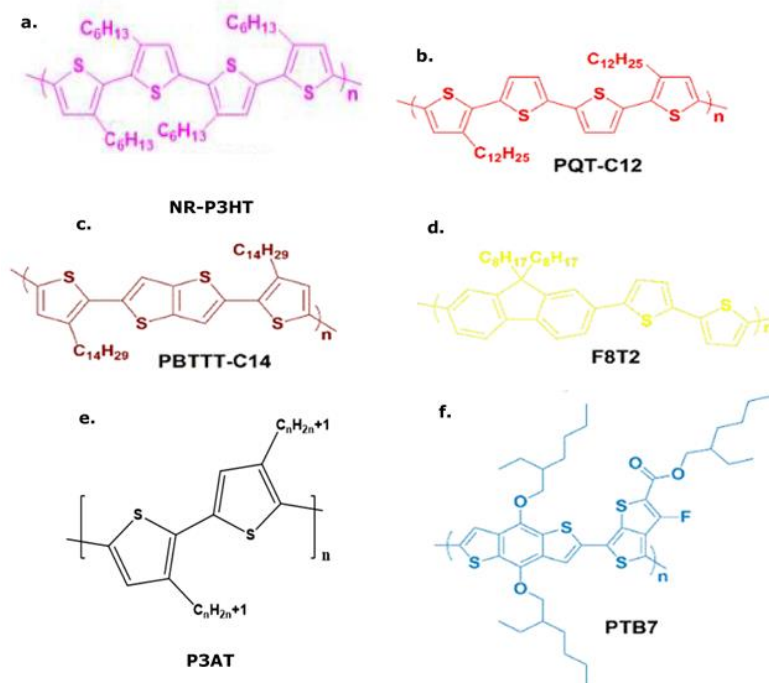


**Figure: 2.1** Chemical structure of different  $\pi$ -conjugated semiconducting polymers like NR-P3HT (a), PQT-C12 (b), PBTTT-C14 (c), F8T2 (d) regioregular P3ATs (e) and PTB7(f).

## 2.2 Deposition Method

### 2.2.1 Spin Coating

Spin coating is one of the mostly used for thin film deposition of various types of conducting semiconducting and insulating organic materials after making in the form of solution. For making the film, first of all we drop a small amount of material in center according size of substrate and makes it spin for a sort duration. The dropped solution started to spread in all direction due centrifugal force and the excess material ejected from the edges of the substrate and make the solid thin film. The film thickness cab be optimized based on such parameters, concentration of material, spinning speed, acceleration and time is the controlling factor of film thickness. In figure 2.2 shown the thin film fabrication process by spin coating method.

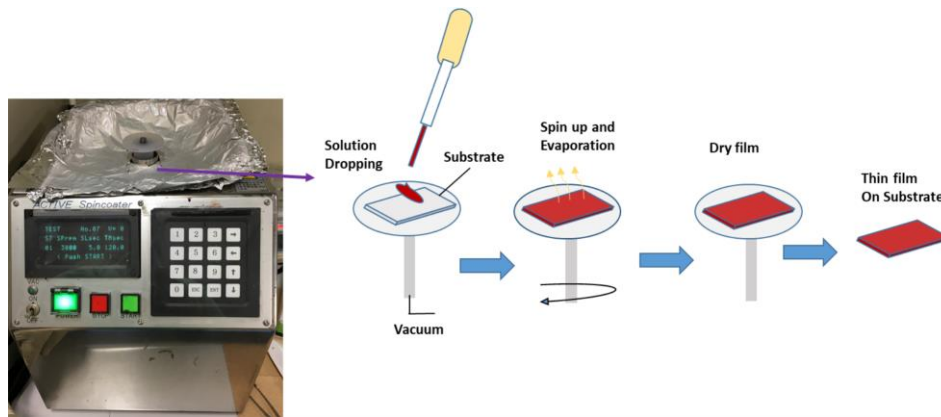


**Figure: 2.2** Picture of the spin coater used step wise for making the thin film

Although this process is known for best reproducible thin film fabrication but it is sensitive to presence of dust particle. This technique is generally used in clean room environment .Some more drawbacks of this technique is not suitable for large area fabrication.

### 2.2.2 Dynamic Floating Film Transfer Method

A novel and simple thin film fabrication method was developed in 2009 in our laboratory to easily make a conjugated polymer film on hydrophilic liquid substrate by using floating film transfer method [11,12].

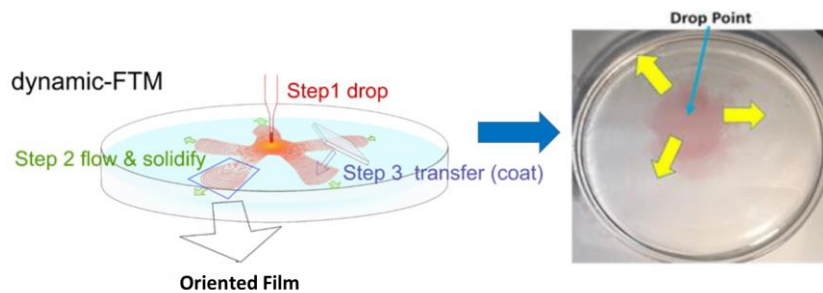


**Figure: 2.3** Schematic of thin film fabrication by dynamic floating film transfer method.

In this method, a small amount of hydrophobic polymer solution dropped on hydrophilic liquid substrate and making a floating solid film. This film was easily transferred on desired substrate

without of any morphological damage. Although this method is similar to Langmuir-Blodgett method but there is no any extremal surface force. It is found that this is the best method for making the oriented film of  $\pi$ - conjugated polymer at cm scale by optimizing its parameter such as casting temperature, concentration of polymer solution and viscosity of the liquid substrate [13]. The main advantage of dynamic FTM is solution processable, facile method with cost effective and least material wastage. Apart from this, it have the ability to fabricate multilayer device by multi casting of oriented film with easily controlled thickness.

In FTM , when solvent vaporized slowly after dropping the polymer solution on liquid substrate that provide the floating film known as static FTM [14,15]. Contrary to quick evaporation of solvent known as dynamic FTM and due to this dynamic nature polymer was oriented well. In FTM, the volatile nature of solvent decide the type of FTM like high boiling point solvent such as chlorobenzene where low evaporation and low boiling point solvent chloroform, tetrahydrofuran and dichloromethane leads quick evaporation shown in figure 2.3

Recently further developed the conventional FTM in which existing circumvent issues like non-uniformity and multi-directional film spreading by providing the directionality in a single direction, and make this FTM method for large scale thin film fabrication up to > 20 cm in length and >2 cm in width by adding the assisting slider during the casting and also achieved the high orientation named as ribbon-shaped FTM [16,17].



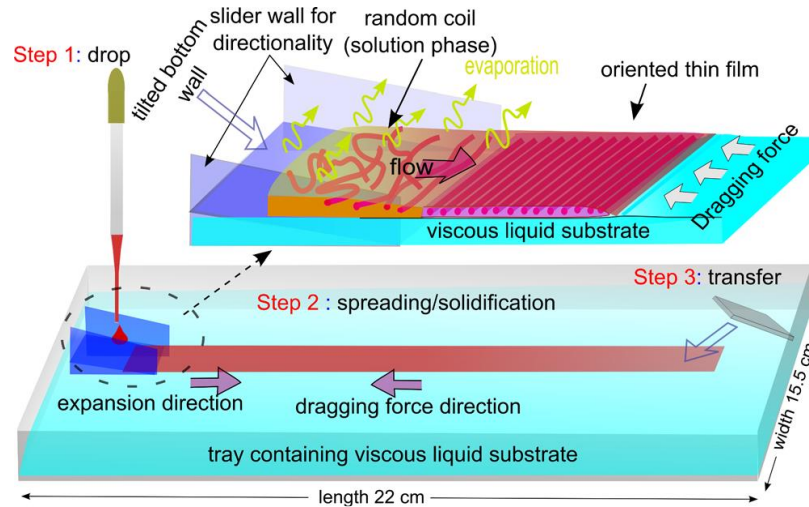


**Figure: 2.4** Schematic demonstration for the fabrication of ribbon-shaped oriented FTM films and its orientation mechanism.

### 2.3.3 Thermal Evaporation

Thermal evaporation is a deposition system where the metal such as gold, silver and aluminum etc. are deposited at very low pressure up to  $10^{-6}$  mbar. For longer mean free path low pressure is required, due to this evaporated particle reached directly to target object without any type of colliding background gases. Apart from pressure some other physical parameter is also important mention in equation 2.1.

$$\lambda_m = \frac{RT}{\sqrt{2} \pi d^2 N_A P} \quad [1]$$

Where the symbols represents.

P, R, T stand for Pressure of the system, Gas Constant and Temperature respectively. While  $N_A$  and d stand for Avogadro's number and diameter of the gas particles in meters.

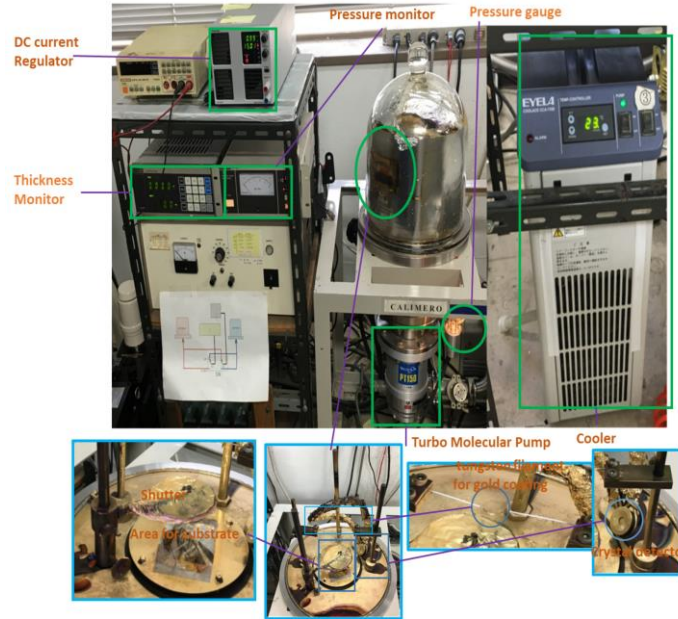


**Figure: 2.5** Thermal evaporation system used for deposition of metal electrodes assembled in our laboratory.

Figure 2.5 shown the setup of thermal evaporation system where two pumps one high vacuum turbo pump backed by another second rotary pump. In this system some important component have the important role for deposition of metals as per requirement. For deposition of metal like gold first wrapped in tungsten filament and setup above the target substrate. For avoid the any types of slippery impurity shutter was used for the protection. Once the sufficient vacuum reached, operating the system then filament tungsten heated on the principle of joule's first law ( $P \propto I^2R$ ). The tungsten was selected as a filament having high melting point ( $\sim 3400$  °C) as compared to gold ( $\sim 1064$  °C) , the gold started to melt around the melting point. During the gold deposition current was increased slowly so that gold properly adhere on filament before the evaporation. The amount of thickness and rate of deposition read by the crystal detector and display on monitor. When the thickness monitor showing the deposition then opened the shutter and reset the thickness start from zero .The rate of deposition slowly increased by dc current regulator till the desired rate

and steady until the desired amount. When desired amount reached, the input current removed and left the deposited substrate for a 15 minutes in high vacuum chamber before taking it out.

## 2.3 Thin Film characterization

### 2.3.1 Ultraviolet-Visible Spectroscopy

Ultraviolet-visible spectroscopy are basically used for optical characterization of any type of solid or solution based samples in the ultraviolet and visible spectral region. According to principle molecules containing  $\pi$ -electrons or nonbonding electrons can absorb the part of incident energy which are incoming and to excite these electrons to higher antibonding molecular orbitals. The more easily excited the electrons the longer the wavelength of light it can absorb. The electronics absorption spectra of any sample either solution or solid film provide the useful information such as various type of electronic transitions and also used in color bearing molecules characterization. These characterization is very helpful for calculation of various parameters such as optical band gap, molecular aggregation and molecular orientation. Figure shown the step wise process for the measurement of electronics absorption spectra. For the measurement of polarized absorption spectra, a polarizer named as Glan-Thomson was used between the sample and incident beam. This polarizer is easily rotate and take the absorption at any desire angle. The polarized absorption spectra was calculated for the estimation of optical anisotropy in terms of dichroic ratio (DR).

$$DR = \frac{\text{Maximum Absorption } \parallel \text{at } (\lambda_{\max} \parallel)}{\text{Absorption } \perp \text{ at } ((\lambda_{\max} \parallel))}$$

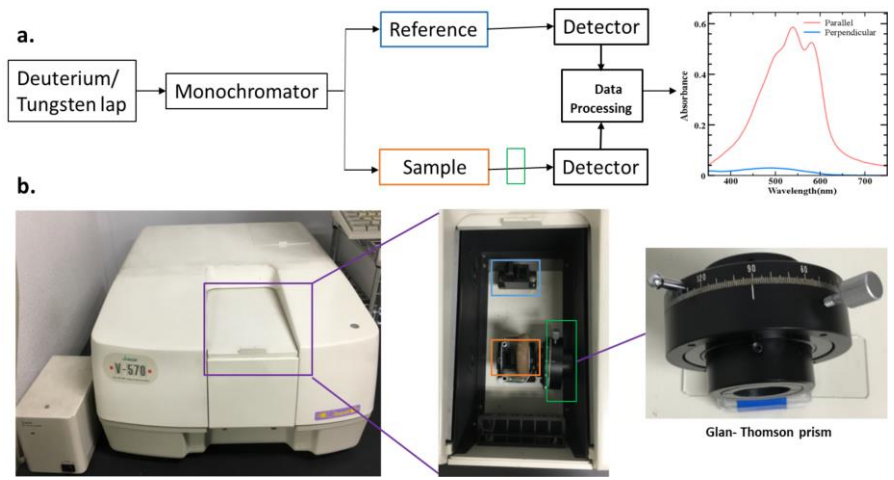


**Figure: 2.6** (a) Schematic representation of the processes involved in absorption spectroscopy and (b) Photograph of the UV-vis spectrophotometer (JASCO V-750). For polarized absorption measurement Glan- Thomson prism is shown in blue-dash square in (a) and (b).

**2.3.2 Interference Microscopy**

Interference microscopy are used for measuring the thickness of the any sample. Figure shown the Eclipse LV150N interference microscopy. This system is combined with digital imaging and advance optical system. It is detected the information easily and display on camera control unit. In addition, the information is automatically converted into appropriate calibration data when changing magnification.



**Figure: 2.7** Set up of Interference Microscopy (Nikon- Eclipse LV150N) utilized for thickness measurement.

### 2.3.3 2-D Positional Mapping

2-D positional mapping is similar to absorption spectroscopy used for the probing the absorption spectra with small interval distance of thin film. Figure 2.8 shown the setup of 2- D positional mapping, where a fixed light source, computer controlled X-Y sample stage and multichannel photodiode array detector was used for the 2-D positional scanning of thin film. It is basically measured by the position dependent absorbance at the respective absorption maximum of the CPs, where absorption peak directly correlates with the thickness.



**Figure: 2.8** 2 D position mapping set up used for analysis of thin film distribution.

### 2.3.4 X-RAY Diffraction

X-ray diffraction is one of the most important material characterization tool to analyze the atomic and molecular structural of the polymer film. The bragg equation is most important for understanding the X-ray diffraction

$$n\lambda = 2 d \sin\theta$$

Where  $n$  is an integer,  $\lambda$  is the wavelength of the X-rays,  $d$  is the interplanar spacing between the atoms, and  $\theta$  is the angle of the X-ray beam with respect to these planes. There are two types of measurement was done in my work. First, out-of-plane diffraction, where we received the stacking

behavior from diffracted lattice plane. This measurement is basically less surface sensitive owing to large incident angle. The out-of-plane process easily understood by shown figure. In this process due to difficulty to achieve the single crystal of polymer and on the other hand the transport properties depend upon arrangement of macromolecules in space of the polymer film. For orientation base polymer film grazing-incidence XRD (GIXD) is suitable reported in [18], where the incident rays are close just above the critical angle it becomes more surface sensitive and refracted beams are stronger.

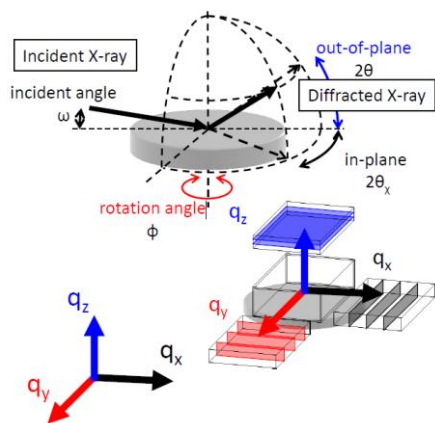


**Figure: 2.9** Schematic geometry of out-of-plane XRD (a) and in-plane GIXD (b).

### 2.3.5 Atomic Force Microscopy

Atomic force microscopy (AFM) also known as Scanning force microscopy (SFM) is very high resolution scanning probe microscopy. It is used for determine the surface topography of any material on the order of fraction of a nanometer. The AFM basically work on the principle of having a cantilever with sharp tip at the end that is used to scan the surface morphology. When the tip contact on the surface of film there is force between the surface and tip lead to deflection of the

cantilever according to Hooke's law [19]. The force consist of different type according to situation, such as mechanical force, van der walls, electrostatic, chemical, capillary and magnetic force etc.



**Figure: 2.10** Set up of AFM system with JEOL-SPM used for AFM measurement.

The tapping mode was used for the scanning the surface of material because the tip could stick the surface in normal contact mode. In backside of the cantilever beam a laser beam is focused and reflects it to the position sensitive photodetector, which convert it in electrical signal. AFM image were taken by JEOL SPM 5200 with Olympus probe (OMCL-AC200 TS-C3) in tapping mode and AFM set up was shown in figure.

### **2.3.6 Gel Permeation Chromatography**

Gel permeation chromatography (GPC) is a type of size exclusion chromatography (SEC) that separates the dissolved macromolecules by size based according to elution form columns filled with a porous gel. It is basically known for triple detection coupled with light scattering, viscometer and concentration detection. It is used for the measurement of molecular weight, molecule size and intrinsic viscosity and also produce the important information on the macromolecular structure, conformation, aggregation and branching. Apart from molecular weight, it can characterized molecules such as synthetic polymers as well as natural polymer. It

can be also characterized by a variety of definitions for molecular weight including the number average molecular weight ( $M_n$ ), the weight average molecular weight ( $M_w$ ) and calculate the polydispersity (PDI).

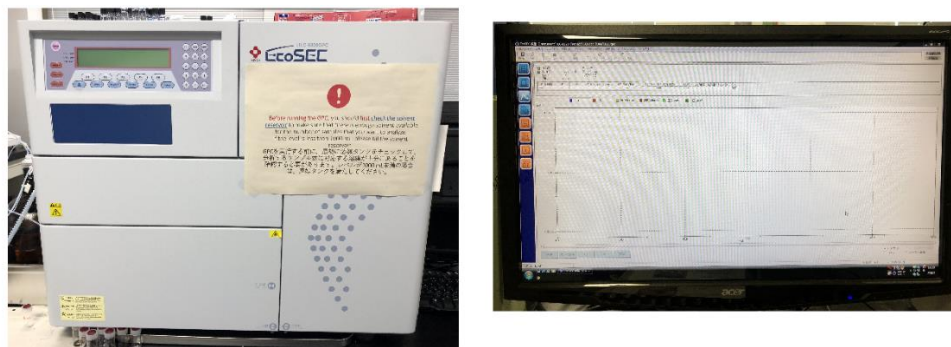


**Figure 2.11** Set up of GPC measurement system for estimation of molecular weight and PDI of the polymer.

## 2.4 Device Fabrication

### 2.4.1 Surface Treatment

Bottom gate top contact OFET was fabricated on highly doped Si substrate having 300nm of grown  $\text{SiO}_2$  insulating layer. For making the devices, Si substrate was cut into a small pieces up to size of  $\sim 1 \text{ cm}^2$ . It is important to note that the wafer should be cut on clean soft cloth to avoiding the any types of scratch on insulator interface during the cutting because one small scratch act as an interface for active semiconducting layer. The pieces of substrate was cleaned in ultrasonic bath 5 minute each by rinsing the substrate into acetone and isopropanol and dry it at  $100 \text{ }^\circ\text{C}$  for a few minutes. The  $\text{SiO}_2$  layer act as a gate dielectric insulator having the capacitance  $10 \text{ nF/cm}^2$ . The insulating layer was modified by making it more hydrophobic as per requirement. In my experimental work two types of hydrophobic preparation was done on  $\text{SiO}_2$  surface such as CYTOP TM and octadecyl (trichloro) silane (OTS).



For making the CYTOP layer on SiO<sub>2</sub>, the solution of CYTOP drop on SiO<sub>2</sub> substrate and spin coated at 3000 rpm for 120 second followed by annealing at 150 °C for a duration of 1 hour. After coating the CYTOP on SiO<sub>2</sub> the value of capacitance was changed and found 8 nF/cm<sup>2</sup>. For OTS treatment, the SiO<sub>2</sub> surface was immersed in a closed glass container filled with 2 mM solution of octadecyltrichlorosilane (OTS) in dehydrated toluene and heated 90°C for 2 hours followed by annealing at 130°C for 30 min. to make the self-assembled monolayer of OTS on SiO<sub>2</sub> surface.

### 2.4.2 Deposition of Semiconductor Layers and Electrodes

For making the OFETs, oriented semiconductor layer was deposited by FTM method followed by masking which show anisotropic nature, while for comparison non-oriented layer was deposited by spin coating method show isotropic. Masking position was set according to the orientation direction oriented before the electrode (source and drain) deposition. Figure 2.12 shown the procedure of electrode deposition by using the mask. After the deposition of electrode the unwanted area outside the mask was removed for avoid the any type of leakage at the edges during the OFET operation. For characterization, source, drain and gate terminal was connected to the 50 μm gold wire with the help of silver pest for characterization.

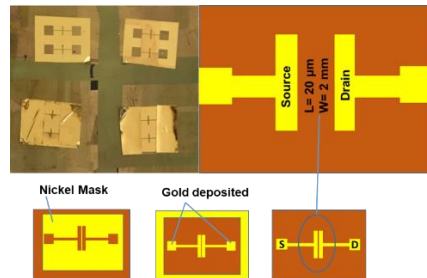


**Figure: 2.12** (a) Photograph of nickel shadow mask on substrates and (b) schematic flow diagram of the various steps from semiconductor layer to full ready OFET for measurement. The channel length ‘L’ and width ‘W’ was 20 μm and 2 mm, respectively.

### 2.4.3 Electrical Characterization

The OFETs measurement was done in vacuum where the normal pressure up to  $10^{-3}$  torr shown in figure. The set up was made in acrylic box for the connection of source, drain and gate using the gold wire (50 $\mu$ m in diameter). The set up box headed in vacuum chamber and start the pump for creating the vacuum. The electrical characterization such as output and transfer characteristics were measured with computer controlled two channel electrometer (Keithley 2612). OFET parameter such as field effect mobility ( $\mu$ ), threshold voltage ( $V_{th}$ ) and on/off ratio was calculated from the transfer characteristics .

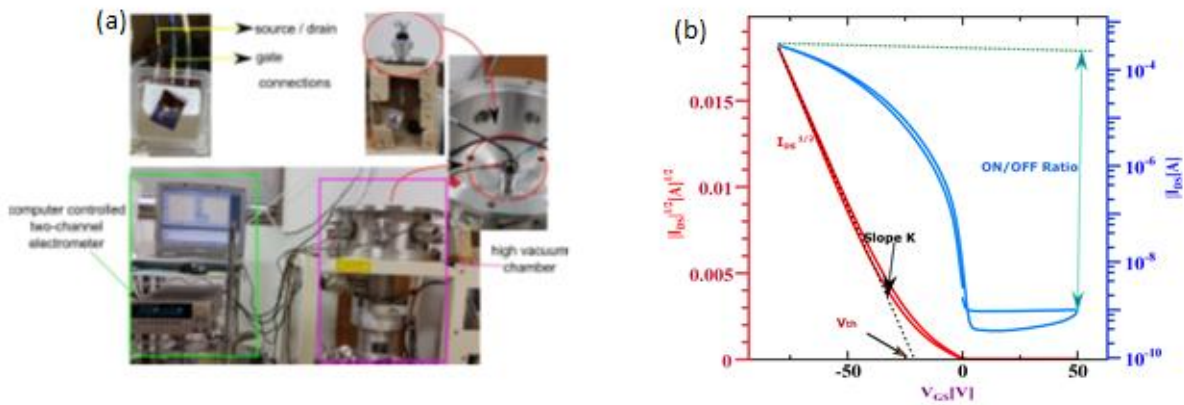


**Figure 2.13** Set up of OFETs electrical characterization (a) with one typical example of transfer characteristics of PQT-C12 as an active material (b).

Figure shown the transfer characteristics of OFET at saturation region in  $I_{DS}$  vs  $V_{GS}$ . Mobility and threshold voltage was measured by the calculation of  $\sqrt{I_{DS}}$  vs  $V_{GS}$ . The drain current equation at saturation region represent the value of drain current. By solving the drain equation for mobility we found that it depends upon the slope  $k$  in equation that was mention in graph of transfer characteristics. The threshold voltage was also calculated by the intersection of the line with the axis of  $V_{GS}$ .

$$I_{DS,Sat} = \frac{W}{2L} C_i \mu (V_{GS} - V_{th})^2 \quad (2)$$

$$\sqrt{I_{DS,Sat}} = \sqrt{\frac{W}{2L} C_i \mu} (V_{GS} - V_{th}) \quad (3)$$

$$K = \sqrt{\frac{W}{2L} C_i \mu} \quad (4)$$

$$\mu = \frac{2k^2}{C_i \frac{W}{L}} \quad (5)$$

## References:

- [1] R.H. Lohwasser, M. Thelakkat, Toward perfect control of end groups and polydispersity in poly(3-hexylthiophene) via catalyst transfer polymerization, *Macromolecules*. 44 (2011) 3388–3397. doi:10.1021/ma200119s.
- [2] S. Amou, O. Haba, K. Shirato, T. Hayakawa, M. Ueda, K. Takeuchi, M. Asai, Head-to-tail regioregularity of poly(3-hexylthiophene) in oxidative coupling polymerization with FeCl<sub>3</sub>, *J. Polym. Sci. Part A Polym. Chem.* 37 (1999) 1943–1948. doi:10.1002/(SICI)1099-0518(19990701)37:13<1943::AID-POLA7>3.0.CO;2-X.
- [3] S. Ong, Y. Wu, P. Liu, S. Gardner, High-Performance Semiconducting Polythiophenes for Organic Thin-Film Transistors High-Performance Semiconducting Polythiophenes for Organic Thin-Film Transistors, (2004) 3378–3379. doi:10.1021/ja039772w.
- [4] M.R. Andersson, D. Selse, M. Berggren, H. Järvinen, T. Hjertberg, O. Inganäs, O. Wennerström, J.E. Österholm, Regioselective Polymerization of 3-(4-Octylphenyl)thiophene with FeCl<sub>3</sub>, *Macromolecules*. 27 (1994) 6503–6506. doi:10.1021/ma00100a039.
- [5] M. Trznadel, A. Pron, M. Zagorska, R. Chrzaszcz, J. Pielichowski, Effect of molecular weight on spectroscopic and spectroelectrochemical properties of regioregular poly(3-hexylthiophene), *Macromolecules*. 31 (1998) 5051–5058. doi:10.1021/ma970627a.
- [6] M. Pandey, S. Nagamatsu, S.S. Pandey, S. Hayase, W. Takashima, Orientation Characteristics of Non-regiocontrolled Poly (3-hexyl-thiophene) Film by FTM on Various Liquid Substrates, *J. Phys. Conf. Ser.* 704 (2016). doi:10.1088/1742-6596/704/1/012005.
- [7] T. Kushida, T. Nagase, H. Naito, Angular distribution of field-effect mobility in oriented poly[5,5'-bis(3-dodecyl-2-thienyl)-2,2'-bithiophene] fabricated by roll-transfer printing, *Appl. Phys. Lett.* 104 (2014). doi:10.1063/1.4867980.
- [8] S. Thienothiophene, *Advanced Materials Interfaces Rapid formation of Macroscopic Self-Assembly of Liquid Crystalline , High Mobility , (n.d.)*.
- [9] A. Dauendorffer, S. Nagamatsu, W. Takashima, K. Kaneto, Optical and transport anisotropy in poly(9,9'-dioctyl-fluorene-alt- bithiophene) films prepared by floating film transfer method, *Jpn. J. Appl. Phys.* 51 (2012). doi:10.1143/JJAP.51.055802.
- [10] E. Lim, B.J. Jung, H.K. Shim, Synthesis and characterization of a new light-emitting fluorene-thieno[3,2-b]thiophene-based conjugated copolymer, *Macromolecules*. 36 (2003) 4288–4293. doi:10.1021/ma034168r.
- [11] T. Morita, V. Singh, S. Nagamatsu, S. Oku, W. Takashima, K. Kaneto, Enhancement of transport characteristics in poly(3-hexylthiophene) films deposited with floating film transfer method, *Appl. Phys. Express.* 2 (2009) 1–4. doi:10.1143/APEX.2.111502.
- [12] D. Arnaud, R.K. Pandey, S. Miyajima, S. Nagamatsu, R. Prakash, W. Takashima, S. Hayase, K. Kaneto, Fabrication of large-scale drop-cast films of  $\pi$ -conjugated polymers with floating-film transfer method., *Trans. Mater. Res. Soc. Japan.* 38 (2013) 305–308.

doi:10.14723/tmrsj.38.305.

- [13] M. Pandey, S.S. Pandey, S. Nagamatsu, S. Hayase, W. Takashima, Controlling Factors for Orientation of Conjugated Polymer Films in Dynamic Floating-Film Transfer Method, *J. Nanosci. Nanotechnol.* 17 (2017) 1915–1922. doi:10.1166/jnn.2017.12816.
- [14] M. Pandey, S.S. Pandey, S. Nagamatsu, S. Hayase, W. Takashima, Solvent driven performance in thin floating-films of PBTTT for organic field effect transistor: Role of macroscopic orientation, *Org. Electron. Physics, Mater. Appl.* 43 (2017) 240–246. doi:10.1016/j.orgel.2017.01.031.
- [15] J. Noh, S. Jeong, J.Y. Lee, Ultrafast formation of air-processable and high-quality polymer films on an aqueous substrate, *Nat. Commun.* 7 (2016) 1–9. doi:10.1038/ncomms12374.
- [16] A. Tripathi, M. Pandey, S. Nagamatsu, S.S. Pandey, S. Hayase, W. Takashima, Casting Control of Floating-films into Ribbon-shape Structure by modified Dynamic FTM, *J. Phys. Conf. Ser.* 924 (2017). doi:10.1088/1742-6596/924/1/012014.
- [17] A.S.M. Tripathi, M. Pandey, S. Sadakata, S. Nagamatsu, Anisotropic charge transport in highly oriented films of semiconducting polymer prepared by ribbon-shaped floating film, (n.d.). doi:10.1063/1.5000566.
- [18] M.L. Chabinye, X-ray scattering from films of semiconducting polymers, 2008. doi:10.1080/15583720802231734.
- [19] [https://en.wikipedia.org/wiki/Surface\\_Science\\_Reports](https://en.wikipedia.org/wiki/Surface_Science_Reports).

## *Chapter: 3 Ribbon-shaped FTM: parametric optimizations*

### **3.1 Introduction**

In the recent past Conjugated polymers (CPs) have captivated a lot of attentions for their potential applications in the area of organic field effect transistors (OFETs), light emitting diodes, (LEDs) photovoltaics and different type of sensors etc. The CPs having solution processing capability, which is one of the important features rendering their suitability towards potential application in the area of flexible electronics owing to the cost efficient process for fabrication of thin films. The quality of thin film morphology, plays an important factor in deciding the charge transport properties, which commence from the self-assembly promoted aggregation of macromolecules while solid phase condensation. The casting procedures to prepare the thin film semiconducting layer by using CPs is, therefore, an important and best way to characterize the transport performance. Although thin film fabricated by spin coating is one of the well documented and mostly preferred techniques but unfortunately, the random spatial arrangement of polymeric main-chains bounds its usage for fabricating high performance organic electronic devices [1]. Recent past years one of the amicable solutions for this problem is developed by the introduction of macromolecular alignment of CPs. Now days various methods are used for the preparation of oriented thin-films in which some methods such as friction transfer method [2], mechanical rubbing [3], solution flow [4], capillary action [5], solution shearing [6], slide coating [7] and strain alignment [8] etc. have been developed and also investigated the analysis of orientation and charge transport characteristics in details. Although the oriented film of CPs fabricated by these techniques have demonstrated high performance in organic electronics devices from the last one decade, but some important challenges such as fabrication process in simple way and multilayer

oriented thin film fabrication without harming the film morphology are yet to be taken into consideration. After looking such type of challenges our group developed a dynamic casting of thin floating-film of CPs on orthogonal liquid-substrate and make a floating solid film that is easily transfer on a desired substrate named as dynamic-FTM. This is simple and quick casting method and provide the oriented film of CPs with cost effective. The oriented film are at centimeter-scale which enables us to construct multilayered thin-films with the preserved oriented morphology. [9-11] However, remaining obstacles like non-uniformity in thickness and control of orientation direction are still remaining challenges which have to be solved. In order to resolve such issues, we have developed a new casting method by modifying in casting of conventional floating films into the ribbon-shape by introducing a custom-made slider during the casting and control the spreading of the oriented films. In this study, we have compared the film characteristics prepared by this ribbon-shaped dynamic-FTM and conventional dynamic-FTM. The importance of individual casting parameters such as solution concentration, viscosity of liquid substrate and casting temperature have been investigated by polarized electronic absorption spectroscopy.

### **3.2 Experimental**

In this study non-regiocontrolled poly (3-hexylthiophene) (NR-P3HT) was selected as the representative polymeric material. It has been synthesized by chemical oxidative polymerization using FeCl<sub>3</sub> catalyst and purified as per our earlier publication. [15] The regioregularity (head-to-tail coupling content) was confirmed to be about 80 % by proton nuclear magnetic resonance investigations. The dehydrated chloroform as a solvent, purchased from Wako Chemicals, was used for the thin film casting. The synthesized NR-P3HT was highly soluble in the dehydrated chloroform and used to prepare three types of solutions, 0.5%, 1% and 2% (wt/wt). Procedure to cast the ribbon shaped floating-film has been schematically shown in the Fig. 1.

The hydrophilic liquid mixture was first made and poured into a rectangular tray which serves the purpose of liquid-substrate. A hand-made assisting slider made of PTFE was put near the one of edges in the tray. About 15  $\mu\text{l}$  of NR-P3HT solution in chloroform was dropped in center of slider. When the droplet touched the boundary of slider/liquid-substrate, there was a quick spreading of the polymer solution in unidirectional and followed by continuous solidification due to evaporation of solvent and leading to the fabrication of ribbon-shaped floating-film. After this casting, the obtained solid floating-film was left for 5 minutes to ensure complete evaporation of the remaining solvent. Since the orientation of CP in the floating-film was of macroscopic in order, it was manually confirmed by a sheet of polarizer film with the naked eyes before the measurement and easily understand the orientation direction. The resulted solid floating film was stamped on transparent solid-substrates for the orientation analysis.

Before the film transfer, the surface of the solid substrates were treated with hexamethyldisilazane (HMDS) to enhance the hydrophobicity of the solid substrate in order to ensure easy and better adhesion of the thin floating-films during the film transfer. The transferred film surface was washed with methanol in order to remove any remaining liquid substrate on the stamped surface followed by drying. In order to investigate the effect of viscous liquid-substrate on the molecular orientation, a variety of binary mixtures such as water and ethylene glycol (Wt/Eg) or ethylene glycol and glycerol (Eg/Gl) were used to prepare the liquid-substrates as per our earlier reported manuscript. [14,15] The polarized electronics absorption spectra were obtained by utilizing a Glan-Thompson prism with JASCO V-570 spectrophotometer for investigation of optical anisotropy in the oriented thin films. The orientation intensity of the NR-P3HT based films was calculated in terms of optical dichroic ratio (DR) by using polarized absorption spectra.



### 3.3 Result and Discussion

#### 3.3.1 Casting of Floating Film

The casting of oriented film on liquid substrate is very simple and quick method and easily transfer on a desired substrate. In Figure 3.1 demonstrated the real photographic images of the obtained floating-films prepared by the conventional as well as Ribbon-shaped FTM methods, respectively. The both method casted on liquid substrate by utilizing the same polymeric solution but certain change during the dropping and clearly observed that the obtained shape of the floating-film drastically changes depending on the employed method of the film casting under dynamic FTM. The floating film in circular shape with some dispersive parts formed in the floating film can be clearly seen for the thin film fabrication using previous used conventional dynamic-FTM.

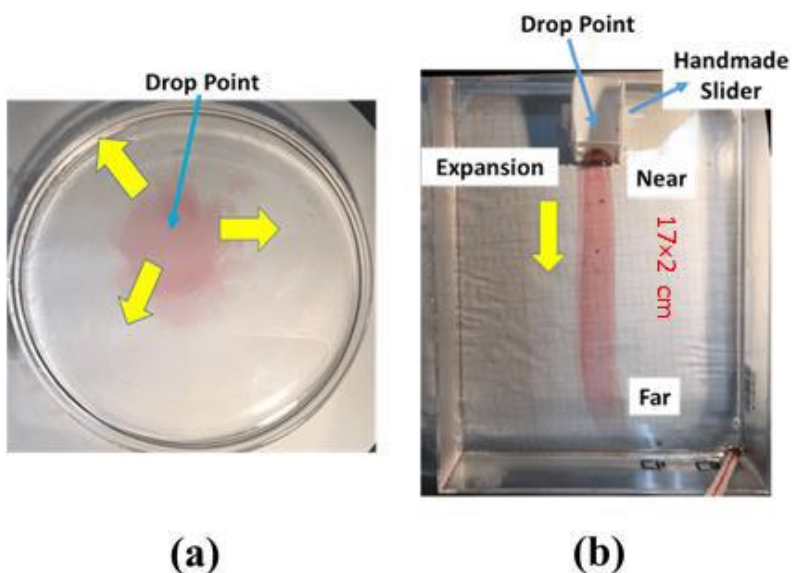


**Figure: 3.1** Optical photographs of casting with (a) conventional dynamic FTM and (b) Ribbon-shape FTM procedure, respectively.

On the other hand, after this newly developed handmade custom slider as solution dropper during the casting changed the shape of the floating-film into the Ribbon-shaped one. It is obvious

that after changing the setting-up method in conventional FTM has advantages in terms for the analysis the orientation manually as well as ease of handling the transfer process due to its rectangular shape in one direction. For the investigation of orientation, polarized electronic absorption spectra was taken by transferring the oriented film of Ribbon-shaped floating-film on hydrophobically treated glass substrate demonstrated in the Figure 3.2. In order to compare the behavior of oriented film a non-polarized electronic absorption spectra of a spin-coated NR-P3HT film has been also incorporated. The obtain DR of the Ribbon-shaped floating-films was found to be 2.4 after calculating the ratio at  $\lambda_{\max}$  at  $\parallel$  and  $\lambda_{\perp}$  at  $\lambda_{\max} \parallel$ . It can be easily seen that absorption maximum ( $\lambda_{\max}$ ) in the electronic absorption spectrum of parallel oriented NR-P3HT film was located at 520 nm along with the presence of vibronic shoulders. Interestingly,  $\lambda_{\max}$  in the electronic absorption spectrum of spin-coated film was found to be at 508 nm with a clear red shift of 12 nm in the Ribbon-shaped FTM film. The vibronic shoulders around 540 nm and 602 were appeared in the similar manner to that observed for the conventional dynamic-FTM.

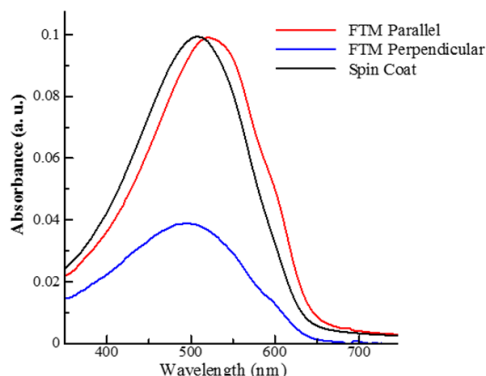


**Figure: 3.2** Polarized electronic absorption spectra of NR-P3HT thin films prepared by spin coating as well as Ribbon-shape FTM.

These obtain resultant indicate the presence of the increased  $\pi$ -orbital delocalization on main-chain of the polymer. [16] The results also support that the films fabricated by this newly

developed method also have enhanced in  $\pi$ -stacking and such type of films are appropriate for the fabrication of optoelectronic devices. Although a relatively small DR of 2.4 observed in this ribbon-shaped oriented film indicates that developed slider method provides a weak orientation as compared to that of the conventional dynamic-FTM. A clear reason for this cannot be assigned at the present stage but further development and optimization of the slider shape is required for achieving the high orientation. The orientation intensity is small in the ribbon-shaped films, it is worthy to note that the  $\lambda_{\max}$  is clearly red-shifted even in NR-P3HT as discussed above. As reported in our previous work, that thin film casted via dynamic-FTM is found to show high transport performance as compared to that of the spin-coat film. [12] In addition, the orientation size can be reached up to centimeter-scale in single direction as compared to conventional dynamic-FTM.

### **3.3.2 Controlling the Casting Parameter**

#### **3.3.2.1 Casting Temperature**

During the orientation optimization in ribbon shaped FTM, casting temperature such as temperature of polymer solution and viscous liquid substrate play important role because it can change the evaporation speed as well as viscosity of the liquid substrate. If we have used the polymer solution associated with temperature, the polymer solution spreads large area and it will take long time for evaporation of solvent, while in opposite at high temperature the evaporation of solvent was rapid and in a short duration polymer solution spread. On the other hand in case of liquid substrate temperature the polymer expansion was also affected. Likewise polymer solution, at low temperature of viscous liquid temperature, it reduces the spreading speed because of relatively high viscosity of liquid substrate, while at high temperature it provide the rapid expansion. After this discussion it is clear that both factors are important during the optimization

film orientation under the dynamic FTM and achieve the maximum possible orientation. For quantitate investigation polarized electronic absorption spectra of FTM films at different temperatures were measured in order to elucidate its implication on the molecular orientation of NR-P3HT films and demonstrated in Figure 3.3

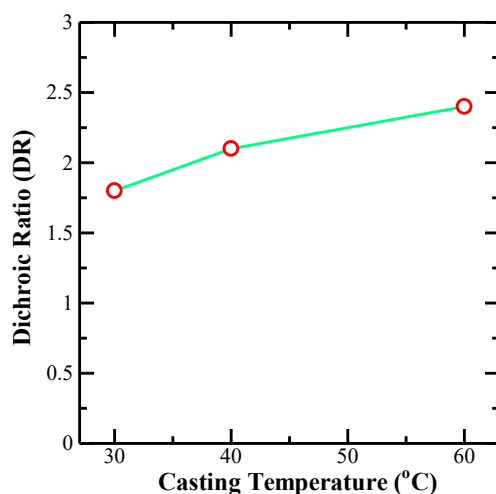


**Figure: 3.3** Effect of casting temperature on dichroic ratio.

### 3.3.2.2 Polymer Concentration

In dynamic FTM, polymer concentration play important role for controlling the film orientation. An optimized concentration is required to achieve the maximum orientation in any polymer by dynamic FTM. For this investigation we have prepared the 0.5%, 1% and 2% concentration of polymer solution and find out that when the polymer concentration is high, the solvent evaporation and the polymer solidification are too rapid hindering the polymers to expand and to generate a uniform floating-film on the liquid-substrate. On the other hand, in the case at very low concentration, dropped solution parts easily spread on the whole of the liquid surface before its solidification. For this investigation polarized absorption was taken of different concentration and observed the affect in spectral feature and orientation intensity. A red shifted absorption maximum

( $\lambda_{\max}$ ) along with clear vibronic shoulders can be seen when the concentration of NR-P3HT solution was increased from 0.5 to 1% (w/w) suggesting the increase in the effective  $\pi$ -conjugation length of the polymer main chains. Further increase in the concentration up to 2% (w/w) leads to not only the blue-shifted of  $\lambda_{\max}$  but relatively less-defined vibronic shoulder also. These findings clearly show that the solution concentration is an important factor for the orientation of main chain for dynamic-FTM. The orientation intensity in terms of DR at several different concentrations is shown in the Figure 3.4. The figure clarifies that increase in the solution concentration from 0.5 to 1% (w/w) promotes the orientation then turned to decrease in the orientation with further increase in the concentration of the polymer solution. These results suggest the mechanism to cause the orientation in dynamic-FTM.

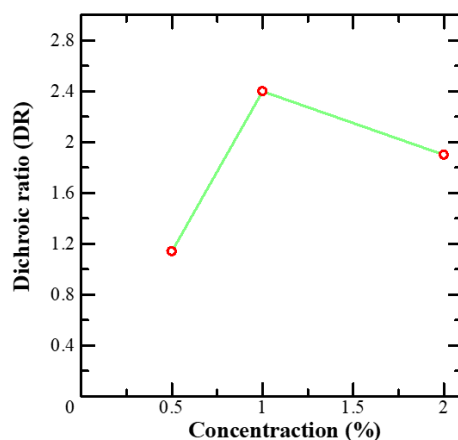


**Figure: 3.4** Effect of polymer concentration on dichroic ratio.

Figure 3.5 shows the location dependence of DR as well as the absorbance at the  $\lambda_{\max}$ . Absorbance at  $\lambda_{\max}$  at difference location of the ribbon-shaped FTM was also measured in order to investigate variation in thickness of the films at different locations of the casted films. It is important to note that thin films casted towards the slider end in the Ribbon-shaped FTM up to >

10 cm exhibit nearly no change in the measured DR values. This indicates that the Ribbon-shaped casting method provides relatively uniform orientation especially towards the slider side. The film thickness tends to be thinner as a function of increasing distance of the casted film from slider side to opposite end. These location dependences were also observed even after changing the concentration of the polymer solution. Such information about the distribution of large-scale orientation is highly desired for the in-depth discussion about the orientation mechanism. In this context, Ribbon-shaped thin film casting procedure proposed here provides the considerable knowledge of orientation characteristics by dynamic-FTM. It is interesting to note that there is appreciable enhancement in the observed DR at the far area in the Ribbon-shaped floating-film. This could be explained considering the fact that at the initial stage of solidification of floating film due fast solvent evaporation and dragging viscous force from the liquid substrate, there is induction of molecular orientation, which continues further with the advancing floating film.

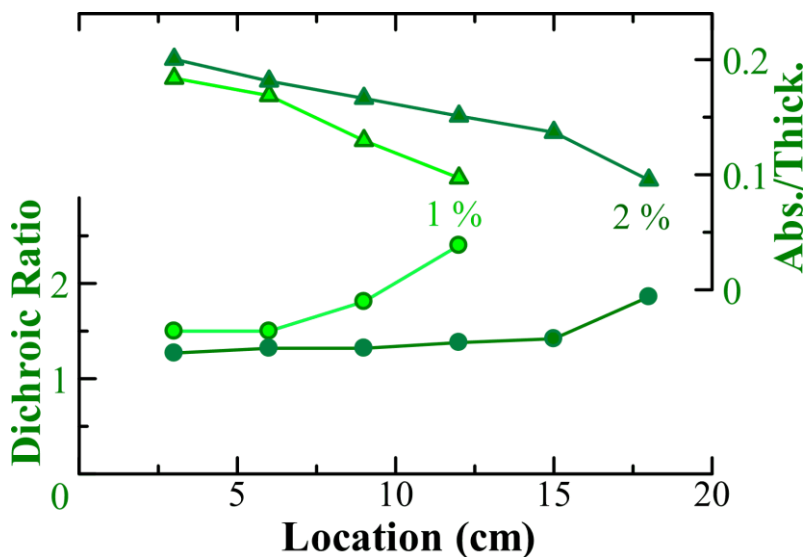


**Figure: 3.5** Location dependence of DR as well as the absorbance at the  $\lambda_{\max}$ .

### 3.3.2.3 Liquid Substrate Viscosity

In dynamic FTM, viscosity of liquid substrate also play one of the important role to controlling the molecular orientation. It acts as a dragging force in opposite direction during the propagation of polymer solution, thereby affecting the self-organization of polymer leading to the orientation. The liquid substrate viscosity can be change by mixing the two different liquid having different viscosities. In this study, different varieties of liquids such as pure water, ethylene glycol (EG) and glycerol (GL) used as a base liquid having viscosity 0.79, 14.41 and 487.64 centistoke respectively. By mixing this base liquid we can make the optimized binary liquid for control of viscosities. It has been clearly observed that increasing the viscosity affect the propagation of the FTM film on liquid substrate. In case of very low viscosity in case of 100% pure water the polymer solution spreading all over the area of liquid substrate and decrease while increasing the viscosity. These findings suggest that a dragging force hindering the FTM films to a confined area.

Figure 3.6 depicts the liquid substrate viscosity dependence of observed DR in the Ribbon-shaped floating-film where the viscosity was controlled by mixing the two miscible hydrophilic solvents of varying viscosities. All of the DR plotted here are taken at the farthest position giving the best orientation. Although DR is small as mentioned above, the orientation characteristics are quite the same of the floating-films obtained by the conventional dynamic-FTM as reported previously. [14]. This fact also indicates that even by changing floating film fabrication method as mentioned above with Fig.2, the essential orientation characteristics remain well conserved. This is also very important to note that the Ribbon-shaped dynamic-FTM is useful for investigating the mechanism with various casting factors aiming towards the attainment of high molecular orientation. The proposed Ribbon-shaped dynamic-FTM is utilized for researching the orientation mechanism in dynamic-FTM and for optimizing the orientation condition towards the practical use.

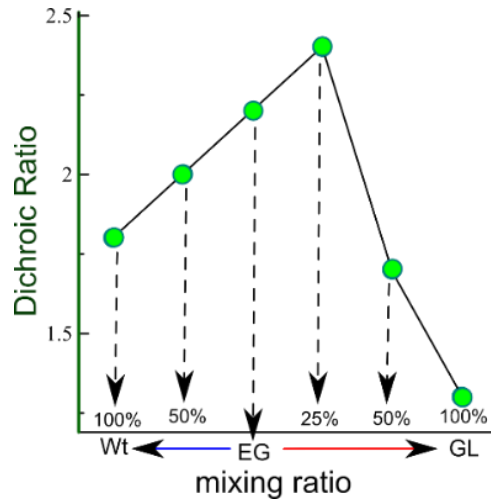


**Figure: 3.6** DR dependence on the binary mixture of water, EG or GL as casting liquid substrate.

### 3.4 Conclusion

We have developed a modified dynamic-FTM by changing the shape of conventional FTM circular to rectangular shape and obtain the Ribbon-shaped floating-films. The resulting floating-films were confirmed to be oriented to perpendicular against the propagation direction. The orientation intensity given by the dichroic ratio (DR) was 2.4, which was relatively small as compared to the conventional dynamic-FTM. DR dependences on the distance from the dropping point, solution concentration and liquid-substrate were investigated as a preliminary investigation. These results exhibit almost the same characteristics as compared that observed in conventional dynamic FTM. The developed casting way can be utilized for investigating the orientation mechanism as well as for the optimizing the casting condition in dynamic-FTM.



### 3.4 References

- [1] K.E. Strawhecker, S.K. Kumar, J.F. Douglas, A. Karim, The critical role of solvent evaporation on the roughness of spin-cast polymer films [1], *Macromolecules*. 34 (2001) 4669–4672. doi:10.1021/ma001440d.
- [2] S. Nagamatsu, W. Takashima, K. Kaneto, Y. Yoshida, N. Tanigaki, K. Yase, K. Omote, Backbone arrangement in “friction-transferred” regioregular poly(3-alkylthiophene)s, *Macromolecules*. 36 (2003) 5252–5257. doi:10.1021/ma025887t.
- [3] L. Hartmann, K. Tremel, S. Uttiya, E. Crossland, S. Ludwigs, N. Kayunkid, C. Vergnat, M. Brinkmann, 2D versus 3D crystalline order in thin films of regioregular poly(3-hexylthiophene) oriented by mechanical rubbing and epitaxy, *Adv. Funct. Mater.* 21 (2011) 4047–4057. doi:10.1002/adfm.201101139.
- [4] N. Yamasaki, Y. Miyake, H. Yoshida, A. Fujii, M. Ozaki, Solution flow assisted fabrication method of oriented  $\pi$ -conjugated polymer films by using geometrically-asymmetric sandwich structures, *Jpn. J. Appl. Phys.* 50 (2011). doi:10.1143/JJAP.50.020205.
- [5] T. Higashi, N. Yamasaki, H. Utsumi, H. Yoshida, A. Fujii, M. Ozaki, Anisotropic properties of aligned  $\pi$ -conjugated polymer films fabricated by capillary action and their post-annealing effects, *Appl. Phys. Express*. 4 (2011) 3–6. doi:10.1143/APEX.4.091602.
- [6] G. Giri, D.M. DeLongchamp, J. Reinspach, D.A. Fischer, L.J. Richter, J. Xu, S. Benight, A. Ayzner, M. He, L. Fang, G. Xue, M.F. Toney, Z. Bao, Effect of solution shearing method on packing and disorder of organic semiconductor polymers, *Chem. Mater.* 27 (2015) 2350–2359. doi:10.1021/cm503780u.
- [7] M. Karakawa, M. Chikamatsu, Y. Yoshida, M. Oishi, R. Azumi, K. Yase, High-performance poly(3-hexylthiophene) field-effect transistors fabricated by a slide-coating method, *Appl. Phys. Express*. 1 (2008) 0618021–0618023. doi:10.1143/APEX.1.061802.
- [8] B. O’Connor, R.J. Kline, B.R. Conrad, L.J. Richter, D. Gundlach, M.F. Toney, D.M. DeLongchamp, Anisotropic structure and charge transport in highly strain-aligned regioregular poly(3-hexylthiophene), *Adv. Funct. Mater.* 21 (2011) 3697–3705. doi:10.1002/adfm.201100904.
- [9] T. Morita, V. Singh, S. Nagamatsu, S. Oku, W. Takashima, K. Kaneto, Enhancement of transport characteristics in poly(3-hexylthiophene) films deposited with floating film transfer method, *Appl. Phys. Express*. 2 (2009) 1–4. doi:10.1143/APEX.2.111502.
- [10] T. Morita, V. Singh, S. Oku, S. Nagamatsu, W. Takashima, S. Hayase, K. Kaneto, Ambipolar transport in bilayer organic field-effect transistor based on poly(3-hexylthiophene) and fullerene derivatives, *Jpn. J. Appl. Phys.* 49 (2010) 0416011–0416015. doi:10.1143/JJAP.49.041601.
- [11] J. Noh, S. Jeong, J.Y. Lee, Ultrafast formation of air-processable and high-quality polymer films on an aqueous substrate, *Nat. Commun.* 7 (2016) 1–9. doi:10.1038/ncomms12374.

- [12] M. Pandey, S. Nagamatsu, S.S. Pandey, S. Hayase, W. Takashima, Enhancement of carrier mobility along with anisotropic transport in non-regiocontrolled poly (3-hexylthiophene) films processed by floating film transfer method, *Org. Electron. Physics, Mater. Appl.* 38 (2016) 115–120. doi:10.1016/j.orgel.2016.08.003.
- [13] A. Dauendorffer, S. Miyajima, S. Nagamatsu, W. Takashima, S. Hayase, K. Kaneto, One-step deposition of self-oriented  $\beta$ -phase polyfluorene thin films for polarized polymer light-emitting diodes, *Appl. Phys. Express.* 5 (2012). doi:10.1143/APEX.5.092101.
- [14] M. Pandey, S.S. Pandey, S. Nagamatsu, S. Hayase, W. Takashima, Controlling Factors for Orientation of Conjugated Polymer Films in Dynamic Floating-Film Transfer Method, *J. Nanosci. Nanotechnol.* 17 (2017) 1915–1922. doi:doi:10.1166/jnn.2017.12816.
- [15] M. Pandey, S. Nagamatsu, S.S. Pandey, S. Hayase, W. Takashima, Orientation Characteristics of Non-regiocontrolled Poly (3-hexyl-thiophene) Film by FTM on Various Liquid Substrates, *J. Phys. Conf. Ser.* 704 (2016). doi:10.1088/1742-6596/704/1/012005.
- [16] M. Pandey, S.S. Pandey, S. Nagamatsu, S. Hayase, W. Takashima, Influence of backbone structure on orientation of conjugated polymers in the dynamic casting of thin floating-films, *Thin Solid Films.* 619 (2016) 125–130. doi:10.1016/j.tsf.2016.11.015.

## ***Chapter 4: Charge transport in poly (dodecylquaterthiophene): Implication of optical anisotropy and molecular weight***

### **4.1 Introduction**

Advent of solution processable conjugated polymers (CP) have drawn a good deal of attentions of materials science community since about last three decades owing to their application potentials in the area of low cost disposable and flexible electronic devices such as organic field effect transistors (OFETs), light emitting diodes and solar cells.[1] Interests in CPs was geared considering their features like mechanical flexibility, self-assembly and tuning of their electronic functionality. Inherent one-dimensionality and extended  $\pi$ -conjugation of CPs renders them highly susceptible for molecular self-assembly in condensed state. Unidirectional alignment CP macromolecules are highly desired for the facile in-plane charge transport along the orientation direction leading to the fabrication of high performance OFETs. Now days OFETs are more studied research for the development of electronics consisting of amplifying and switching action.[2] For the commercialization of OFET based electronics devices high performance OFETs are required by controlling the several types of issue such as enhancement in field effect mobility,[3] operation stability,[4] passivation method[5,6] and high- performance reproducibility[7,8]. As reported by the some groups, OFETs performance were optimized based on fabrication conditions [9–11]. Some literature study was also reported that OFETs mobility dependence on average chain length of polymer. The mobility was enhanced in order to increasing molecular weight reported for P3HT and other thiophene based polymer [9,11–13]. Apart from these , CPs stringently depends on their film morphology leading to the proposal of various film fabrication techniques although spin coating has been most widely utilized [14–16]. A number of methods have been proposed to orient CPs, however, most of them either uses shear forces offering

preferred face-on orientation. At the same time existing possibility of physicochemical damages to the underlying soft polymeric layers also cannot be ruled out [17,18]. However, direct deposition of thin films via slow solvent evaporation from the polymer solution inherently results in to the thermodynamically favored edge-on orientation of CP macromolecules, which is highly favorable for planer devices like OFETs [19,20].

In this chapter, we have reported a facile and cost control strategy for fabricating the oriented thin films of CPs on the viscous hydrophilic liquid substrates and named as floating film transfer method (FTM [15,20]. In this method, solid film formation takes place by simultaneous rapid spreading and compression of film by dragging force offered through viscous liquid substrate in opposite direction [14,20]. Interestingly, highly oriented thin floating films at very large scale up to several centimeters (15-20 cm) with a small variation in the film thickness as well as orientation intensity. Apart from this we also show the importance of molecular weight and PDI in the fabrication of orientated thin film and as well as in OFET. Importantly, in this discussion it demonstrate that the effect of molecular weight and PDI on orientation are a function of mobility.

## **4.2 Experimental Work**

### **Materials and Optimization**

In this work poly(3,3'-didodecyl quaterthiophene)(PQT) was synthesized as per our previous publication and used as representative CP in the present work[21]. On the other hand, PQT-C12 are also synthesis by changing the synthesis parameter and achieved the four PQT-C12 extract of varied molecular weight and PDI. Dehydrated chloroform was purchased from sigma Aldrich as a solvent. Polymer solution was prepared 2% and 0.5% w/w for making the solid film prepared by ribbon shaped FTM and spin coating respectively. For making the solid film by FTM we drop a

15-20  $\mu\text{l}$  of polymer solution in center of the assisting slider which placed in one edge of partly filled rectangular tray. On the other hand spin coating film was also prepared by the condition of 3000 rpm spinning speed and 5 s acceleration for the duration of 120 sec. Film thickness was measured by interference microscopy (Nikon Eclipse LV150). Optical characterization was done by using polarized UV visible absorption spectrophotometer (JASCO V 570) equipped with Glan-Thompson Prism.

Bottom gate top contact OFETs were fabricated for investigation of electrical characterization. For making the OFETs, highly doped Si substrate was used with 300 nm grown  $\text{SiO}_2$  layer. Before transfer the FTM film surface treatment was done by introducing addition self-assembled monolayer on  $\text{SiO}_2$  surface. In this treatment substrate was dip in 2 mM solution of octadecyltrichlorosilane (OTS) in dehydrated toluene and heated  $90^\circ\text{C}$  for 2 hours followed by annealing at  $130^\circ\text{C}$  for 30 mins. The estimated dielectric capacitance was about to  $C_i = 10 \text{ nF/cm}^2$ . FTM film was transferred on OTS treated  $\text{SiO}_2$  layer by stamping. 50 nm electrode (source and drain) was deposited by thermal evaporation on base pressure  $10^{-6}$  torr by using nickel shadow mask having the channel length  $20\mu\text{m}$  and width 2mm. Electrical characterization was done by computer controlled 2 channel source meter unit (Keithley-2612) in vacuum at  $10^{-3}$  torr pressure .

A custom-made slider consisted of polytetrafluoroethylene was designed and used to provide directionality while film spreading. Slider was dipped in a rectangular tray (22 cm x 15.5 cm) in such a manner that half of its slope should be immersed in viscous liquid substrate (Fig.1) acting as liquid substrate. Viscosity of the liquid substrate plays a dominant role and decides not only the thickness but also the molecular orientation which was optimized by taking the different viscous liquid substarte. We have used mixture of ethylene glycol (EG) and Glycerol (GL) in the ratio of 3:1 as optimized viscous liquid substrate and 25  $\mu\text{l}$  of the polymer solution was dropped in the

center of the slider. This dropped polymer solution rapidly spreads and expands in the form of a ribbon up to 15-20 cm from the drop point. However, unlikely to our standard FTM reported previously, spreading in this case took place only in one direction due to the tilted bottom wall of the slider as illustrated schematically in the Fig.1. Orientation was qualitatively verified by naked eye using a polarizer film followed by its transfer on the glass slides (1.1 cm × 2.5 cm) by stamping for quantitative analysis. Spin-coated films were also prepared from the 0.5 % (w/w) PQT solution in chloroform by spin coating at 3000 rpm for 120 s for comparison. PQT coated glass substrates were annealed at 60°C for 5 min in order to ensure the complete evaporation of any remaining solvent. Polarized electronic absorption spectra were measured with UV-visible-NIR spectrophotometer (JASCO V-570) equipped with Glan Thomson prism. In order to quantify the molecular orientation and optical anisotropy in the FTM processed films, optical dichroic ratio (DR) was also estimated from the polarized optical absorption spectrum. Optical DR was defined as  $DR = A_{\parallel}/A_{\perp}$ , where  $A_{\parallel}$  and  $A_{\perp}$  are absorption maximum ( $\lambda_{\max}$ ) of the film along the  $\parallel$  and  $\perp$  direction of the orientation, respectively [20].

## 4.3 Results and Discussion

### 4.3.1 Molecular Orientation

Fig 4.1 (a) show the polarized electronic absorption spectra of the oriented ribbon shaped FTM as well as spin-coated thin films of PQT for the comparison. Spin-coated PQT film spectra show the featureless absorption spectrum with ill-defined vibronic modes as compared to that of oriented films fabricated by FTM. In parallel oriented PQT thin films exhibit clear peaks at  $\lambda_{\max}$  around 537 nm and 580 nm along with vibronic shoulder at 505 nm. These vibronic peak around 580 nm indicates the formation of higher structural ordering in the condensed state and enhanced  $\pi$ - $\pi$

lamella stacking [21]. The absorption spectra of oriented thin film shown in Fig. 4.1(a) that shows 22 dichroic ratio, which is one of the highest optical anisotropy reported for the oriented PQT films. Interestingly, Pandey et al have also worked on orientation in the PQT films by using our conventional FTM and found the low DR along with less pronounced vibronic features [21]. These prominent resolution of the 0-0 vibronic transition at 580 nm indicates the higher planarization of polymeric chains and enhanced molecular ordering due to higher unidirectional orientation [22].

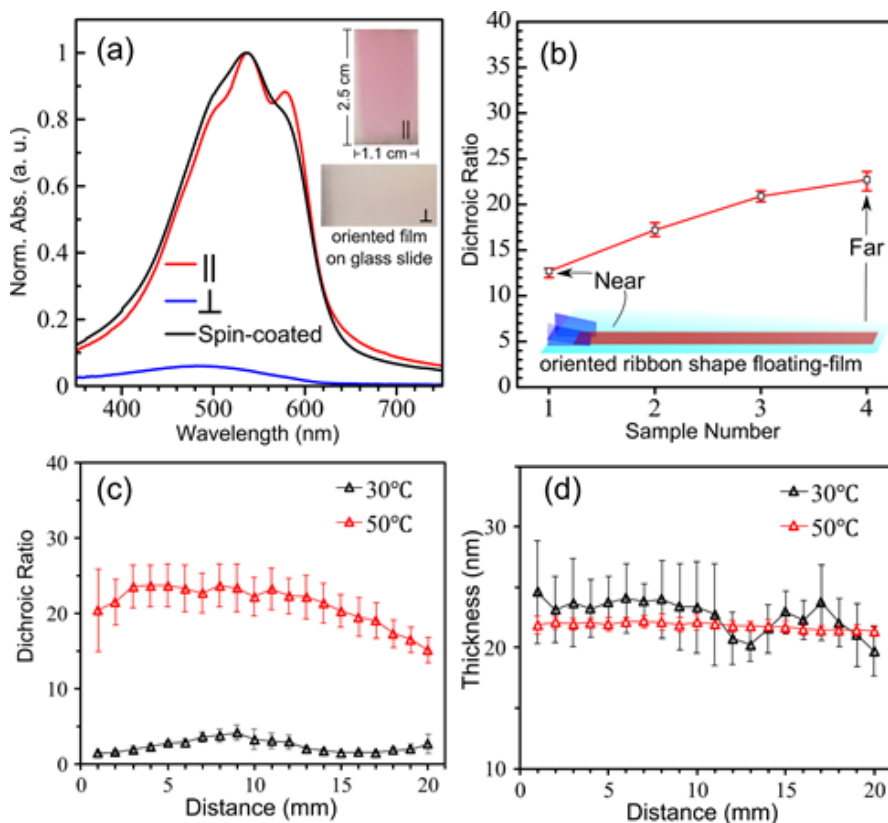


**Figure: 4.1** (a) Polarized electronic absorption spectra of oriented film and (b) Variation of DR from near to far with samples taken at equidistant interval in a 15 cm long ribbon shaped oriented film. (c) Variation in DR and (d) film thickness of the oriented film casted on glass substrate with area of  $2 \times 2 \text{ cm}^2$ . Inset in (a) is the photograph of the oriented film transferred on glass slide with  $\parallel$  and  $\perp$  orientations. The dark color shows parallel ( $\parallel$ ) and almost colorless shows perpendicular ( $\perp$ ) when angle of the polarizer was rotated from  $00^\circ$  to  $90^\circ$ .

The oriented films with  $\perp$  absorption spectra show featureless  $\lambda_{\max}$  at 489 nm like as in solution which, clearly indicates the polymer chain are randomly distributed [20,23]. Since in FTM films molecular orientation results from synergistic interaction between the solvent evaporation and viscous dragging force of liquid substrate, it is obvious to have some variation in the calculated DR of oriented film at large scale shown in the Fig. 4.1(b). A perusal of this figure corroborates that calculated DR at the far end of film is relatively higher as compared to that at the near end of film from the solution dropping point. It is attributed to the fact that the progressing film towards the far end has to pass through the additional viscous dragging force posed by the viscous liquid substrate prior to film solidification. The thin film homogeneity in terms of their thickness and molecular orientation plays the important role for controlling the device performance. Thickness have been measured by Interference microscopy (Nikon Eclipse LV150). Fig. 4.1(c) and (d) shows the variation in DR and thickness at intervals of 1 mm in the oriented film with point source photonic analyzer connected with the computer controlled mobile stage for holding the PQT coated glass substrate. It can be seen that the thickness of oriented films fabricated at optimized casting temperature at 50°C is rather uniform (variation  $\pm 1$  nm) as compared to that non optimized condition at 30°C showing relatively large thickness non-homogeneity (variation  $\pm 6$ ) in the latter case. Relatively inhomogeneous films fabricated at lower temperature could be associated with the slow solvent evaporation and non-homogeneous film expansion.

In this work four categories of PQT-C12 Extract having different molecular weight and PDI were also used for the investigation. Figure 4.2 shown the polarized absorption spectra of four categories of PQT-C12 having different molecular weight and PDI, where found the red shift in parallel FTM as compared to spin coated. All the selected of PQT-C12 extract spectral features such as maximum absorption spectra in parallel/perpendicular, vibronic shoulder and optical anisotropy in terms of



DR summarized in table 1. Amongst all, PQT-C12 extract having highest molecular weight and PDI exhibit maximum absorption spectra in  $\parallel$  FTM at 546 nm which is 8nm red shifted with clear vibronic shoulder exhibit at 586nm as compared to spin coated film. On the other hand in case of lowest molecular weight and PDI show the maximum absorption spectra in  $\parallel$  FTM at 544 nm which is 6nm red shifted as compared to spin coated film along with clear vibronic shoulder at 584nm. In middle, two of PQT-C12 extract in which one show maximum absorption spectra in  $\parallel$  FTM at 550nm which is 10 nm red shifted as compared to spin coating along with clear vibronic shoulder at 588nm and in second one of remaining PQT-C12 extract show the maximum absorption spectra in parallel FTM at 538 nm which is red shifted 22 nm as compared to spin coated film along with vibronic shoulder at 582 nm. Such type of spectral features such as red shift and existence of vibronic shoulder indicate the structural ordering in the condensed state and improve the  $\pi$ - $\pi$  stacking [15].

Absorption spectra shown in figure 4.2 (a) clear indicate the spectral difference according to molecular weight and PDI. These resultant show the importance of Molecular weight and PDI as a function of changing the spectral features such as variation in absorption peak as well as vibronic shoulder. Apart from this spectral features, also play important role for the changing the orientation characteristics. As per reported by Pingle at al. molecular weight and PDI dependence spectral features by selecting three PQT C-12 extract such as high ( $M_w=26500$  g/mol,  $PDI=1.66$ ) medium ( $M_w= 7000-9000$  g/mol,  $PDI=1.17-1.29$ ) and low ( $M_w= 1700$  g/mol,  $PDI=1.03$ ) molecular weight and compared to it with similar three group of P3HT counterpart [22]. According to him, high and medium molecular weight of absorption spectral features of PQT-C12 extract almost resemble each other and the spectral feature started to degrade such as blue shift and featureless absorption spectra when going from higher to lower molecular weight in both of case. For P3HT such degrade

was described in terms of smaller crystallinity in medium molecular weight means a large no of chain are contained in disorder area and exhibit less plagiarized backbone conformation [11,24] In low molecular weight of PQT-C12 there is a reverse trend such as narrow well absorption spectra and small red shift as compared to medium molecular weight and further degrade in P3HT. Its features can be interpreted in terms of prevalence of planarized chain conformation and high solid-state order [25,26]. Although in my case I selected four PQT-C12 extract having different molecular weight and PDI noted in table1. The resultant show the importance of both is equally, when we increase the molecular weight and PDI from first type to second the spectral features and vibronic transition was featureless but increasing the molecular weight in third group enhance the spectral feature. Further increase in molecular weight again slightly decrease the spectral feature as compared to third. It might be the main reason the value of the PDI. Although it was increased after increasing the molecular weight, which was clearly reflected from the table1 and Pingal at al. resultant [22]. According to me and other groups resultant clearly reported optimization of PDI is so difficult during the polymerization. Apart from spectral feature the orientation was also increase after increasing the molecular weight from first to third and further start to degrade in case of next type. The orientation was expressed in terms of DR and its average quantitative values from first to third be 4.5, 4.9, 8.7 and 6.8 in case of four. Figure 4.2 (b) show one of the typical absorption spectra of third group PQT-C12 extract in parallel and in perpendicular which is one of the highest value among four. Figure 4.2 (c) and (d) show the molecular weight and PDI dependence dichroic ratio measured by the polarized absorption spectroscopy. For the reproducibility we prepared 6 sample for each type of PQT-C12 extract and taking the average DR. These resultant show importance of molecular weight and PDI limitation for optimizing the orientation. In my case the one of the optimized PQT-C12 have 42500 molecular weight and 2.1 PDI and achieved the one of

highest DR > 10 and average DR= 8.7. The main reason to achieve this highest DR due to possibility of combination of high molecular weight and average low value of PDI.

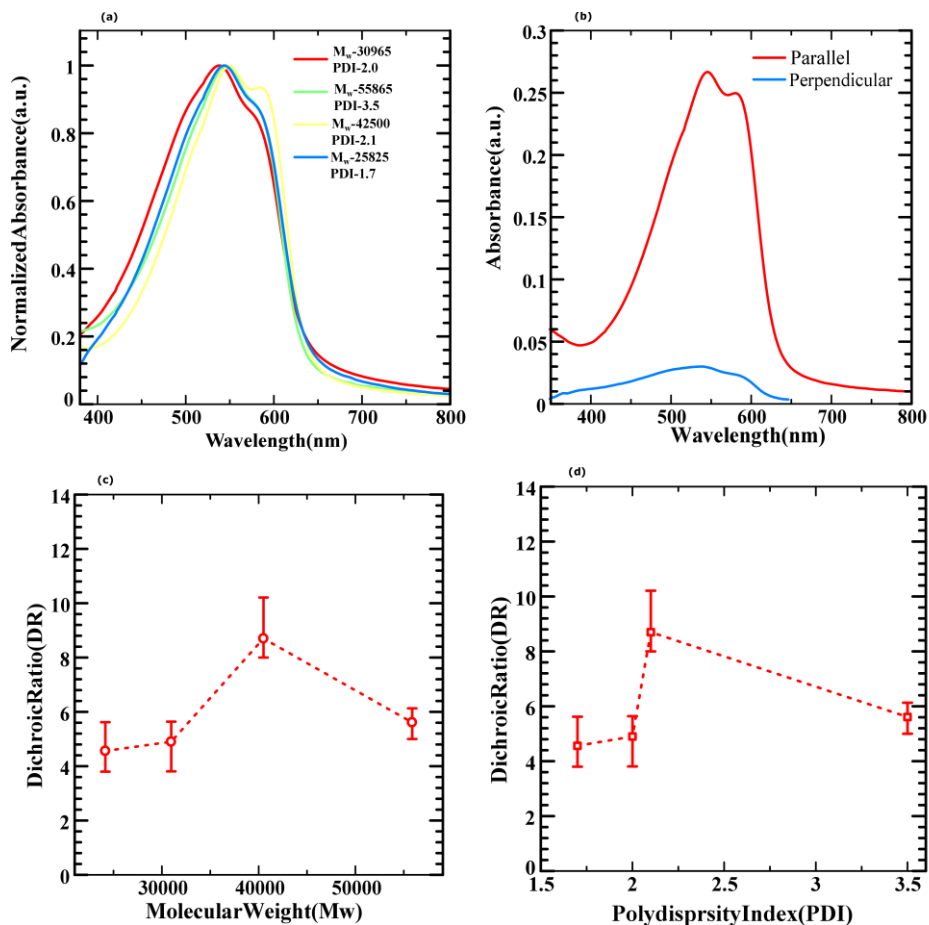


**Figure: 4.2** Polarized Electronic absorption spectra of PQT-C12 prepared by ribbon- shaped FTM of different molecular weight and PDI in Parallel (a) typical absorption spectra in parallel and perpendicular having highest DR>10 for molecular weight 42500 g/mol and PDI=2.1 (b) Molecular weight dependence DR (c) PDI dependence DR(d).

Tabel-1 Optical parameters for spin coated and ribbon shaped FTM films from the solid-state electronic absorption spectra.

Polymer PQT C-12		Film Condition	Absorption Max (nm)	Dichroic Ratio (DR)	Vibronic Shoulder (nm)
Mw	PDI				
25825	1.7	Spin coat	528	4.56	586
		Parallel FTM	544		586
		Perpendicular FTM	524		590
30965	2.0	Spin coat	516	4.9	578
		Parallel FTM	538		582
		Perpendicular FTM	496		582
42500	2.1	Spin coat	540	8.7	586
		Parallel FTM	550		588
		Perpendicular FTM	538		592
55865	3.5	Spin coat	538	6.13	590
		Parallel FTM	546		586
		Perpendicular FTM	532		590

#### 4.3.2 Probing Orientation by XRD

The in-plane GIXD measurements were also taken in order to analyze the conformation of the backbones in the FTM processed films, which is shown in the Figure 4.3 The measurements were taken by casting the oriented films on the bare silicon wafers following the measurement geometry (inset of Fig. 4.3 (a)) [18]. It can be seen that all of the diffraction peaks related to lamellar alkyl-stacking are absent and only 010 peak associated with  $\pi$ - $\pi$  staking was appeared at  $21^\circ$  in the as-cast film when the incident X-ray was  $\parallel$  ( $\chi = 90^\circ$ ) to the orientation direction [27,28]. Interestingly,

same peak at  $21^\circ$  completely disappears when the incident X-ray was  $\perp$  ( $\chi = 00^\circ$ ) to the orientation direction. These results implies that the polymers are uni-directionally oriented with conjugation as well  $\pi$ - $\pi$  stacking axis are in plane of the substrate (edge-on orientation).

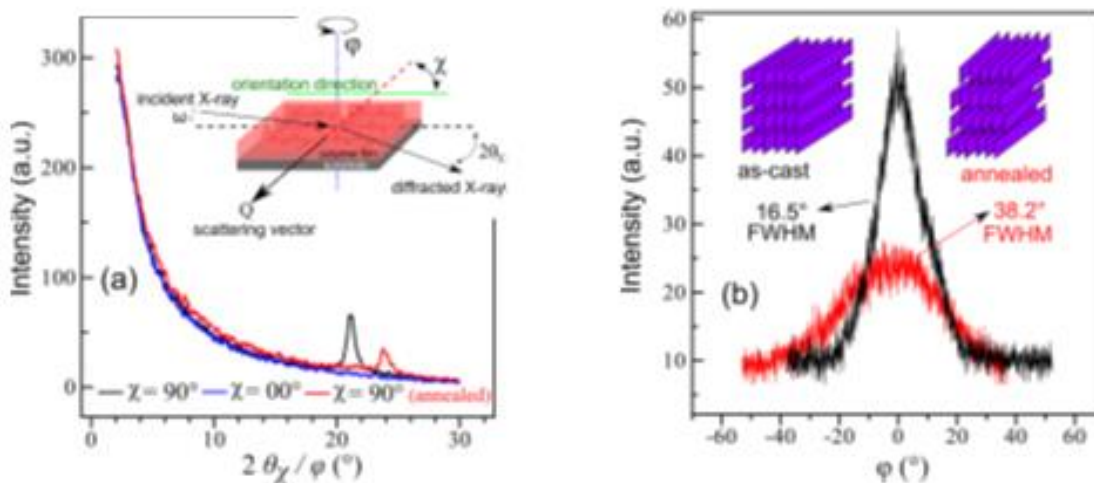


**Figure : 4.3** (a) In-plane GIXD of oriented PQT film before and after thermal annealing, (b)  $\phi$  scan of 010 peak of as-cast and annealed oriented film. GIXD along  $\chi = 00^\circ$  and  $\chi = 90^\circ$  represents the diffraction pattern along the perpendicular and parallel to the orientation direction, respectively. The inset in (a) represents the experimental geometry for in-plane GIXD set-up and inset in (b) is schematic view of orientation pattern in edge-on oriented film before and after annealing.

### 4.3.3 Electrical Characterizations

This is crucial for devices like OFETs where charge transport take place at the interface of the insulator/semiconductor and presence on any alkyl sidechains in the channel direction acts as resistive barriers for hopping of the charge carriers [29]. It has been reported that PQT possesses liquid crystalline (LC) behavior whose alkyl side-chains melts around  $130^\circ\text{C}$  [30]. In our case, when as cast and highly oriented film was annealed at LC phase transition temperature for 5 min, 010 peak shifted at  $24^\circ$  representing more dense packing in the films. Since there was no

remarkable change in the extent of orientation after annealing, therefore, this could have originated from the disturbance in the polymer stacking. In order to probe this,  $\phi$ -scan were also performed on 010 peak of as-cast and annealed films as shown in Fig. 4.3 (b). The  $\phi$ -scan yielded a full width at half maximum (FWHM) of  $16.5^\circ$  in the as-cast film which increased drastically to  $38.2^\circ$  for annealed films. This clearly indicates that although the  $\pi$ - $\pi$  stacking goes under more dense state once annealed but there was a disturbance in the molecular arrangement during  $\pi$ - $\pi$  stacking. It is also worth to note here that these value of FWHM are very close to oriented poly(3-hexylthiophene) prepared by mechanical rubbing and friction transferred techniques, however, those methods yielded face-on orientation with alkyl chains lying in-plane to the substrate.[18,31]

OFETs were fabricated by stamping the oriented PQT films on the CYTOP coated  $\text{SiO}_2 / \text{Si(p++)}$  substrates having the capacitance of  $8 \text{ nF/cm}^2$  in the bottom gate and to contact device configuration as shown in Fig. 4.4 (a). Gold electrodes (50 nm) were deposited for source and drain terminals using thermal evaporation at  $10^{-6}$  Torr on the top of PQT film with nickel shadow mask having channel length ( $L = 20 \text{ }\mu\text{m}$ ) and width ( $W = 2 \text{ mm}$ ). Electrical characterization was made under dark with computer controlled two-channel electrometer (keithley-2612) at  $10^{-3}$  Torr. All of the electronic parameters for OFETs were extracted as per our earlier publication and field effect mobility ( $\mu$ ) was extracted in the saturation regime of the transfer curves using Eq.

$$I_{\text{DS}} = \frac{W}{2L} \mu C_i (V_{\text{GS}} - V_{\text{TH}})^2$$

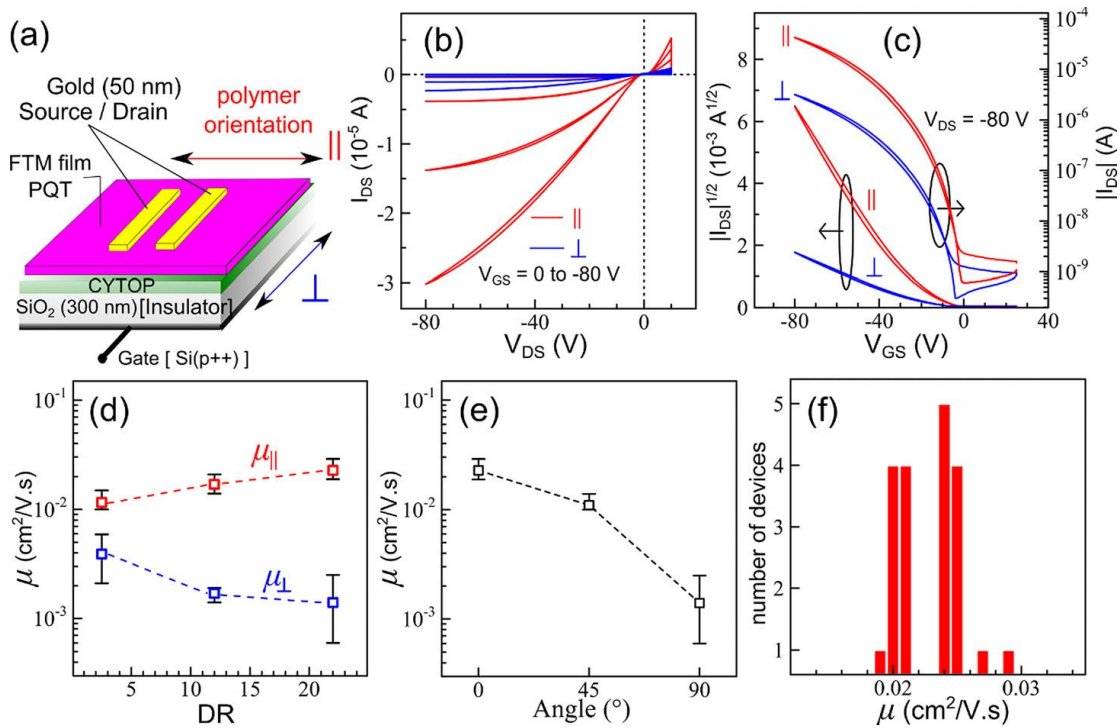


**Figure: 4.4** Device architecture of the OFETs (a), their output (b) and transfer curves (c) using oriented PQT film having the DR of 22. Variation in  $\mu$  for the OFETs using oriented PQT of variable DR (d) where,  $\mu_{\parallel}$  and  $\mu_{\perp}$  represent the  $\mu$  along the  $\parallel$  and  $\perp$  direction, respectively. PQT film with low DR ( $\sim 2$ ) was casted at  $30^{\circ}\text{C}$  while that with intermediate DR ( $\sim 12$ ) was casted at the proximal end of the oriented ribbon shaped film prepared at  $50^{\circ}\text{C}$ . (e) Angle dependence mobility at  $0^{\circ}$ ,  $45^{\circ}$  and  $90^{\circ}$  (f) Statistical analysis of FET performance showing large scale homogeneous film.

Charge transport was evaluated for PQT in both of the orientation directions viz. with channel  $\parallel$  to the orientation direction as well as channel  $\perp$  to orientation direction (Fig. 4.4(a)). Parallel and perpendicular OFETs were fabricated on the same substrates and in similar device configurations in order to pinpoint the implication of molecular orientation only and avoiding the substrate dependent deviations. Fig. 4.4 (b) shows the typical  $I$ - $V$  characteristics with a clear p-type behavior, where higher output currents were observed when channel was  $\parallel$  as compared to devices when channel was  $\perp$  with respect to the orientation direction of the polymer backbone. There was about an order of magnitude higher output current for devices as compared to  $\perp$  one at a fixed gate

bias. Figure 4.4 (c) shows the transfer characteristic of the same OFETs (DR = 22) with average (maximum) 0.026 (0.029)  $\text{cm}^2/\text{Vs}$  and 0.0025 (0.0013)  $\text{cm}^2/\text{Vs}$  along the  $\parallel$  and  $\perp$  directions, respectively. Although mobility have been achieved lower as reported by other group [27,32,33] because of various factor to improve the mobility in which some of the factors like polymer synthesis techniques, molecular weight, fabrication technique, surface treatment and post treatment. It might be the possibility of lower mobility due to the lower molecular weight ( $M_w=10000$  g/M) as compared to other group with high molecular weight ( $M_w=22900$  g/Mole).

These molecular weight dependence mobility also support by this article [22]. All of the OFETs using  $\parallel$  oriented PQT films exhibited nearly similar on/off ratio typically in the order of  $10^5$ . On the other hand, relatively lower on current and nearly similar off current for OFETs fabricated with perpendicularly oriented PQT films led to one order of magnitude lower ( $10^4$ ) ON/OFF ratio. Possibility of fabrication of PQT films with variable optical anisotropies by controlling the film casting conditions under ribbon-shaped FTM encouraged us to explore the implication of extent of molecular orientation on the anisotropic charge transport. To accomplish this, OFETs were fabricated using oriented PQT films with varying optical anisotropy and DR dependent field effect mobility for parallel and perpendicular oriented PQT films ( $\mu_{\parallel}$  and  $\mu_{\perp}$ ) are shown in the Figure 4.4 (d). It can be clearly seen that mobility anisotropy ( $\mu_{\parallel} / \mu_{\perp}$ ) increases with the increasing DR, which clearly indicates that the significance of increasing the molecular orientation on the charge transport. Beniek et al have reported that nature of the molecular orientation and extent of their distribution (edge-on/face-on) in CPs play dominant role in controlling the charge carrier transport anisotropy ( $\mu_{\parallel} / \mu_{\perp}$ )[31]. Therefore, almost one order of magnitude change in  $\mu_{\parallel} / \mu_{\perp}$  for PQT films in spite of having relatively small DR is in well agreement with the GIXD results, where a well-stacked edge-on conformation was clearly evidenced. Angular dependence mobility have been



measured to investigate the anisotropy based transport phenomenon shown in figure 4.4 (e), Where mobility was decreased after increase the angle in orientation direction. To investigate the homogeneous large scale oriented films quality, we have been fabricated many OFETs and its performance statistical analysis demonstrated in figure 4.4(f).

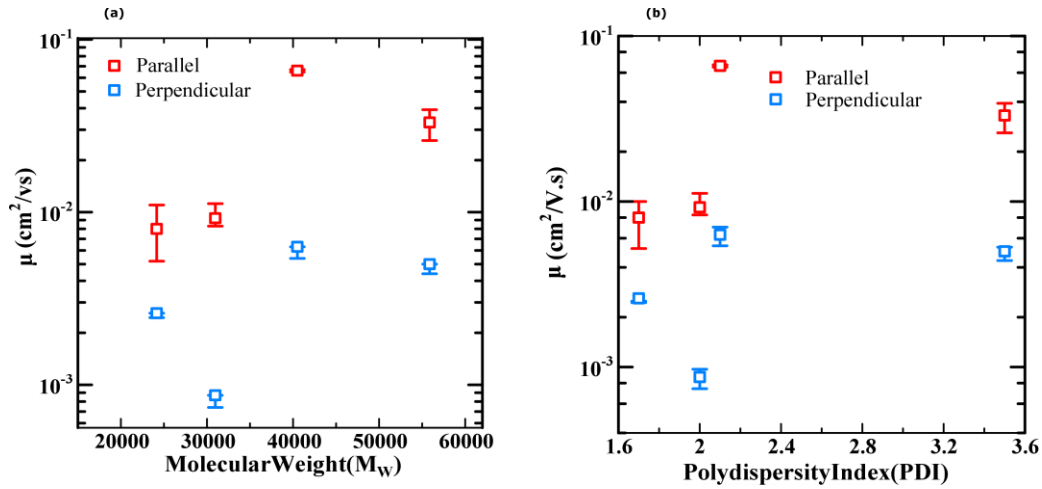


**Figure: 4.5** mobility of oriented thin film in parallel and perpendicular based on molecular weight (a) and dependence on PDI (b).

In this work, OFETs were also fabricated in similar manner of above geometry for the investigation of charge transport anisotropy of four extract of PQT-C12 having different molecular weight and PDI. Detailed summary was summarized in table 2 where four types of PQT-C12 extract having different molecular weight and PDI were used for the investigation. Resultant show when molecular weight increases from first to third type PQT-C12 the maximum mobility in parallel was increased in order of  $0.8 \times 10^{-2} \text{ cm}^2/\text{Vs}$ ,  $1.12 \times 10^{-2} \text{ cm}^2/\text{Vs}$  and  $6.7 \times 10^{-2} \text{ cm}^2/\text{Vs}$  respectively. But after further increment in molecular weight it start to decrease  $3.92 \times 10^{-2} \text{ cm}^2/\text{Vs}$ . In all PQT-C12 extract, third type of extract having one of the highest mobility  $6.7 \times 10^{-2} \text{ cm}^2/\text{Vs}$  in parallel and one order less in perpendicular  $7.0 \times 10^{-3} \text{ cm}^2/\text{Vs}$  however Ong.et al and my previous publication also reported the mobility  $0.02 - 0.05 \text{ cm}^2/\text{Vs}$  and  $0.029$  having  $M_n = 17300 \text{ g/mol}$

and  $M_w=10080$  g/mol respectively [27,34]. Apart from these pingle et.al also reported mobility in the range of  $10^{-3}$  cm<sup>2</sup>/Vs having  $M_n= 1650$  g/mol [22]. In this article third type of PQT-C12 having highest mobility might be the possibility high molecular weight 42500 with of optimized value of PDI 2.1 which is different to fourth types of extract having high molecular weight 55865 and with high PDI 3.5. Note that in this investigation to check the reproducibility the mobility of four types of PQT-C12 are averages over measurements on 5-6 transistors each.

Figure 4.5 show mobility graph as a function of molecular weight and PDI. In figure 4.5 (a) clearly indicate mobility was increased with molecular weight below 45000 and slightly decrease after further increment. The mobility was demonstrated in parallel and perpendicular for the analysis of charge transport anisotropy. The charge transport anisotropy was achieved very high upto 10 having molecular weight above 30000 and below 45000 and slightly decreased above 45000. There are many reason to increase in mobility with molecular weight reported by some group such as charge trapping at the end, the density of chemical defects, regioregularity of the polymer chain and variation in energy level because of PDI etc.[9]. In all the one group reported that regioregularity in polymer chain are play important role for enhancement in mobility because chain pack each other [35]. In figure 4.5 (b) show PDI as a function of mobility as well as anisotropy. The mobility and charge transport anisotropy was increased when PDI was 2 and 2.1 and slightly decreased at 3.5. The reason of decrease in mobility having high PDI was explained as having longer chain statically provide longer conjugation length that acts as trap site and reduced in band gap [35].

Table-2 Device parameters deduced from OFETs prepared thin films of PQT-C12 extract fabricated by ribbon-shaped FTM.

<b>PQT-C12</b>		$\mu_{\parallel}$	$\mu_{\perp}$	$\mu_{\parallel}/\mu_{\perp}$	$I_{ON}/I_{OFF}$	<b>DR</b>
<b>Mw</b>	<b>PDI</b>	<b>FTM</b>	<b>FTM</b>			
<b>25825</b>	1.7	$5.3 \times 10^{-3}$	$3.0 \times 10^{-3}$	4.5	$10^4$	4.56
<b>30965</b>	2.0	$9.2 \times 10^{-3}$	$8.7 \times 10^{-4}$	10	$10^5$	4.9
<b>42500</b>	2.1	$6.6 \times 10^{-2}$	$6.3 \times 10^{-3}$	10	$10^6$	8.7
<b>55865</b>	3.5	$3.3 \times 10^{-2}$	$5.0 \times 10^{-3}$	7.4	$10^5$	5.61

#### 4.4 Conclusion

In conclusion, we have demonstrated a novel and cost effective method for the fabrication of large area, uniform and highly oriented floating films. It has been shown that oriented films of PQT up to 20 cm in length can be easily cast with just 25  $\mu$ l of the polymer solution. Polarized electronic absorption spectra of the oriented PQT films exhibited very high optical anisotropy (DR=22) which is one of the best reported values amongst CPs oriented by different methods. Investigation pertaining to the film uniformity in terms of extent orientation and thickness revealed high uniformity for the films fabricated under optimized casting conditions. The in-plane GIXD results also clarified the well-stacked backbone conformation with ideal edge-on orientation. At the same

time  $\varphi$ -scan suggested that although PQT shows thermotropic LC phase but main chains are ideally aligned in edge-on conformation without any thermal treatment at LC phase transition temperature. DR dependent charge transport anisotropy has also been demonstrated and is well correlated with the results of polarized electronic absorption spectroscopy as well as GIXD supporting the fact that increase in DR leads to increased  $\mu_{\parallel}$ , decreased  $\mu_{\perp}$  and vice versa.

Apart from this four PQT-C12 extract having different molecular weight and PDI obtain after optimized the synthesis parameter. These different molecular weight and PDI is a key function of changing the orientation as well as charge carrier transport in OFETs. By increasing a molecular weight and low PDI upto limit achieved the high performance oriented film having DR>10 and  $6.7 \times 10^{-2} \text{ cm}^2/\text{Vs}$  charge transport in parallel and one order lower in perpendicular without any post treatment. Apart from this it also shows more than >10 optical and electrical anisotropy with  $I_{\text{ON}}/I_{\text{OFF}}$  ratio in the range of  $10^6$  in parallel and one order lower  $10^5$  in perpendicular.

## 4.5 References

- [1] C. Applications, A. Facchetti,  $\pi$ -Conjugated Polymers for Organic Electronics and Photovoltaic, (2011) 733–758.
- [2] R. Dost, S.K. Ray, A. Das, M. Grell, Oscillator circuit based on a single organic transistor, *Appl. Phys. Lett.* 93 (2008) 1–4.
- [3] J.E. Anthony, Functionalized acenes and heteroacenes for organic electronics, *Chem. Rev.* 106 (2006) 5028–5048.
- [4] B. Lee, A. Wan, D. Mastrogiovanni, J.E. Anthony, E. Garfunkel, V. Podzorov, Origin of the bias stress instability in single-crystal organic field-effect transistors, *Phys. Rev. B - Condens. Matter Mater. Phys.* 82 (2010) 3–6.
- [5] C.L. Fan, Y.Z. Lin, P.C. Chiu, S.J. Wang, W. Der Lee, Teflon/SiO<sub>2</sub> bilayer passivation for improving the electrical reliability of pentacene-based organic thin-film transistors, *Org. Electron. Physics, Mater. Appl.* 14 (2013) 2228–2232.
- [6] S. Park, S. Nam, L. Kim, M. Park, J. Kim, T.K. An, W.M. Yun, J. Jang, J. Hwang, C.E. Park, Synthesis and characterization of a fluorinated oligosiloxane-containing encapsulation material for organic field-effect transistors, prepared via a non-hydrolytic sol-gel process, *Org. Electron. Physics, Mater. Appl.* 13 (2012) 2786–2792.
- [7] J. Hoon Park, H. Lim, H. Cheong, K. Min Lee, H. Chul Sohn, G. Lee, S. Im, Anisotropic mobility of small molecule-polymer blend channel in organic transistor: Characterization of channel materials and orientation, *Org. Electron. Physics, Mater. Appl.* 13 (2012) 1250–1254.
- [8] S.O. Kim, T.K. An, J. Chen, I. Kang, S.H. Kang, D.S. Chung, C.E. Park, Y.H. Kim, S.K. Kwon, H-aggregation strategy in the design of molecular semiconductors for highly reliable organic thin film transistors, *Adv. Funct. Mater.* 21 (2011) 1616–1623.
- [9] R.J. Kline, M.D. McGehee, E.N. Kadnikova, J. Liu, J.M.J. Fréchet, Controlling the field-effect mobility of regioregular polythiophene by changing the molecular weight, *Adv. Mater.* 15 (2003) 1519–1522.
- [10] H. Sirringhaus, Device physics of solution-processed organic field-effect transistors, *Adv. Mater.* 17 (2005) 2411–2425.
- [11] A. Zen, J. Pflaum, S. Hirschmann, W. Zhuang, F. Jaiser, U. Asawapirom, J.P. Rabe, U. Scherf, D. Neher, Effect of molecular weight and annealing of poly(3-hexylthiophene)s on the performance of organic field-effect transistors, *Adv. Funct. Mater.* 14 (2004) 757–764.
- [12] R. Zhang, B. Li, M.C. Iovu, M. Jeffries-El, G. Sauvé, J. Cooper, S. Jia, S. Tristram-Nagle, D.M. Smilgies, D.N. Lambeth, R.D. McCullough, T. Kowalewski, Nanostructure dependence of field-effect mobility in regioregular poly(3-hexylthiophene) thin film field effect transistors, *J. Am. Chem. Soc.* 128 (2006) 3480–3481.
- [13] J.M. Verilhac, R. Pokrop, G. LeBlevenec, I. Kulszewicz-Bajer, K. Buga, M. Zagorska, S. Sadki, A. Pron, Molecular weight dependent charge carrier mobility in poly(3,3"-dioctyl-

- 2,2';5',2''-terthiophene), *J. Phys. Chem. B.* 110 (2006) 13305–13309.
- [14] J.F. Chang, B. Sun, D.W. Breiby, M.M. Nielsen, T.I. Sölling, M. Giles, I. McCulloch, H. Sirringhaus, Enhanced Mobility of poly(3-hexylthiophene) transistors by spin-coating from high-boiling-point solvents, *Chem. Mater.* 16 (2004) 4772–4776.
- [15] M. Pandey, S. Nagamatsu, S.S. Pandey, S. Hayase, W. Takashima, Enhancement of carrier mobility along with anisotropic transport in non-regiocontrolled poly(3-hexylthiophene) films processed by floating film transfer method, *Org. Electron. Physics, Mater. Appl.* 38 (2016) 115–120.
- [16] M. Pandey, S. Nagamatsu, W. Takashima, S.S. Pandey, S. Hayase, Interplay of Orientation and Blending: Synergistic Enhancement of Field Effect Mobility in Thiophene-Based Conjugated Polymers, *J. Phys. Chem. C.* 121 (2017) 11184–11193.
- [17] M. Brinkmann, L. Hartmann, L. Biniak, K. Tremel, N. Kayunkid, Orienting semi-conducting pi-conjugated polymers, *Macromol. Rapid Commun.* 35 (2014) 9–26.
- [18] S. Nagamatsu, W. Takashima, K. Kaneto, Y. Yoshida, N. Tanigaki, K. Yase, K. Omote, Backbone arrangement in “friction-transferred” regioregular poly(3-alkylthiophene)s, *Macromolecules.* 36 (2003) 5252–5257.
- [19] M. Pandey, S.S. Pandey, S. Nagamatsu, S. Hayase, W. Takashima, Solvent driven performance in thin floating-films of PBTTT for organic field effect transistor: Role of macroscopic orientation, *Org. Electron. Physics, Mater. Appl.* 43 (2017) 240–246.
- [20] M. Pandey, A. Gowda, S. Nagamatsu, S. Kumar, W. Takashima, S. Hayase, S.S. Pandey, Rapid Formation and Macroscopic Self-Assembly of Thienothiophene, 1700875 (2018) 1–11.
- [21] R.K. Pandey, A.K. Singh, R. Prakash, Directed self-assembly of poly(3,3'-dialkylquaterthiophene) polymer thin film: Effect of annealing temperature, *J. Phys. Chem. C.* 118 (2014) 22943–22951.
- [22] P. Pingel, A. Zen, D. Neher, I. Lieberwirth, G. Wegner, S. Allard, U. Scherf, Unexpectedly high field-effect mobility of a soluble, low molecular weight oligoquaterthiophene fraction with low polydispersity, *Appl. Phys. A Mater. Sci. Process.* 95 (2009) 67–72.
- [23] A. Hamidi-Sakr, L. Biniak, J.L. Bantignies, D. Maurin, L. Herrmann, N. Leclerc, P. Lévêque, V. Vijayakumar, N. Zimmermann, M. Brinkmann, A Versatile Method to Fabricate Highly In-Plane Aligned Conducting Polymer Films with Anisotropic Charge Transport and Thermoelectric Properties: The Key Role of Alkyl Side Chain Layers on the Doping Mechanism, *Adv. Funct. Mater.* 27 (2017) 1–13.
- [24] A. Zen, M. Saphiannikova, D. Neher, J. Grenzer, S. Grigorian, U. Pietsch, U. Asawapirom, S. Janietz, U. Scherf, I. Lieberwirth, G. Wegner, Effect of molecular weight on the structure and crystallinity of poly(3-hexylthiophene), *Macromolecules.* 39 (2006) 2162–2171.
- [25] J.F. Chang, J. Clark, N. Zhao, H. Sirringhaus, D.W. Breiby, J.W. Andreasen, M.M. Nielsen, M. Giles, M. Heeney, I. McCulloch, Molecular-weight dependence of interchain polaron delocalization and exciton bandwidth in high-mobility conjugated polymers, *Phys. Rev. B*

- *Condens. Matter Mater. Phys.* 74 (2006) 1–12.
- [26] J. Gierschner, J. Cornil, H.J. Egelhaaf, Optical bandgaps of  $\pi$ -conjugated organic materials at the polymer limit: Experiment and theory, *Adv. Mater.* 19 (2007) 173–191.
- [27] B.S. Ong, Y. Wu, P. Liu, Structurally Ordered Polythiophene Nanoparticles for High-Performance Organic Thin-Film Transistors \*\*, (2005) 1141–1144.
- [28] T. Kushida, T. Nagase, H. Naito, Mobility enhancement in solution-processable organic transistors through polymer chain alignment by roll-transfer printing, *Org. Electron. Physics, Mater. Appl.* 12 (2011) 2140–2143.
- [29] H. Sirringhaus, P.J. Brown, R.H. Friend, M.M. Nielsen, K. Bechgaard, A.J.H. Spiering, Two-dimensional charge transport in conjugated polymers, (1999) 685–688.
- [30] S. Ong, Y. Wu, P. Liu, S. Gardner, High-Performance Semiconducting Polythiophenes for Organic Thin-Film Transistors High-Performance Semiconducting Polythiophenes for Organic Thin-Film Transistors, (2004) 3378–3379.
- [31] L. Biniek, N. Leclerc, T. Heiser, R. Bechara, M. Brinkmann, Large scale alignment and charge transport anisotropy of pBTTT films oriented by high temperature rubbing, *Macromolecules.* 46 (2013) 4014–4023.
- [32] T. Kushida, T. Nagase, H. Naito, Angular distribution of field-effect mobility in oriented poly[5,5'-bis(3-dodecyl-2-thienyl)-2,2'-bithiophene] fabricated by roll-transfer printing, *Appl. Phys. Lett.* 104 (2014).
- [33] J. Lee, Extraction of high charge density of states in electrolyte-gated polymer thin-film transistor with temperature-dependent measurements Extraction of high charge density of states in electrolyte-gated polymer thin-film transistor with temperature-dependent , 203302 (2016) 1–5.
- [34] A.S.M. Tripathi, M. Pandey, S. Sadakata, S. Nagamatsu, Anisotropic charge transport in highly oriented films of semiconducting polymer prepared by ribbon-shaped floating film, *Appl. Phys. Lett.* (2018)**112**, 123301 (n.d.).
- [35] A. Menon, H. Dong, Z.I. Niazimbetova, L.J. Rothberg, M.E. Galvin, Polydispersity effects on conjugated polymer light-emitting diodes, *Chem. Mater.* 14 (2002) 3668–3675.

## ***Chapter: 5 Optoelectronic properties of conjugated polymers prepared by ribbon-shaped FTM***

### **5.1 Introduction**

The advent of conjugated polymers (CPs) and their semiconducting properties for the use in various technological fields such as solar cells, organic light emitting diodes and organic field effect transistors (OFETs) make them strong contender amongst organic semiconductors in the area of organic electronics [1,2]. CPs can be functionalized by main chain and side chain substitutions [3,4], which facilitates solution processing and variety of applications [5-7]. In CPs intrinsic one- dimensionality and extended  $\pi$ -conjugation of CPs make them susceptible to molecular self-assembly in condensed state. In this attainment of an ordered structure is driven by the different interactions like hydrogen bonding, hydrophobic, electrostatic, van der Waals interaction and  $\pi$ - $\pi$  stacking etc. Controlling the molecular self-assembly in order to get ordered structure is one of the requirements for providing the high-performance to optoelectronics devices. Orientation of CPs has been reported for enhancing the charge transport, polarized luminescence and electroluminescence [8-11]. Controlling the thin film morphology by molecular alignment of the polymer chains has been demonstrated to be critical for enhancing the photoresponse in the optoelectronic devices like photosensitive field effect transistors [12]. At the same time, molecular orientation of CPs support in-plane transport owing to the planarity of  $\pi$ -conjugated backbone leading to high-performance in organic OFETs [10]. A number of methods such as mechanical rubbing [10], friction transfer [13], high-temperature rubbing [14], drawing [15], strain alignment [16] and solution flow [17] etc. have already been used for the orientation of the CPs. Although these techniques have been found to impart molecular orientation but exiting some problems such as mechanical damage, static charge accumulation, solubility of the under layers, material wastage and lack of multilayer formation have to be solved amicably. Apart from these, use of shear force



in these methods generally provide face-on orientation, which is not much suitable for planer devices like OFETs. On the other hand, deposition of thin film using polymeric solution with slow solvent evaporation results into thermodynamically favored edge-on orientation, which is highly essential for in-plane charge transport in the planner devices [18-20].

We have developed a novel and low-cost method for the fabrication uniform and oriented thin films on the viscous liquid substrate and named as floating film transfer method (FTM) [21,22]. Orthogonality of the solvents used for the preparation of liquid substrate and solution of CPs are important requirements for thin film fabrication under FTM. Application of a drop of polymer solution with low boiling solvent on an orthogonal liquid substrate leads to fabrication of thin floating film via film spreading and solvent evaporation. Competing processes like evaporation of solvent used for polymer solution and viscous force of liquid substrate provide molecular orientation to the floating film. Such floating films can be easily transferred to the desired substrate for further characterization as well as applications. It has been found that film thickness and orientation intensity can be controlled by optimizing film-casting parameters like concentration of the polymer solution, temperature and viscosity of the liquid substrates [23]. Apart from the optimization of film casting conditions during FTM, the nature of the polymeric backbone also plays a dominant role in controlling the molecular orientation and affects the finally attainable optical anisotropies [24]. In order to circumvent issues like non-uniformity and multi-directional film spreading, we have recently reported an improvisation in our conventional FTM [25]. Utilization of a custom-made slider during film spreading for providing directionality to the spreading film in FTM led to the large area (14-20 cm long) and highly oriented film formation named as Ribbon- shaped FTM [26].

Present work deals with the fabrication and characterization of very large area oriented thin films of CPs using our newly developed ribbon-shaped FTM. To expedite the investigations pertaining to the nature of the polymeric backbone on molecular orientation, five different CPs (homopolymer and copolymer) belonging to the thiophene family have been taken into consideration. Molecular orientation in these large area oriented films have been probed by polarized electronic absorption spectroscopy, while anisotropic charge transport has been studied after the fabrication OFETs in the bottom gate top contact device architecture.

## 5.2 Experimental Work

In this work five different CPs such as poly(didodecyl-quaterthiophene) (**PQT-C12**), poly[(9,9-dioctyl-9H-fluorene-2,7-diyl)-alt-2,2'-bithiophene]-5,5'-diyl] (**F8T2**), non-regiocontrolled poly(3-hexyl thiophene) (**NR-P3HT**), poly[2,5-bis(3-tetradecylthiophen-2-yl)thieno[3,2-b]thiophene] (**PBTTT-C14**) and poly[4,8-bis[(2-ethylhexyl)oxy]benzo[1,2-b:4,5-b']dithiophene-2,6-diyl][3-fluoro-2-[(2-ethylhexyl)carbonyl]thieno[3,4-b]thiophenediyl] (**PTB7**) have been used for the investigation of orientation. Chemical structure of the CPs are demonstrated in the Figure 5.1.

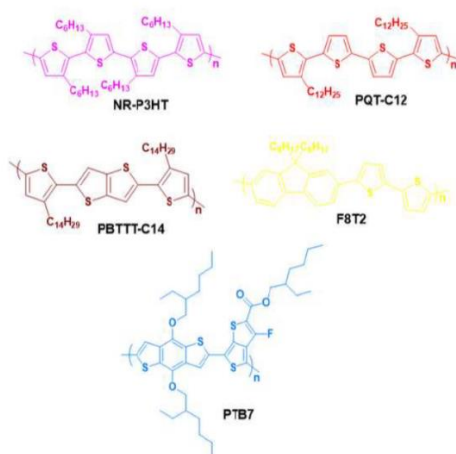


**Figure: 5.1** Chemical structure of conjugated polymer utilized for probing molecular orientation and anisotropic charge transport.

NR-P3HT and PQT-C12 were chemically synthesized using  $\text{FeCl}_3$  catalyzed oxidative polymerization and purified by soxhlet extraction as per our earlier publications [27-29]. Copolymer F8T2 was synthesized by Suzuki coupling following the method reported by Lim et al [30]. Copolymer PTB7 and homopolymer PBTTC-C14 were purchased from 1-Material and Sigma Aldrich, respectively. Both of these two polymers were used without any further purifications. In order to fabricate thin films by FTM, 1 % solution (w/w) of the respective CPs was prepared in the dehydrated chloroform. The oriented thin films of the CPs were prepared using a rectangular tray having size (23 cm  $\times$  15 cm) filled with hydrophilic viscous liquid substrate. The optimized viscous liquid substrate was consisted of a binary mixture of ethylene glycol (EG) and glycerol (GL) in the 3:1 ratio. A custom-made slider (PTFE) was placed at one of the longer sides of the rectangular tray as schematically shown in the Figure 5.2.

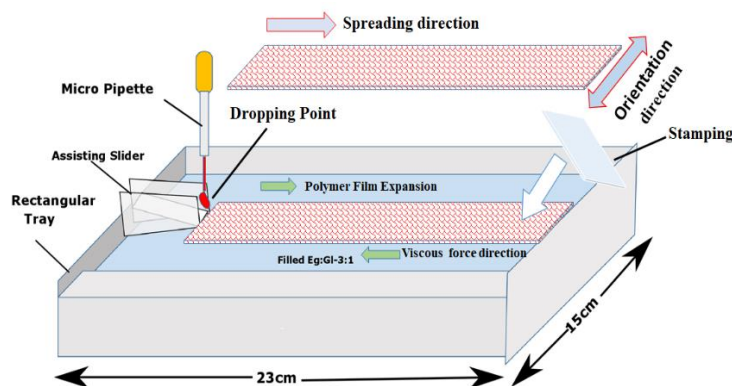


**Figure: 5.2.** Schematic representation for fabrication of oriented thin film by ribbon-shaped FTM.

The amount of solution about 25  $\mu\text{l}$  of respective polymers in dehydrated chloroform was dropped in the center of the slider where the edge of the slider touch the hydrophilic liquid substrate. The slider play important role for assisting the spreading of a polymer solution in single direction

followed by continuous evaporation of chloroform owing to its low boiling point finally leading to large area ribbon-shaped oriented floating film. Before the transfer the film orientation was verified manually by naked eye using a polarizer film and transferred on a glass and Si/SiO<sub>2</sub> substrates by stamping for investigations pertaining to the estimation of optical as well as electrical anisotropy after fabrication of the OFETs respectively. Apart from that, isotropic spin-coated films of CPs under investigation were also prepared by using 0.5 % (w/w) polymer solution at spinning speed of 3000 rpm for 120 s to compare their optoelectronic behaviour. Polarized electronic absorption spectra were measured by UV-visible NIR spectrophotometer (JASCO-570) equipped with Glan Thomson prism. To measure the absorption coefficient, film thickness was measured by the interference microscope [Nikon Eclipse LV150]. Electrical characterization was made after OFET fabrication in bottom gate top contact (BGTC) configuration using respective CP films fabricated by spin coating as well as FTM method. OFET was fabricated by using highly p-doped silicon having 300 nm of SiO<sub>2</sub> insulating layer as a gate dielectric with the capacitance of 10 nF/cm<sup>2</sup>. Prior to the semiconductor deposition, SiO<sub>2</sub> surface was treated with 2 mM solution of octadecyltrichlorosilane (OTS) in dehydrated toluene at 90°C for 2 hours followed by annealing at 130°C for 30 min. to make the self-assembled monolayer of OTS on SiO<sub>2</sub> surface. 50 nm source and the drain electrodes were then deposited by thermal evaporation at a base pressure of 10<sup>-6</sup> Torr followed by Ni shadow mask on oriented film having channel length (L= 20 μm) and width (W=2 mm). Electrical characterization of OFETs was done with computer controlled two-channel source measure unit (Keithley-2612) having the pressure of 10<sup>-3</sup> Torr.

## **5.2 Result and Discussion**

As discussed earlier, orientation intensity in FTM can be controlled by controlling the speed of film spreading and solvent evaporation forming thin film on the viscous hydrophilic liquid

substrate. At the same time, the extent of orientation and film thickness can also be controlled by controlling the film casting parameters like concentration of the polymer solution along with the temperature and viscosity of the liquid substrate [23]. During FTM, compressive force posed by the viscous liquid substrate and solvent evaporation of polymer solution synergistically assist the molecular alignment. These ribbon-shaped films have been found to orient in the tangential direction to the film spreading. An optimized condition such as hydrophilic liquid substrate consisted of EG/GL (3:1), the temperature of 60°C and polymer concentration 1% (w/w) in chloroform was found to be optimum for NR-P3HT. Utilization of PTFE slider and NR-P3HT, we have recently demonstrated the fabrication of very large area [(20 cm (L) × 2cm (W))], uniform and oriented under ribbon-shaped Film [25]. In order to check the versatility of this ribbon-shaped FTM, a number of organic CPs like PQT-C12, F8T2, NR-P3HT, PBTTT-C14 and PTB7 were utilized for the fabrication of large area oriented thin films. All of these CPs were subjected to thin film fabrication under optimized casting condition of NR-P3HT aiming towards implication of nature of polymeric backbone on their optoelectronic properties. Fabricated thin films for various CPs are shown in the Fig. 5.3. It can be clearly seen from this figure that all of the CPs under investigation form very large area [20 cm (L) × 2 cm (W)] thin films like a ribbon under FTM similar to that of NR-P3HT as reported by us previously. Observation of these films under polarizer exhibited a contrast in the color when polarizer was rotated at 90° indicating that these films are oriented too. The direction of the film orientation was perpendicular to the film spreading direction.

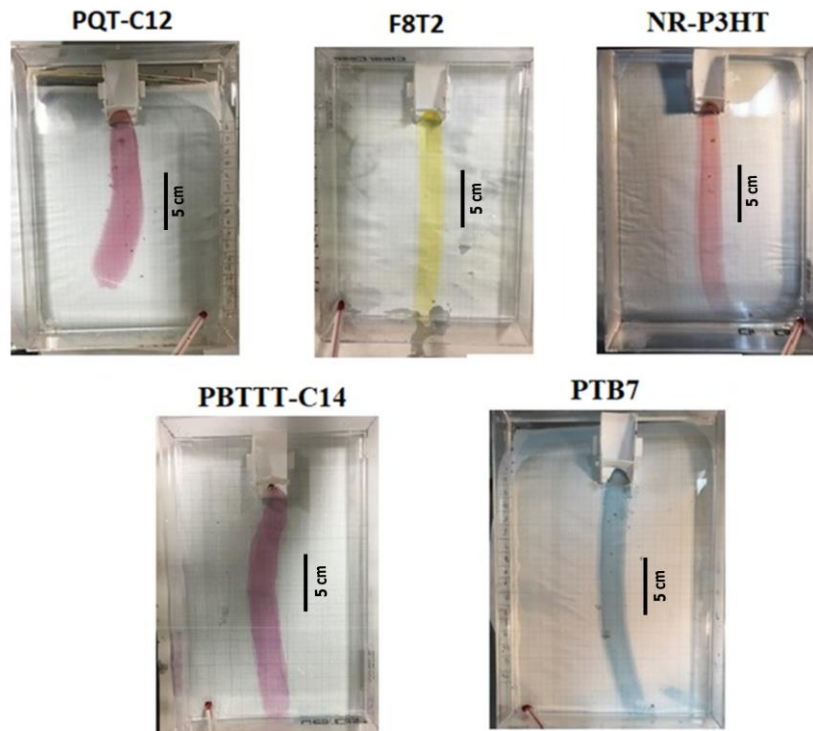


Figure 5.3. Photographic images of thin films of various CPs fabricated by ribbon- shaped FTM under identical casting conditions [liquid substrate-EG: GL (3:1), temperature 60°C, concentration 1 % (w/w) in chloroform.

Fabrication of homogeneously uniform films is one of the important requirements for utilization of thin film fabrication technology towards their application for devices with high reproducibility. In order to investigate the homogeneity of large area thin films fabricated by ribbon- shaped FTM, variation in thickness over centimeter scale was measured by measuring the position dependent absorbance at the respective absorption maximum of the CPs. It is well known that peak absorbance directly correlates with the thickness, therefore, it was measured using 2-dimensional position scanning of absorbance with a step size of 1 mm interval. A fixed light source, computer controlled X-Y sample stage and multichannel photodiode array detector was used for the 2-D positional scanning. Results of the 2D-positional mapping of the film uniformity is shown in the Fig. 5.4. It can be clearly seen that thin films of all of the CPs are highly uniform. Moreover, this film uniformity continues up to cm scale not only in the length but also in the width directions.

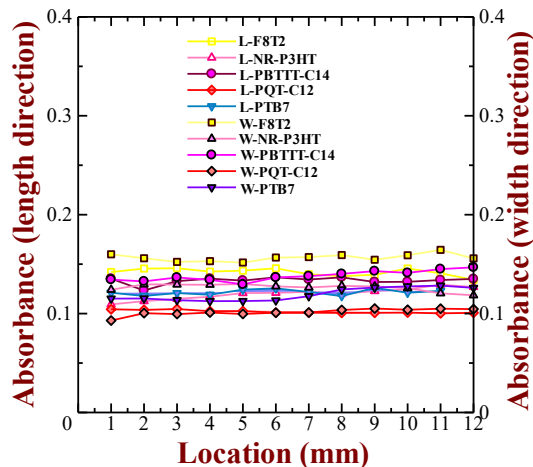
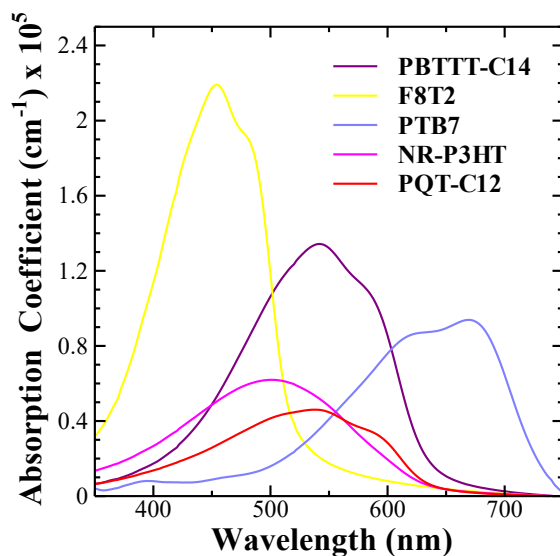


Figure 5.4. Variation of peak absorption intensity across about 1 cm in the length and width directions for the thin films of CPs casted on a glass substrate.

### 5.3.1 Non-Polarized Absorption Spectra

The respective five CPs were first subjected to optical characterization of coated thin films fabricated by conventional spin coating prior to the anisotropic optical characterization using oriented thin films fabricated by ribbon-shaped FTM. The electronic absorption spectra of spin-coated films of all respective CPs under investigation are demonstrated in the Figure 5.5 and its detail summarization values related to of their absorption maxima ( $\lambda_{\max}$ ) in the table 1. Although all of the CPs belong to the thiophene family but differ in absorption spectral features depend on the extent of  $\pi$ -conjugation.



**Figure: 5.5** Electronic absorption spectra various conjugated polymers on glass prepared by spin coating method.

Amongst CPs used F8T2 absorption spectra shows most hypsochromically shifted  $\lambda_{\max}$  at 454 nm and vibronic shoulder at 482 nm along with highest value of extinction coefficient of  $2.27 \times 10^5 \text{ cm}^{-1}$ . However, PTB7 resultant show largest bathochromically shifted  $\lambda_{\max}$  at 670 nm combined with  $\pi$ - $\pi^*$  electronic transition and vibronic shoulder at 622 nm. The increased extent of  $\pi$ -conjugation in the monomer block along with high planarity is attributed to the observation of showing high value of  $\lambda_{\max}$  in this polymer. If we have to consider PQT-C12 and NR-P3HT, they are structurally very similar but exhibit  $\lambda_{\max}$  at 538 nm and 508 nm, respectively. At that instant, we can observe the clear vibronic shoulder at 587 nm for PQT-C12, while such vibronic shoulder is not present in NR-P3HT. It is already reported that regioregular P3HT exhibit not only red-shifted  $\lambda_{\max}$  but also clear vibronic shoulder due enhanced effective  $\pi$ -conjugation and crystallinity as compared to their non-regiocontrolled counterparts [31]. Therefore, the presence of higher extent of regioregularity in PQT-C12 owing to its molecular structure could be responsible for its



red-shifted  $\lambda_{\max}$  along with clear vibronic shoulder compared to that of NR-P3HT. PBTTT-C14 is a liquid crystalline CP and exhibit  $\lambda_{\max}$  at 542 nm associated with  $\pi$ - $\pi^*$  electronic transition along with vibronic shoulder appearing at 586 nm. It is interesting to note that absorption coefficient of NR-P3HT ( $6.6 \times 10^4 \text{ cm}^{-1}$ ) is higher than that of PQT-C12 ( $4.8 \times 10^4 \text{ cm}^{-1}$ ), which could be explained considering the density or compaction of  $\pi$ -electrons in the polymeric backbone. In an interesting report, Takashima et al have reported that in the regioregular poly(3-alkylthiophenes), absorption coefficients of CPs decreases with the alkyl chain length [32]. Therefore, presence long alkyl chain (dodecyl) in PQT-C12 could be responsible for its lower absorption coefficient as compared to NR-P3HT having relatively smaller alkyl chain (hexyl) substituents. It can be seen that PBTTT-C14 exhibits highest red- shift amongst the CPs except for PTB7, which is associated with very large effective  $\pi$ -conjugation length and enhanced molecular self-assembly facilitated by its high degree of planarity and presence of fused thienothiophene ring.

### 5.3.2 Polarized Absorption Spectra

As mentioned previously, ribbon-shaped FTM not only leads to large area homogeneous thin films but also imparts the molecular orientation. In order to quantitatively analyze the molecular orientation of CPs, oriented polymer films were transferred on to glass substrate and subjected to polarized electronic absorption spectral investigations by measuring the absorbance of the films after rotating the angle of the polarizer at  $00^\circ$  (parallel) and  $90^\circ$  (perpendicular). Figure 5.6 shows the anisotropic electronic absorption spectra for thin films of PQT-C12, F8T2, NR-P3HT, PBTTT-C14 and PTB7. At the same time, optical parameters like absorption maxima for parallel/perpendicular orientation, vibronic shoulders and optical anisotropy in terms of dichroic ratio (DR) have been summarized in table 1. Electronic absorption spectra of PQT-C12 in the

parallel orientation exhibits  $\lambda_{\max}$  at 547 nm, which is 9 nm red-shifted as compared to non-polarized spin coated film. Apart from red shift, it exhibits vibronic shoulder at 589 nm, which indicates the structural ordering in the condensed state and enhanced  $\pi$ - $\pi$  stacking [29]. The dichroic ratio ( $A_{\parallel}/A_{\perp}$ ) for this CP was found to be 5.1, which was maximum amongst the CPs used for present investigation.

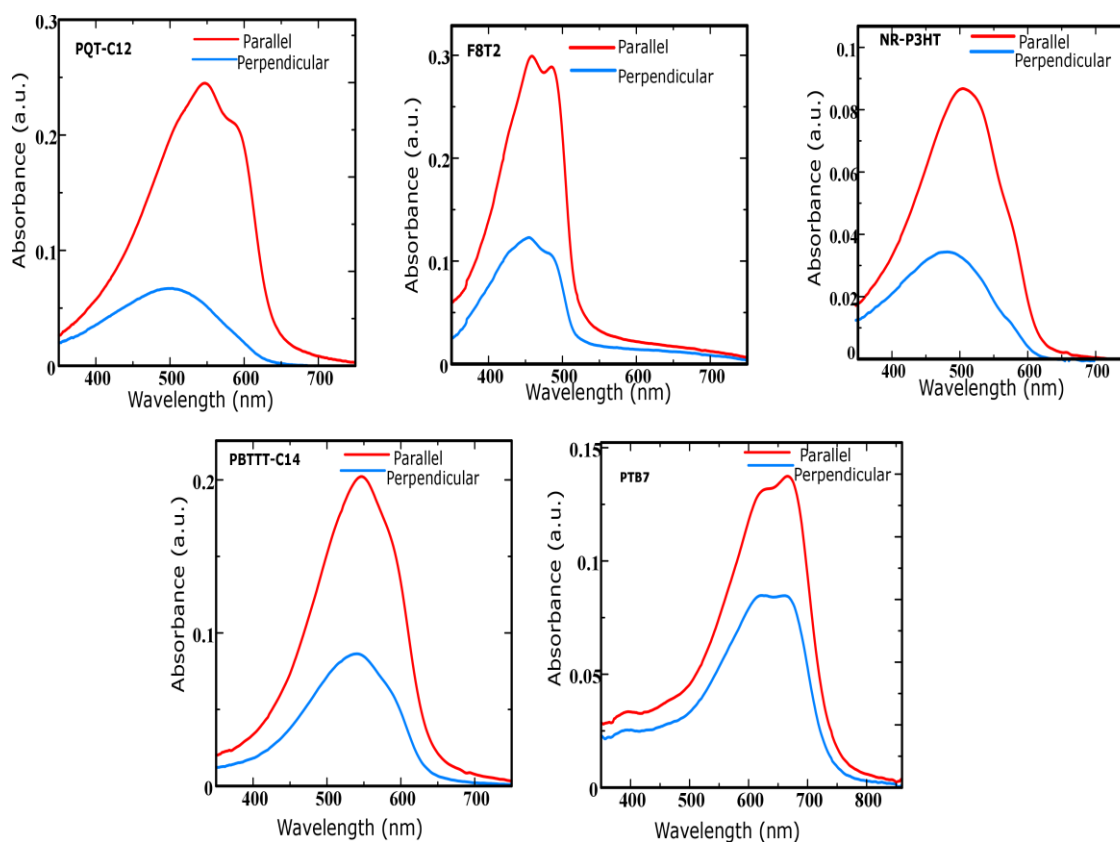


**Figure: 5.6** Polarized electronic absorption spectra of oriented CPs on glass substrate prepared by Slider based FTM.

Oriented F8T2 films exhibit an intense absorption associated with  $\pi$ - $\pi$  transition appearing at  $\lambda_{\max}$  of 486 nm, which is not only 5 nm red-shifted as compared to spin-coated films but also shows clear vibronic shoulder indicating backbone alignment [11]. Oriented NR-P3HT films exhibited

$\lambda_{\max}$  at 520 nm with pronounced red-shift and clear vibronic shoulders at 562 nm and 587 nm, which are very similar to the spectral features of regioregular P3HT and absent in the spin-coated films [25]. PBTTC-C14 shows  $\lambda_{\max}$  at 546 nm, which is slightly red-shifted (4 nm) as compared to non-polarized Spin coated films. In spite of molecular rigidity and well-known liquid crystalline nature, red-shifted  $\lambda_{\max}$  and vibronic shoulder clearly indicates enhanced effective  $\pi$ -electron delocalization in the FTM processed oriented films owing to applied viscous force from the liquid substrate during the solidification after film spreading [29,33,34]. Interestingly, FTM processed PTB7 exhibits nearly similar spectral features as compared to that of spin-coated films and smallest optical anisotropy (DR = 1.7) also supports that polymeric chains are less prone to align further.

A perusal of Figure 5.4 and table 1 clearly corroborates that ribbon-shaped FTM is not only able to make large area homogeneous thin films of all of the CPs under investigation but also exhibit optical anisotropy too. Although extent of orientation (represented by DR) is different, which was highest for PQT-C12 and lowest for PTB7. It has been previously reported by us that extent of orientation depends not only on FTM parameters but also on the crystallinity, molecular packing, liquid crystalline behaviour and nature of polymeric backbones [24-25, 35]. It has been observed that rigid rod-like crystalline CPs are relatively less prone to orientation under FTM, which can be explained considering the fact that molecular orientation is facilitated by viscous dragging force applied during film spreading and solidification on the liquid substrate. This is the reason why regioregular (RR) P3HT exhibits relatively small orientation as compared it its non-regiocontrolled NR-P3HT under identical film casting conditions during FTM [27].

Tabel-1 Optical parameters for spin coated and ribbon shaped FTM films for various CPs deduced from the solid-state electronic absorption spectra.

Polymer	Film conditions	Absorption Maximum (nm)	Dichroic Ratio (DR)	Vibronic Shoulder (nm)
<b>PQT-C12</b>	Spin Coat	538	5.1	587
	FTM Parallel	547		589
	FTM Perpendicular	502		Absent
<b>F8T2</b>	Spin Coat	454	2.5	482
	FTM Parallel	459		486
	FTM Perpendicular	455		485
<b>NR-P3HT</b>	Spin Coat	508	2.4	Absent
	FTM Parallel	520		602
	FTM Perpendicular	496		Absent
<b>PBTTT-C14</b>	Spin Coat	542	2.2	586
	FTM Parallel	546		594
	FTM Perpendicular	540		590
<b>PTB7</b>	Spin Coat	670	1.7	620
	FTM Parallel	670		624
	FTM Perpendicular	662		618

In an interesting review, Kuei and Gomez discussed in detail about molecular chain conformation of CPs and their implications on the phase behaviour and optoelectronic properties and advocated about the persistent length ( $L_p$ ) in order to correlate and compare the chain conformation of the CPs quantitatively [36]. Actually,  $L_p$  is the distance taken by polymeric backbone to bend it by  $90^\circ$  and a smaller value leads to attaining flexible coil-like conformation while a high  $L_p$  represents

stiff, rod-like and crystalline polymeric backbone. Using small angle neutron scattering experiments, McCulloch et al reported a small  $L_p$  of 0.9 and 1.4 for regiorandom and NR-P3HT, which was much higher for RR-P3HT (2.9) [37]. Therefore, lower value of  $L_p$  could be attributed to lower DR under FTM for RR-P3HT reported by us previously. At the same time, a  $L_p$  value 9.0 and 8.2 have been reported by Zhao et al and Li et al for PBTTT and PTB7, respectively [38]. This indicates that both of these polymers are stiff rigid rod-like and highly crystalline, which make them less prone to orient easily during FTM as indicated by their lower values of DR as shown in the table 1. One can argue that in spite of lower  $L_p$  for PTB7 (8.2) than PBTTT-C14 (9.0), why it exhibits relatively lower molecular orientation (DR= 1.7) as compared to PBTTT-C14 (DR= 2.2) under ribbon-shaped FTM. This can be explained considering the nature of polymeric backbone in to consideration. Although, PTB7 and PBTTT-C14 both bear fused thienothiophene ring providing enhanced planarity and intermolecular interactions but former has hydrophilic ester group while later has only hydrophobic alkyl chains. We have recently reported that thin films PBTTT-C14 prepared by FTM exhibits edge-on orientation and its hydrophobicity-assisted repulsion from hydrophilic liquid substrate promote this edge-on orientation [39]. Contrary to this, presence of hydrophilic ester group in PTB7 offers attractive interaction of the polymeric main-chain with hydrophilic liquid substrate posing hindrance in the orientation leading to drastically reduced DR of 1.7 in the oriented films of PTB7 prepared under ribbon-shaped FTM.

### **5.3.2 Anisotropic Charge Transport**

The BGTC device architectures for OFETs have been adopted to investigate the effect of molecular orientation on anisotropic charge transport. This device architecture was selected because this work lies in the fact that  $\text{SiO}_2$  grown insulator are most commonly being used, easily available from different commercial sources and there is no damage to the dielectric layer while

adopting solution processable organic semiconductors. At the same time, contact resistance has been reported to be small for BGTC device structures as compared to that of the BGBC device structure counterparts [40]. The device architecture of the fabricated OFET is shown in the Fig. 5.7 (a), where thin film were deposited by ribbon-shaped FTM along with the spin coating for comparison. Prior to transfer the oriented film for device fabrication, direction of aligned FTM films was first confirmed by polarizer film followed by its transfer on SiO<sub>2</sub>/Si substrate in order to assign the alignment direction. The electrode, source-drain metal contacts were then thermally evaporated on top on semiconductor layer by using shadow mask by placing the mask in parallel and perpendicular with respect to the orientation direction. The device field effect mobility (  $\mu$  ) was calculated from the transfer characteristics, when the device reached in condition of saturation region using the equation 1 as follows:

$$I_{DS} = \frac{W}{2L} \mu C_i (V_{GS} - V_{TH})^2$$

Where,  $I_{DS}$ ,  $W$ ,  $L$ ,  $\mu$ ,  $C_i$ ,  $V_{GS}$  and  $V_{TH}$  are representing saturated output current, channel width, channel length, charge carrier mobility, capacitance of gate insulator, applied gate bias voltage and threshold voltage, respectively. A typical output characteristics OFETs using oriented thin films of PQT-C12 fabricated by ribbon-shaped FTM is shown in the Fig. 5.7(b), where varying gate bias voltage as a function of OFETs. In figure 5.6(b) that OFET shows typical p-type semiconducting behaviour since it is being operated at negative gate bias voltages and show high current in case of parallel oriented film.

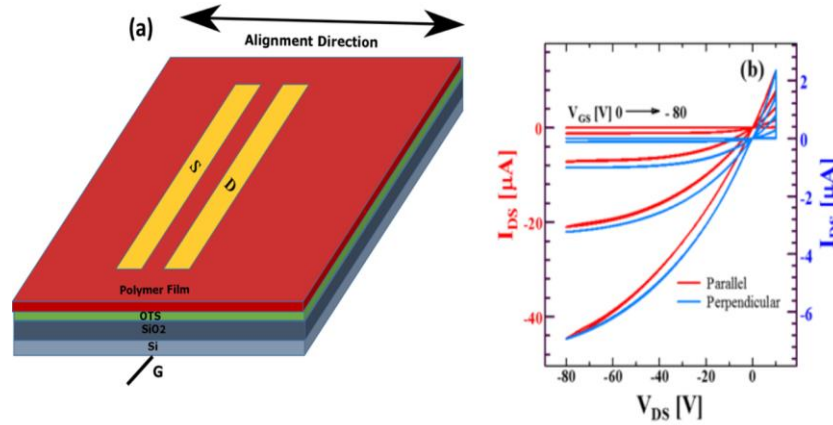


**Figure: 5.7** Device architecture (a) and representative output characteristics of OFETs (b) fabricated using parallel and perpendicularly oriented PQT-C12 films at various applied gate bias.

In order to extract the electrical parameters of the OFETs, transfer characteristics ( $I_{DS}-V_{GS}$ ) of the OFETs operated at  $V_{DS} = -80$  V, which are demonstrated in the Fig. 8. These parameter like  $\mu$ , ON/OFF ratio, electronic anisotropy ( $\mu_{||} / \mu_{\perp}$ ) etc. calculated from the transfer characteristic curves for all of the CPs along with corresponding isotropic spin coated films (for comparison) have been summarized in the table 2.

**Table-2** Anisotropic electrical parameters deduced from OFETs using thin films of different CPs fabricated by ribbon-shaped FTM.

Conducting Polymers	FTM [ $\mu_{  }$ ] ( $\text{cm}^2 \cdot \text{V}^{-1} \cdot \text{s}^{-1}$ )	FTM [ $\mu_{\perp}$ ] ( $\text{cm}^2 \cdot \text{V}^{-1} \cdot \text{s}^{-1}$ )	Spin coated ( $\text{cm}^2 \cdot \text{V}^{-1} \cdot \text{s}^{-1}$ )	( $\mu_{  } / \mu_{\perp}$ )	$I_{ON}/I_{OFF}$	DR
PQT-C12	$5 \times 10^{-2}$	$7 \times 10^{-3}$	$6.7 \times 10^{-4}$	7.1	$10^6$	5.1
F8T2	$1.05 \times 10^{-3}$	$3.7 \times 10^{-4}$	$2.0 \times 10^{-4}$	2.9	$10^4$	2.5
NR-P3HT	$4.2 \times 10^{-3}$	$1.2 \times 10^{-3}$	$1.0 \times 10^{-5}$	3.5	$10^4$	2.4
PBTTT-C14	$7.5 \times 10^{-3}$	$5 \times 10^{-3}$	$5.2 \times 10^{-3}$	1.5	$10^4$	2.2
PTB7	$1.9 \times 10^{-4}$	$5.5 \times 10^{-5}$	$1.1 \times 10^{-4}$	3.5	$10^3$	1.7

A perusal of the transfer characteristics shown Figure 5.8 and table 2 corroborates that amongst CPs used PQT-C12 exhibited highest charge carrier mobility of  $0.05 \text{ cm}^2/\text{vs}$  for FTM films oriented parallel to channel direction, which was about 7 times higher ( $7.0 \times 10^{-3} \text{ cm}^2/\text{vs}$ ) as compared to the corresponding FTM films in the perpendicular orientation. An electrical and optical anisotropies of 7.1 and 5.1, respectively, also correlate the implication of anisotropic charge transport in the OFETs based on PQT-C12. At the same time, parallel oriented film of PQT-C12 show nearly 75 times enhancement in the mobility in comparison to its spin coated counterparts ( $6.7 \times 10^{-4} \text{ cm}^2/\text{vs}$ ) portrays the importance of molecular orientation on the facile charge carrier transport. Although, highest mobility of PQT-C12 was reported but in this work is a lower as compared to the benchmark values ( $> 0.1 \text{ cm}^2/\text{vs}$ ), reason behind this optimization of other factors such as dielectric interface, molecular weight, polydispersity index, processing conditions and channel length etc. apart from molecular orientation [ 41]. Parallel FTM oriented F8T2 exhibits although about 5 times higher mobility as compared to its corresponding spin coated films but it is lower than the reported mobility of high performance OFETs ( $4.3 \times 10^{-2} \text{ cm}^2/\text{vs}$ ) for this material by Endo et al [42] . This high mobility was reported along with for highly oriented F8T2 films having (DR>10) achieved under stringent conditions such as annealing at its very high liquid crystalline temperature of  $280^\circ\text{C}$  and alignment of polymer chains due to mechanical rubbing. NR-P3HT based OFETs exhibited maximum charge carrier mobilities of  $4.2 \times 10^{-3} \text{ cm}^2/\text{vs}$ ,  $1.2 \times 10^{-3} \text{ cm}^2/\text{vs}$  and  $1.0 \times 10^{-5} \text{ cm}^2/\text{vs}$  in oriented film of parallel, perpendicular and spin coating films, respectively. This resultant shows that charge transport in parallel oriented thin films of NR-P3HT was  $>10^2$  times higher as compared to its spin-coated thin film counterparts.



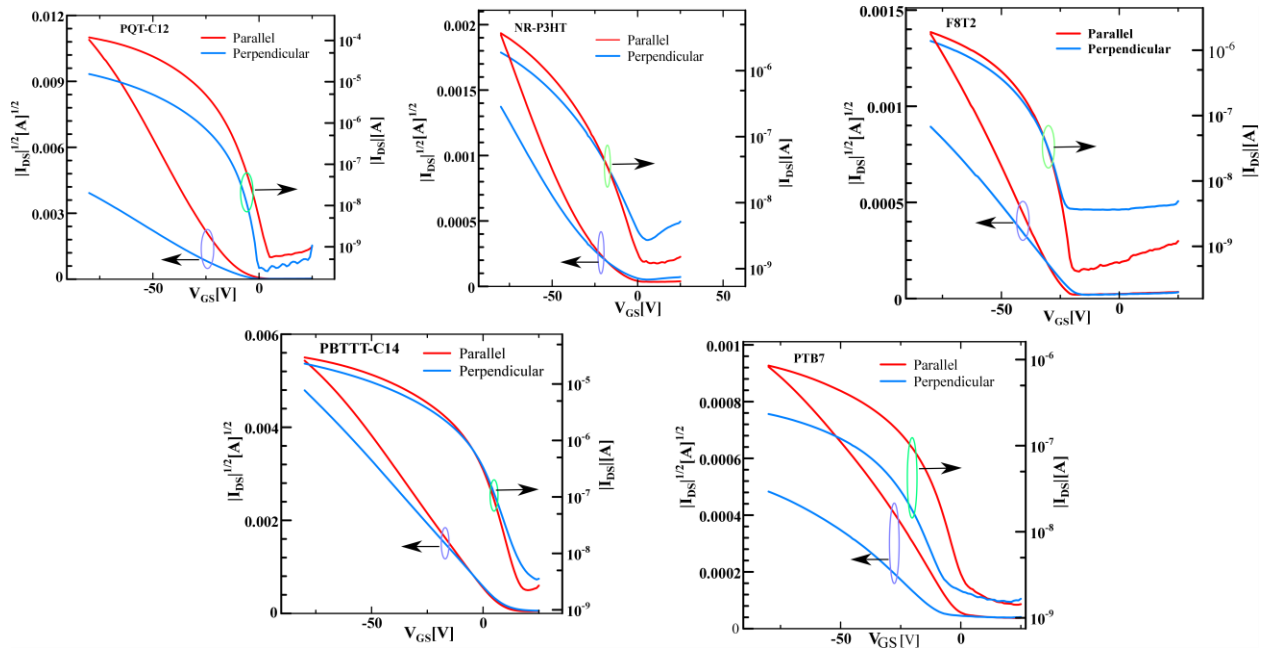


**Figure: 5.8** Transfer characteristics of OFETs operated at gate bias voltage of -60 V in parallel and perpendicular orientation for various thin films fabricated using ribbon-shaped FTM.

Charge carrier mobilities in the FTM processed parallel oriented thin films of PBTTT-C14, PTB7 were slightly higher than that of corresponding spin-coated films, and electrical anisotropy follows the trend of optical anisotropy. In spite of large area homogeneous thin films of PBTTT-C14 prepared by ribbon-shaped FTM, mobility of parallel oriented film ( $7.5 \times 10^{-3} \text{ cm}^2/\text{vs}$ ) was lower than that reported by M. Pandey et al by conventional FTM under optimized condition ( $0.11 \text{ cm}^2/\text{Vs}$ ) [20]. In this work, similar casting condition was used for the ribbon shaped FTM of all of the CPs for structure-property correlation, which might not be optimum for PBTTT-C14, Therefore, lower molecular orientation of this material in the present case might be responsible for hampered value of observed carrier mobility. In line with smallest molecular orientation, parallel oriented FTM films of PTB7 exhibited FET mobility of  $1.9 \times 10^{-4} \text{ cm}^2/\text{vs}$ , which is smallest amongst the CPs used in this work. Although observed mobility is nearly similar to that reported

by Xu et al ( $6.0 \times 10^{-4} \text{ cm}^2/\text{Vs}$ ), smallest value of molecular orientation (1.7) and nearly similar value compared to that of spin-coated film [43] suggest that hindrance in most favorable edge-on orientation owing to its molecular structure could be responsible for hampered charge transport along the channel. One can argue that in spite of very low optical anisotropy in PTB7 (DR = 1.7), what the cause of large electrical anisotropy ( $\mu_{\parallel} / \mu_{\perp} = 3.5$ ). In general, sheer-force assisted molecular orientation leads to face-on molecular orientation which is not much favored for planer devices and presence of large alkyl chains in the plane of the channel results in to highly hindered charge transport perpendicular to the channel leading to very high electrical anisotropy. Using poorly soluble polythiophene derive and aligning them by friction-transfer method. Hosakawa et al. [44] have also reported very high  $\mu_{\parallel} / \mu_{\perp}$  value. Therefore, hindered edge-on orientation in PTB7 as discussed earlier could be responsible for relatively higher mobility anisotropy in spite of low optical anisotropy.

## 5.4 Conclusion

Ribbon-shaped FTM has been successfully utilized for the fabrication of large area [20 cm (L)  $\times$  2 cm (W)] uniform and oriented thin films. The main advantage of this method single direction uniform thin film fabrication was demonstrated using a number of CPs belonging to polythiophene family. There is a least material wastage during thin film fabrication in ribbon-shaped FTM can be justified considering the fact that by using only one drop (20  $\mu\text{l}$ ) of polymer solution, it is possible to fabricate >100 OFETs. Parametric optimization of FTM for a CP is necessary in order to get optimum molecular orientation but under identical casting condition, order of molecular orientation was found to be PQT-C12>F8T2>NR-P3HT>PBTTT-C14>PTB7. The correlation of structure-property in terms of polymeric structure and molecular orientation was explained in terms of nature and rigidity of polymeric chains in the light of reported values of persistent length.

A clear anisotropic charge transport was demonstrated by all of the CPs used in this work. Amongst CPs used, PQT-C12 exhibits highest optical as well as electrical charge transport anisotropy, and achieved best device performance with having  $5 \times 10^{-2} \text{ Cm}^2/\text{Vs}$  charge carrier mobility in parallel orientation.

## 5.4 References

- [1] H. Sirringhaus, 25th anniversary article: Organic field-effect transistors: The path beyond amorphous silicon, *Adv. Mater.* 26 (2014) 1319–1335. doi:10.1002/adma.201304346.
- [2] C. Applications, A. Facchetti,  $\pi$ -Conjugated Polymers for Organic Electronics and Photovoltaic, (2011) 733–758. doi:10.1021/cm102419z.
- [3] T.-A. Chen, R.D. Rieke, Upon 4, *J. Am. Chem. Soc.* 114 (1992) 10087–10088.
- [4] C.L. Gettinger, A.J. Heeger, J.M. Drake, D.J. Pine, A photoluminescence study of poly(phenylene vinylene) derivatives: The effect of intrinsic persistence length, *J. Chem. Phys.* 101 (1994) 1673–1678. doi:10.1063/1.468438.
- [5] S.N. Patel, G.M. Su, C. Luo, M. Wang, L.A. Perez, D.A. Fischer, D. Prendergast, G.C. Bazan, A.J. Heeger, M.L. Chabiny, E.J. Kramer, NEXAFS Spectroscopy Reveals the Molecular Orientation in Blade-Coated Pyridal[2,1,3]thiadiazole-Containing Conjugated Polymer Thin Films, *Macromolecules.* 48 (2015) 6606–6616. doi:10.1021/acs.macromol.5b01647.
- [6] H. Youn, H. J. Park and L. J. Guo, *Energy Technoloy*, 3 (2015) 340–350.
- [7] B. Döring, V. Vohra, T.T. Dao, M. Garriga, H. Murata, M. Campoy-Quiles, Uniaxial macroscopic alignment of conjugated polymer systems by directional crystallization during blade coating, *J. Mater. Chem. C.* 2 (2014) 3303–3310. doi:10.1039/c3tc32056a.
- [8] M. Grell, D.D.C. Bradley, Polarized luminescence from oriented molecular materials, *Adv. Mater.* 11 (1999) 895–905. doi:10.1002/(SICI)1521-4095(199908)11:11<895::AID-ADMA895>3.0.CO;2-Y.
- [9] E.J.W. Crossland, K. Tremel, F. Fischer, K. Rahimi, G. Reiter, U. Steiner, S. Ludwigs, Anisotropic charge transport in spherulitic Poly(3-hexylthiophene) films, *Adv. Mater.* 24 (2012) 839–844. doi:10.1002/adma.201104284.
- [10] M. Brinkmann, L. Hartmann, L. Biniek, K. Tremel, N. Kayunkid, Orienting semi-conducting pi-conjugated polymers, *Macromol. Rapid Commun.* 35 (2014) 9–26. doi:10.1002/marc.201300712.
- [11] H. Sirringhaus, R.J. Wilson, R.H. Friend, M. Inbasekaran, W. Wu, E.P. Woo, M. Grell, D.D.C. Bradley, H. Sirringhaus, R.J. Wilson, R.H. Friend, Mobility enhancement in conjugated polymer field-effect transistors through chain alignment in a liquid-crystalline phase Mobility enhancement in conjugated polymer field-effect transistors through chain alignment in a liquid-crystalline phase, *Appl. Phys. Lett.* 77 (2000) 406–408. doi:10.1063/1.126991.
- [12] K. Bhargava, V. Singh, High-sensitivity organic phototransistors prepared by floating film transfer method, *Appl. Phys. Express.* 9 (2016). doi:10.7567/APEX.9.091601.

- [13] S. Nagamatsu, W. Takashima, K. Kaneto, Y. Yoshida, N. Tanigaki, K. Yase, K. Omote, Backbone arrangement in “friction-transferred” regioregular poly(3-alkylthiophene)s, *Macromolecules*. 36 (2003) 5252–5257. doi:10.1021/ma025887t.
- [14] L. Biniek, N. Leclerc, T. Heiser, R. Bechara, M. Brinkmann, Large scale alignment and charge transport anisotropy of pBTTT films oriented by high temperature rubbing, *Macromolecules*. 46 (2013) 4014–4023. doi:10.1021/ma400516d.
- [15] S. Nagamatsu, W. Takashima, K. Kaneto, Y. Yoshida, N. Tanigaki, K. Yase, Polymer field-effect transistors by a drawing method, *Appl. Phys. Lett.* 84 (2004) 4608–4610. doi:10.1063/1.1751222.
- [16] N. Yamasaki, Y. Miyake, H. Yoshida, A. Fujii, M. Ozaki, Solution flow assisted fabrication method of oriented  $\pi$ -conjugated polymer films by using geometrically-asymmetric sandwich structures, *Jpn. J. Appl. Phys.* 50 (2011). doi:10.1143/JJAP.50.020205.
- [17] B. O’Connor, R.J. Kline, B.R. Conrad, L.J. Richter, D. Gundlach, M.F. Toney, D.M. DeLongchamp, Anisotropic structure and charge transport in highly strain-aligned regioregular poly(3-hexylthiophene), *Adv. Funct. Mater.* 21 (2011) 3697–3705. doi:10.1002/adfm.201100904.
- [18] J. Chang, B. Sun, D.W. Breiby, M.M. Nielsen, M. Giles, I. McCulloch, H. Sirringhaus, Enhanced Mobility of Poly ( 3-hexylthiophene ) Transistors by Spin-Coating from High-Boiling-Point Solvents, (2004) 4772–4776. doi:10.1021/cm049617w.
- [19] H. Yang, S.W. Lefevre, C.Y. Ryu, Z. Bao, Solubility-driven thin film structures of regioregular poly(3-hexyl thiophene) using volatile solvents, *Appl. Phys. Lett.* 90 (2007) 2005–2008. doi:10.1063/1.2734387.
- [20] M. Pandey, S.S. Pandey, S. Nagamatsu, S. Hayase, W. Takashima, Solvent driven performance in thin floating-films of PBTTT for organic field effect transistor: Role of macroscopic orientation, *Org. Electron. Physics, Mater. Appl.* 43 (2017) 240–246. doi:10.1016/j.orgel.2017.01.031.
- [21] T. Morita, V. Singh, S. Nagamatsu, S. Oku, W. Takashima, K. Kaneto, Enhancement of transport characteristics in poly(3-hexylthiophene) films deposited with floating film transfer method, *Appl. Phys. Express*. 2 (2009) 1–4. doi:10.1143/APEX.2.111502.
- [22] D. Arnaud, R.K. Pandey, S. Miyajima, S. Nagamatsu, R. Prakash, W. Takashima, S. Hayase, K. Kaneto, Fabrication of large-scale drop-cast films of  $\pi$ -conjugated polymers with floating-film transfer method., *Trans. Mater. Res. Soc. Japan*. 38 (2013) 305–308.
- [23] M. Pandey, S.S. Pandey, S. Nagamatsu, S. Hayase, W. Takashima, Controlling Factors for Orientation of Conjugated Polymer Films in Dynamic Floating-Film Transfer Method, *J. Nanosci. Nanotechnol.* 17 (2017) 1915–1922. doi:doi:10.1166/jnn.2017.12816.

- [24] M. Pandey, S.S. Pandey, S. Nagamatsu, S. Hayase, W. Takashima, Influence of backbone structure on orientation of conjugated polymers in the dynamic casting of thin floating-films, *Thin Solid Films*. 619 (2016) 125–130. doi:10.1016/j.tsf.2016.11.015.
- [25] A. Tripathi, M. Pandey, S. Nagamatsu, S.S. Pandey, S. Hayase, W. Takashima, Casting Control of Floating-films into Ribbon-shape Structure by modified Dynamic FTM, *J. Phys. Conf. Ser.* 924 (2017). doi:10.1088/1742-6596/924/1/012014.
- [26] A.S.M. Tripathi, M. Pandey, S. Sadakata, S. Nagamatsu, Anisotropic charge transport in highly oriented films of semiconducting polymer prepared by ribbon-shaped floating film, (n.d.). doi:10.1063/1.5000566.
- [27] R.H. Lohwasser, M. Thelakkat, Toward perfect control of end groups and polydispersity in poly(3-hexylthiophene) via catalyst transfer polymerization, *Macromolecules*. 44 (2011) 3388–3397. doi:10.1021/ma200119s.
- [28] S. Amou, O. Haba, K. Shirato, T. Hayakawa, M. Ueda, K. Takeuchi, M. Asai, Head-to-tail regioregularity of poly(3-hexylthiophene) in oxidative coupling polymerization with FeCl<sub>3</sub>, *J. Polym. Sci. Part A Polym. Chem.* 37 (1999) 1943–1948.
- [29] S. Ong, Y. Wu, P. Liu, S. Gardner, High-Performance Semiconducting Polythiophenes for Organic Thin-Film Transistors High-Performance Semiconducting Polythiophenes for Organic Thin-Film Transistors, (2004) 3378–3379. doi:10.1021/ja039772w.
- [30] E. Lim, B.J. Jung, H.K. Shim, Synthesis and characterization of a new light-emitting fluorene-thieno[3,2-b]thiophene-based conjugated copolymer, *Macromolecules*. 36 (2003) 4288–4293. doi:10.1021/ma034168r.
- [31] S.S. Pandey, S. Nagamatsu, W. Takashima, K. Kaneto, Mechanism of photocarrier generation and transport in poly(3-alkylthiophene) films, *Japanese J. Appl. Physics, Part 1 Regul. Pap. Short Notes Rev. Pap.* 39 (2000) 6309–6315. doi:10.1143/JJAP.39.6309.
- [32] K. Kaneto, W. Takashima, Fabrication and characteristics of Schottky diodes based on regioregular poly(3-hexylthiophene)/Al junction, *Curr. Appl. Phys.* 1 (2001) 355–361.
- [33] I. McCulloch, M. Heeney, C. Bailey, K. Genevicius, I. MacDonald, M. Shkunov, D. Sparrowe, S. Tierney, R. Wagner, W. Zhang, M.L. Chabiny, R.J. Kline, M.D. McGehee, M.F. Toney, Liquid-crystalline semiconducting polymers with high charge-carrier mobility, *Nat. Mater.* 5 (2006) 328–333. doi:10.1038/nmat1612.
- [34] H. Sirringhaus, Device physics of solution-processed organic field-effect transistors, *Adv. Mater.* 17 (2005) 2411–2425. doi:10.1002/adma.200501152.
- [35] M. Pandey, S. Nagamatsu, S.S. Pandey, Remarkable enhancement of carrier mobility along with anisotropic transport in non-regiocontrolled poly ( 3-hexylthiophene ) films processed by floating film transfer method, (n.d.) 1–8.

- [36] B. Kuei, E.D. Gomez, Chain conformations and phase behavior of conjugated polymers, *Soft Matter*. 13 (2017) 49–67. doi:10.1039/C6SM00979D.
- [37] B. McCulloch, V. Ho, M. Hoarfrost, C. Stanley, C. Do, W.T. Heller, R.A. Segalman, Polymer chain shape of poly(3-alkylthiophenes) in solution using small-angle neutron scattering, *Macromolecules*. 46 (2013) 1899–1907. doi:10.1021/ma302463d.
- [38] J. Li, Y. Zhao, H.S. Tan, Y. Guo, C.A. Di, G. Yu, Y. Liu, M. Lin, S.H. Lim, Y. Zhou, H. Su, B.S. Ong, A stable solution-processed polymer semiconductor with record high-mobility for printed transistors, *Sci. Rep.* 2 (2012) 1–9. doi:10.1038/srep00754.
- [39] S. Thienothiophene, *Advanced Materials Interfaces Rapid formation of Macroscopic Self-Assembly of Liquid Crystalline , High Mobility , (n.d.)*.
- [40] K. Bhargava, A. Bilgaiyan, V. Singh, Two dimensional optoelectronic simulation based comparison of top and bottom contact organic phototransistors, *J. Nanosci. Nanotechnol.* 15 (2015). doi:10.1166/jnn.2015.10737.
- [41] P. Pingel, A. Zen, D. Neher, I. Lieberwirth, G. Wegner, S. Allard, U. Scherf, Unexpectedly high field-effect mobility of a soluble, low molecular weight oligoquaterthiophene fraction with low polydispersity, *Appl. Phys. A Mater. Sci. Process.* 95 (2009) 67–72. doi:10.1007/s00339-008-4994-0.
- [42] T. Endo, T. Nagase, T. Kobayashi, H. Naito, Highly Oriented Polymer Field-Effect Transistors with High Electrical Stability Highly Oriented Polymer Field-Effect Transistors with High Electrical Stability, 121601 (2013) 8–11.
- [43] H. Xu, T. Xiao, J. Li, J. Mai, X. Lu, N. Zhao, In Situ Probing of the Charge Transport Process at the Polymer/Fullerene Heterojunction Interface, *J. Phys. Chem. C*. 119 (2015) 25598–25605. doi:10.1021/acs.jpcc.5b07810.
- [44] Y. Hosokawa, M. Misaki, S. Yamamoto, M. Torii, K. Ishida, Y. Ueda, Molecular orientation and anisotropic carrier mobility in poorly soluble polythiophene thin films, *Appl. Phys. Lett.* 100 (2012). doi:10.1063/1.4718424.

## ***Chapter: 6 Orientation and anomalous charge transport in regioregular poly (3-alkylthiophenes)***

### **6.1 Introduction**

Over the last two-decade conjugated polymer have been the great discussion for various type of application including thin film organic field effect transistors (OFETs)[1-3] photovoltaic cell[4,5] organic light emitting diode[6-7] actuator and sensor. The processing condition such as solution processability and low temperature is very important for low cost and wide area electronics manufacturing. Usually the film preparation in conjugated polymer via solution processing exhibit semi crystalline structure in which the presence of few crystals with a mostly disorder matrix [8,9]. Such type of disorder responsible for degrade the device performance and adverse for efficient charge hopping between transport location [10,11]. A great effort have been made by controlling the thin film morphology and alignment to boost charge carrier mobility for high performance devices.

Present day conjugated polymers of both electron and hole have been developed and their charge carrier mobility reach up to  $10 \text{ cm}^2/\text{Vs}$ , [12-14] which is important switching frequencies for any transistors. Even though this value is 2 orders lower as compared to doped semi crystalline Si but direct contest with amorphous silicon and accompanying them edge of commercialization in various type of flexible display and photovoltaic devices [5,15,16]. To date, various orientation technique have been used to align the conjugated polymers main chain for high performance optoelectronics devices [17]. By considering these a some of technique such as mechanical rubbing,[17] friction transfer method,[18] high temperature rubbing [19] solution flow [20] and drawing[21] etc. Although these techniques have been, make effort to orient the conjugated polymers to achieve their outcome in the development of charge transport of organic FET. On the



other hand, these techniques have some defect like consumption of material, mechanical damage, charge accumulation on surface, solubility in interatrial layer and possibility of some barrier of multilayer casting. To resolve such type of issues have been challenge for the researcher. Our group have been developed a technique to make oriented film easily by casting a polymer solution on orthogonal liquid substrate named as dynamic floating film transfer method with nominal material wastage [22,23]. However, the oriented film having at cm scale but still we have some challenges like film non-uniformity in the form of thickness, directionality by controlling direction. To resolve such type of issues and further extend this method by simple using assisting slider to control the spreading in unidirectional named as ribbon shaped FTM [24,25]. In this method the film formation shape resemble like a large ribbon in unidirectional and easily transfer on desire substrate to further analysis.

In this work, we would like to report about orientation analysis of regioregular poly (3- alkyl thiophene) active semiconducting material (alkyl= butyl, hexyl, octyl, decyl and dodecyl). Film orientation have been demonstrated by ribbon shape FTM and molecular ordering of alkyl group were varied based on alkyl chain length. The effect of edge on and face on orientation was discussed in OFET performance by increasing alkyl carbon number.

## **6.2 Experimental Work**

The regioregular Poly (3 –alkyl thiophene) purchased from sigma Aldrich, having head to tell (HT) coupling 98.5% in case of PHT, PDT and PDDT and 80-90% in case of P BuT. The solvent anhydrous chloroform also purchased from sigma Aldrich for dissolving the all polymers. The molecular weight of P BuT, PDT and PDDT was 54000, 42000 and 60000 kg/M respectively listed in table 1. Polymer solution was prepared 2% and 0.5% (W/W) concentration by dissolving in super dehydrated chloroform with 0.001% of maximum water content for thin film casting of

oriented and spin coated method. Alkyl chain length dependence large area oriented thin film prepared by ribbon shaped floating film transfer method [24,26]. For comparison we also prepared thin film by using spin coating followed by 3000 rpm with time duration 120 sec. The oriented film was transferred on desired substrate for optical and electrical characterization. For the measurement of out of plane XRD, sample was prepared by ribbon shaped FTM with HMDS treated on bare silicon substrate by multiple casting for appropriate thicker film up to 700nm for getting at least significant XRD signal intensity without affecting the film morphology. Polarized electronics absorbance spectra was done by using UV visible NIR spectrophotometer (JASCO V-570) attached with Glan Thompson prism. In order to measure the optical anisotropy, rotating polarizer was used before the detector that was rotated according to the angle setting. Optical anisotropy was estimated by in terms of Dichroic Ratio (DR) by polarized absorbance spectra and calculated by this equation  $DR = A_{\parallel} / A_{\perp}$ , where  $A_{\parallel}$  indicate maximum absorbance when polarization direction  $\parallel$  to the orientation direction and  $A_{\perp}$  indicate absorbance in perpendicular direction ( $\perp$ ) at the same wavelength of  $A_{\parallel}$ .

For electrical characterization, OFETs were fabricated by using highly doped p- type Si substrate with 300 nm grown SiO<sub>2</sub> insulating layer having capacitance ( $C_i = 10 \text{ nf/cm}^2$ ). To make SiO<sub>2</sub> surface treatment was done by octadecyltrichlorosilane for the formation of highly hydrophobic self-assemble monolayer which also support better adhesion of floating film. Si Substrate was dip in 8 mM OTS solution mixed with toluene in packed glass petri dish at 90 °C for 2 hours followed by washing in toluene and dry at 130 °C. Oriented floating film was transferred on OTS treated substrate by stamping. 50 nm Source and drain gold electrode were deposited at the rate of 1.5 Å/s in thermal evaporator chamber with high vacuum pressure  $10^{-6}$  torr using nickel mask. The channel length (L) and width (W) was fixed for all devices 20  $\mu\text{m}$  and 2 mm, respectively. Electrical

characterization were estimated by computer controlled 2 channel electrometer (Kiethley 2612) at vacuum of  $10^{-3}$  torr. For comparison we also prepared spin coated sample with concentration of 0.5 % w/w in chloroform for OFET fabrication.

## **6.3 Result and Discussion**

### **6.3.1 Fabrication of Oriented Thin Films**

Dynamic FTM is a facile method for thin film fabrication in ambient atmosphere without high pressure vacuum so attracted me for further studied. As already reported FTM method, during the film casting polymer solution free to move in all direction and making the floating film in circular shape. This circular shape film little difficult to transfer on desired substrate so we developed this method by changing the shape in rectangular by providing the directionality through handmade assisting slider [24]. Extant of orientation, thickness and size of film were controlled by some casting parameters such as concentration of polymer solution, casting temperature and viscosity of liquid substrate [24,26]. In this studies, even series of carbon chain of Poly (3-alkyl thiophene) were used for making oriented thin film for OFET fabrication. Although this poly (3-alkyl thiophene) series as previously reported by some colleagues and other groups but different method such as spin coating and time of flite (TOF).The main reason to utilized long alkyl chain length because of high solubility in organic solvent [27]. For making film we drop a 20-25  $\mu$ l of polymer solution in center of slider which is dipped in rectangular tray with partly filled hydrophilic liquid substrate consisting of binary mixture of ethylene glycol (Eg) and Glycerol (Gl) proportion of 3:1. The dipped slider are placed in such an order which half portion slope touch the viscous liquid substrate. When polymer solution start to spread, slider tilted bottom walls provide the directionality in a single direction and make a solid film on liquid substrate in a ribbon shape shown in fig 6.1.

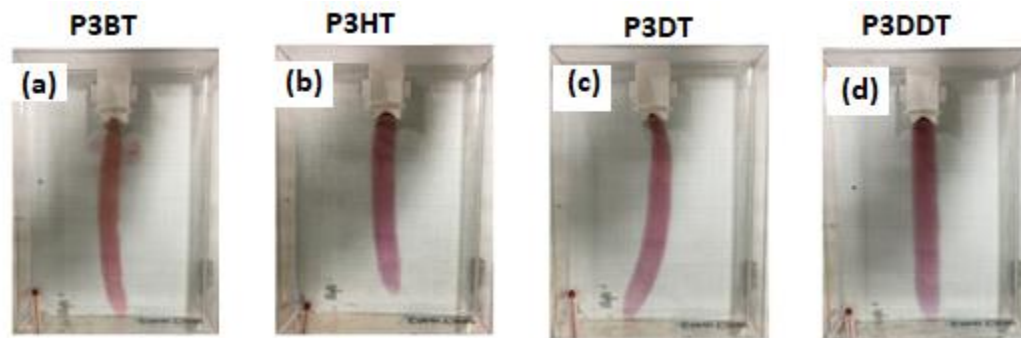


**Figure: 6.1** Floating film casting of regioregular P3ATs on hydrophilic liquid substrate by ribbon-shaped FTM a) Butyl b) hexyl c) decyl and d) dodecyl.

The main key feature of this method is film was prepared by natural self-assembly process without any external force or controlling setup like LB or other method. In this method film was aligned by dynamic solidification by solvent evaporation during spreading and internal compressed force in opposite direction of film expansion try to align the polymer film. During the film expansion most important behavior is also inherent as a lyotropic liquid crystalline phase transition from solution phase to solid, if solidified material have LC characteristics. The film was oriented in perpendicular direction along the spreading direction that is also verified by manually by rotating polarizer film. The oriented film nature like face on and edge on orientation is also play important role for high performance according to device. As per reported, edge on orientation is favored for planer device for example OFETs. However, face on orientation is most preferred for vertical devices i.e. Solar cell and Organic light emitting diode [28,29]. It was already reported to control edge on stacking for some thiophene based conjugated polymer by [25,30,31]. In this discussion we used series of poly(3-alkyl thiophene) with increasing order of alkyl chain for making the film by FTM. After increasing the alkyl chain length it will become more hydrophobic so after casting on hydrophilic liquid which contains large OH group repulsion was also increased according to increase in alkyl chain length and support thermodynamically edge on orientation.

### 6.3.2 Polarized and Non-Polarized Electronic Absorption Spectra

Oriented film prepared by FTM was characterized by electronic absorption spectra and on the other side spin coated film was also characterized to understand the difference between them as shown in Figure 6.2 (a), from figure it is clear that poly (3-alkylthiophene) series have absorption range from 400 to 650 nm. A clear difference of absorption peak in parallel FTM and spin coat was showing by the same color in dark and dashed line for each carbon chain. The difference in absorption peak of carbon chain shows red shift in Parallel FTM as compared to spin coat. In series of poly (3-alkyl thiophene) there was a maximum peak at 516 nm, 542nm, 554nm and 552nm in parallel FTM while 506nm, 530nm, 536nm and 538 nm in spin coated respectively. From these maximum peaks, there was a clear red shift up to 10 nm, 12 nm, 18nm and 16 nm in parallel FTM and blue shift in spin coat. This result indicate alkyl chain length dependence red shift in Poly (3-alkyl thiophene) series. The red shift was increased almost after increasing alkyl chain length. Apart from chain length dependence red shift vibronic shoulder is also clear after increasing the chain length. The 2<sup>nd</sup> vibronic mode 0-0 of alkyl group was similar for C4 and C6 at 600nm on the other hand 606nm for C10 and C12. This vibronic mode was explained by spano associated with electronic structure of excitonic bandwidth (W) with intermolecular coupling transition energy  $E_p$  from equation. [32].

$$\frac{A_{0-0}}{A_{0-1}} = \left[ \frac{1 - 0.24 \frac{W}{E_p}}{1 + 0.073 \frac{W}{E_p}} \right]^2 \quad (1)$$

Where  $A_{0-0}$  and  $A_{0-1}$  intensities of the 0-0 and 0-1 transition. Oriented film optical anisotropy was identified in terms of dichroic ratio (DR). This DR was calculated by the ratio of maximum absorbance parallel at  $\lambda_{\max\parallel}$  to absorbance in perpendicular at  $\lambda_{\max\parallel}$  ( $DR = A_{\parallel}/A_{\perp}$ ).

Figure 6.2 (b) shown the alkyl group dichroic ratio where the dichroic ratio is a function of carbon number. From figure 6.2 (b), C4 have dichroic ratio 1.2 and increase 2.2 in C6 and again slightly decrease in C10 and C12 such as 1.8 and 1.5 respectively. This trend little surprise me because orientation in alkyl group slightly increase and decrease by increasing in carbon number. From my knowledge some body reported orientation in C6 (P3HT) by using different orientation method [33,34]. M. Pandey et al. also reported [35] orientation in C6 RR-P3HT and achieve DR 1.5 which is slightly less as compared to in my case 2.2. This mechanism was further understand by some characterization in next section.

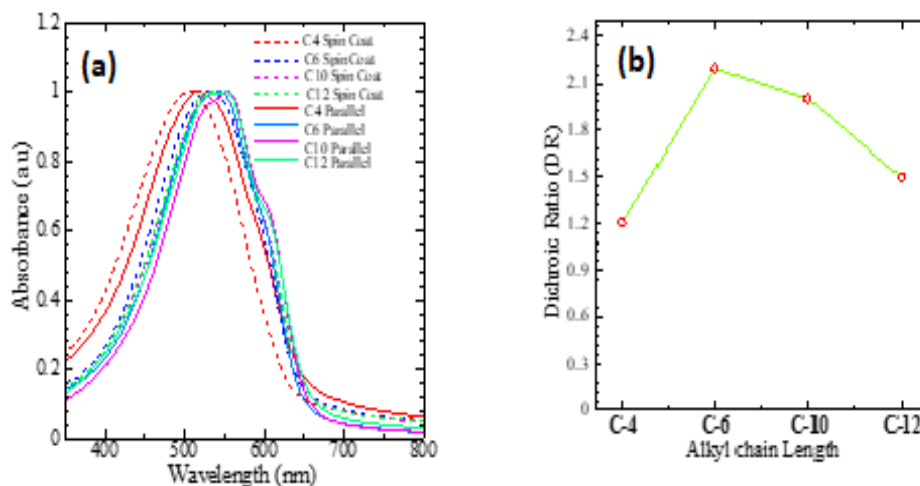


**Figure: 6.2** Absorption spectra of FTM film in parallel (dark color) and spin coat (dashed line) (a) Orientation (DR) is a function of carbon number (b).

### 6.3.2 XRD Analysis

Oriented film prepared by FTM was further studied to investigate crystallinity and stacking by XRD measurement in out of plane. Figure 6.3 (a) shown X-ray diffraction characterization in out of plane for various alkyl chain. There was a sharp peak up to 3 order of (h00) series indicate alkyl stacking in oriented film. These 3 peak full width half maximum (FWHM) showing at low angle region. From figure most important thing is also absorbed after increasing the carbon number these peak shifted at low angle side in PAT series.

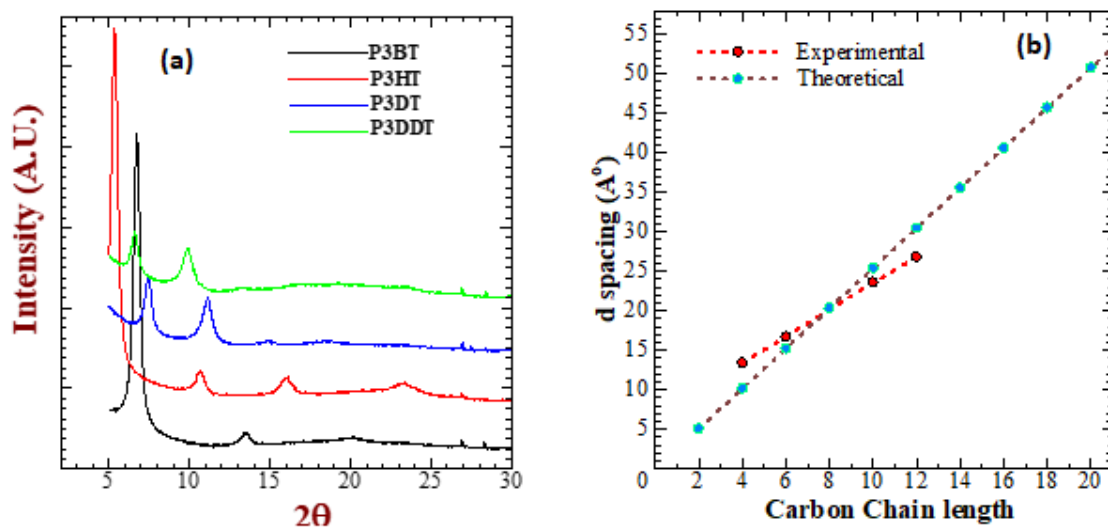


**Figure: 6.3** X-ray diffraction profile in out of plane of various alkyl chain P3AT (a) d space in oriented film calculated by XRD measurement function of alkyl carbon Number (b).

To further understand the mechanism of alkyl PAT in terms of polymer chain distribution in oriented film prepared by FTM we calculated the d spacing by using XRD peak at 2θ angle with the help of Scherer equation. The oriented film d spacing shown in figure 6.3 (b) as function of alkyl carbon number. This graph shows as a sublinear relationship in d spacing and PAT group

while increasing the alkyl carbon number. On the other hand this relationship is little different reported by W. Takashima et al [27] by using spin coat and drop cost method .In this reported method, linear relationship observed while increasing the alkyl carbon number. So this relationship created more interest to further studied to understand the main mechanism.

To investigate the mechanism of slightly decrease orientation in P3AT on the basis of alkyl carbon number was understand by d spacing calculated by manually and XRD measurement. The concept of mechanism possibility was explained from figure 6.4. In figure shown the polymer chain arrangement on the basis of d spacing. The d spacing was decreased when film was prepared by FTM as compared to manually calculation after increment of alkyl carbon number. The d spacing estimation in butyl thiophene was almost same as manually so possibility polymer chain arrangement from one chain to another on at edge. But after increment alkyl carbon number, hexyl thiophene shows slightly decrease in d spacing as compared to manually so polymer chain touch from one chain to another and showing one of the highest DR 2.2 as compared to other .After increment further in carbon number such as decyl and dodecyl thiophene, d spacing further decreased so polymer chain overlap inside and create a problem of inter-digitation. This inter-digitation slightly decrease orientation in alkyl group due to overlap in long chain.

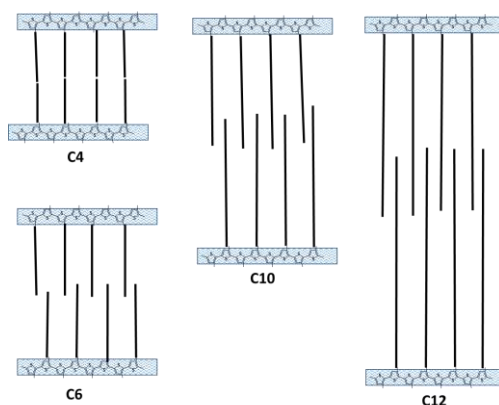
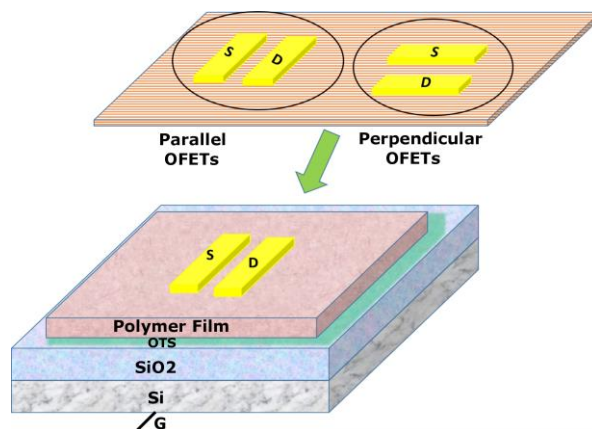




Figure: 6.4 Interdigitation of alkyl chains in the P3AT on the basis of d spacing as a function of theoretically and XRD calculation

### 6.3.2 Anisotropic Charge Transport

To investigate the charge transport bottom gate top contact OFETs are fabricated by using alkyl group as an active semiconducting layer in a channel deposited by FTM shown in figure 6.5. Although similar configuration type of OFET fabricated by some colleague other group by different method such as Spin coat, drop cast and time of flite (TOF) method [32,33,35] by using the PAT as a semiconducting material in channel. These reported method are an isotropic in nature so directly deposited without changing the angle position of mask. But in FTM method mask was used in orientation direction (parallel) as well as its opposite direction (perpendicular) by changing the position of nickel shadow mask that is also shown in figure 6.5



**Figure: 6.5** OFET architecture and mechanism of orientation deposition in parallel and perpendicular by using a nickel shadow mask.

OFETs electrical characterization was measured to check the behavior and its charge transport performance. Figure 6.6 show the one of the typical output and transfer characteristics of regio-regular P3HT in parallel and perpendicular. In figure 6.6 (a) the clear p type transistor behavior

was observed in parallel and perpendicular, where gate to source voltage ( $V_{GS}$ ) varied from 0 to -80 V and achieved  $10^{-5}$   $\mu$ A high drain current at constant drain to source voltage ( $V_{DS}$ ) -80 V. Apart from p-type behavior there was a clear difference in parallel and perpendicular, it reflects because of orientation .charge transport was measured in terms of mobility by using the transfer characteristics shown in Figure 6.6 (b). From figure, there was a clear transfer characteristic in drain current ( $I_D$ ) and gate to source voltage ( $V_{GS}$ ) slightly different in parallel and perpendicular because of orientated film . The mobility was calculated when drain current start to saturate at condition  $V_{DS} \geq V_{GS} - V_{th}$  and constant current flow in channel that is expressed in equation 2.

$$I_D = \frac{1}{2} \mu_n C_{ox} \frac{W}{L} [V_{GS} - V_{th}]^2 \quad (2)$$

In this article, mobility was calculated by using oriented film of P3AT series prepared by FTM. Here mobility was function of alkyl carbon number and slightly varies by increment in carbon number. In butyl thiophene the mobility was observed  $1.4 \times 10^{-2}$   $\text{cm}^2/\text{Vs}$  in parallel and  $1.0 \times 10^{-2}$   $\text{cm}^2/\text{Vs}$  in perpendicular but after increment in carbon number in case hexyl thiophene the mobility was increased up to 2-3 times such as  $3.0 \times 10^{-2}$   $\text{cm}^2/\text{Vs}$  in parallel and  $1.7 \times 10^{-2}$   $\text{cm}^2/\text{Vs}$ . The most important thing after further increment in alkyl carbon number in decyl and dodecyl thiophene, mobility was slightly decrease as compared to hexyl thiophene. This slightly decrease mobility was  $2.6 \times 10^{-2}$  ,  $2.4 \times 10^{-2}$   $\text{cm}^2/\text{Vs}$  in parallel and  $1.9 \times 10^{-2}$ ,  $2.0 \times 10^{-2}$   $\text{cm}^2/\text{Vs}$  in perpendicular respectively. On the other hand , similar type of regio- regular P3AT series was also used for OFETs fabrication by the some previously lab member and some other group member using different isotropic method such as drop cast ,spin coat and time of flight (TOF) method [27]. These reported result little surprised me because there was a large variation in mobility after increase the alkyl carbon number. This large variation mobility was decreased up to 3 order not in 1 or 2 times as per in my case. Charge transport anisotropy was investigated by dividing the ratio of mobility

in parallel and perpendicular ( $\frac{\mu_{\parallel}}{\mu_{\perp}}$ ). Charge transport anisotropy was also reflect similar trend as in case of optical such as 1.4, 1.8, 1.4 and 1.2 respectively mention in table 1. One of the most important parameter was investigated by calculating off current when the device is in off mode  $I_{off}$  and on current when device start  $I_{on}$ . The ratio ( $\frac{I_{on}}{I_{off}}$ ) was decide the switching speed of device. The device ( $\frac{I_{on}}{I_{off}}$ ) was  $10^4$  in case of hexyl, decyl, dodecyl and  $10^3$  in case of butyl noted in table.

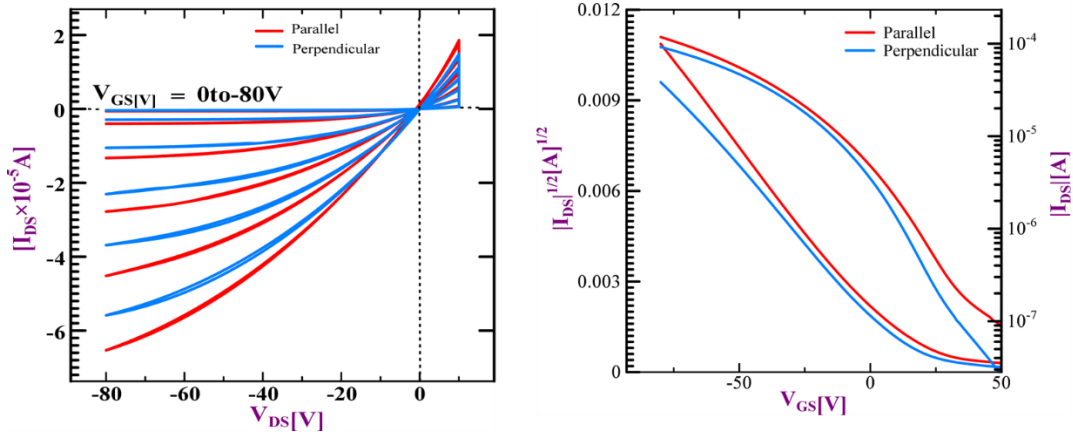
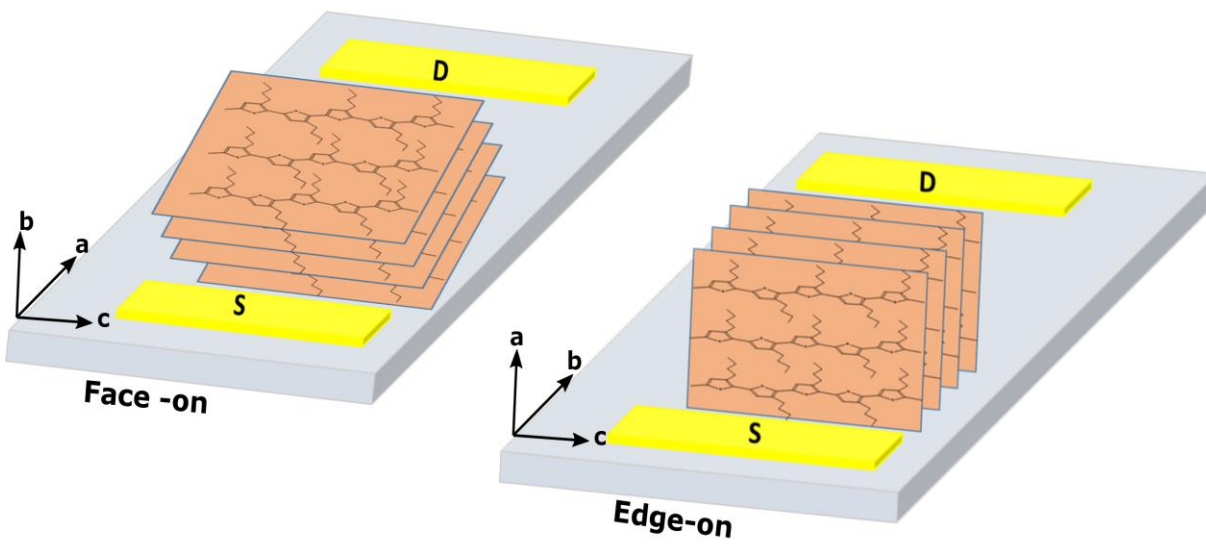


Figure: 6.6 Electrical characterization of OFET in parallel (red) and perpendicular (blue) a) output characteristics b) transfer characteristics.

**Table-1** Anisotropic electrical parameters deduced from OFETs using thin films of P3AT alkyl group of CPs fabricated by ribbon-shaped FTM.

Conducting Polymers	FTM [ $\mu_{\parallel}$ ] ( $\text{cm}^2 \cdot \text{V}^{-1} \cdot \text{s}^{-1}$ )	FTM [ $\mu_{\perp}$ ] ( $\text{cm}^2 \cdot \text{V}^{-1} \cdot \text{s}^{-1}$ )	( $\mu_{\parallel} / \mu_{\perp}$ )	$I_{ON}/I_{OFF}$	DR
C4	$1.4 \times 10^{-2}$	$1.0 \times 10^{-2}$	1.4	$10^3$	1.2
C6	$3.0 \times 10^{-3}$	$1.7 \times 10^{-2}$	1.8	$10^4$	2.2
C10	$2.6 \times 10^{-3}$	$1.9 \times 10^{-2}$	1.4	$10^4$	1.8

C12	$2.4 \times 10^{-3}$	$2.0 \times 10^{-2}$	1.2	$10^4$	1.5
-----	----------------------	----------------------	-----	--------	-----



**Figure: 6.7** Role of face on and edge on orientation of P3ATs for OFET applications

Charge transport unaffected by increasing alkyl chain length was clearly understood by figure 6.7. In figure face on and edge on mechanism was applied in channel and explained charge transport from one electrode (S) to another electrode Drain (D). As per previously reported film prepared by spin coat, drop cast and time of flight (TOF) show face on orientation [27] but on the other hand edge on orientation in FTM film [25]. In face on orientation charge transport transfer from one plain to another plain by hopping on the other hand in edge on orientation charge transfer through polymer chain stacking. Charge transport hopping in face on is difficult because of hopping distance and resultant some charge consumed during hopping decrease in mobility. But in edge on, transport is easy because charge transfer through polymer chain stacking and it is much closed to another stacking. After increase in alkyl carbon number charge hopping is more difficult in face on because distance increased from one polymer chain to other so mobility drastically decreased

up to 3 to 4 order in decyl and dodecyl thiophene. But charge transport not so much disturb by increment in alkyl carbon number in edge on because of polymer chain stacking is more closed.

## 6.4 Conclusion

In summary, we conclude, large area oriented thin film prepared by ribbon shaped FTM. Alkyl chain length dependent orientation was investigated by polarized absorption spectra in parallel and perpendicular and calculated by dichroic ratio. Orientation was slightly decreased after increment in alkyl carbon number because of interdigitation investigated by d spacing based on XRD measurement. In alkyl group poly (3-hexyl thiophene) show one of the highest DR=2.2. The other remaining carbon chain showing slightly decreased in dichroic ratio. Apart from orientation alkyl carbon number dependence charge transport was also investigated and achieved slightly variation in mobility because of edge on orientation unlike to other group. In these alkyl group poly(3-hexyl thiophene) show one of the highest mobility  $3.0 \times 10^{-2} \text{ cm}^2/\text{vs}$ .

## 6.4 References

- [1] B.G. Kim, E.J. Jeong, J.W. Chung, S. Seo, B. Koo, J. Kim, A molecular design principle of lyotropic liquid-crystalline conjugated polymers with directed alignment capability for plastic electronics, *Nat. Mater.* 12 (2013) 659–664. doi:10.1038/nmat3595.
- [2] M. Ikawa, T. Yamada, H. Matsui, H. Minemawari, J. Tsutsumi, Y. Horii, M. Chikamatsu, R. Azumi, R. Kumai, T. Hasegawa, Simple push coating of polymer thin-film transistors, *Nat. Commun.* 3 (2012) 1–8. doi:10.1038/ncomms2190.
- [3] H. Sirringhaus, Device physics of solution-processed organic field-effect transistors, *Adv. Mater.* 17 (2005) 2411–2425. doi:10.1002/adma.200501152.
- [4] M.C. Scharber, On the Efficiency Limit of Conjugated Polymer:Fullerene-Based Bulk Heterojunction Solar Cells, *Adv. Mater.* 28 (2016) 1994–2001. doi:10.1002/adma.201504914.
- [5] G. Li, R. Zhu, Y. Yang, Polymer solar cells, *Nat. Photonics.* 6 (2012) 153–161. doi:10.1038/nphoton.2012.11.
- [6] A. Sandstrom, H.F. Dam, F.C. Krebs, L. Edman, Ambient fabrication of flexible and large-area organic light-emitting devices using slot-die coating, *Nat. Commun.* 3 (2012).
- [7] J. Liang, L. Li, X. Niu, Z. Yu, Q. Pei, Elastomeric polymer light-emitting devices and displays, *Nat. Photonics.* 7 (2013) 817–824. doi:10.1038/nphoton.2013.242.
- [8] H. Tanaka, M. Hirate, S. Watanabe, S. Kuroda, Microscopic Signature of Metallic State in Semicrystalline Conjugated Polymers Doped with Fluoroalkylsilane Molecules, (2014) 2376–2383. doi:10.1002/adma.201304691.
- [9] A. Salleo, R.J. Kline, D.M. DeLongchamp, M.L. Chabinyc, Microstructural characterization and charge transport in thin films of conjugated polymers, *Adv. Mater.* 22 (2010) 3812–3838. doi:10.1002/adma.200903712.
- [10] R. Noriega, J. Rivnay, K. Vandewal, F.P. V Koch, N. Stingelin, P. Smith, M.F. Toney, A. Salleo, A general relationship between disorder, aggregation and charge transport in conjugated polymers, *Nat. Mater.* 12 (2013) 1038–1044. doi:10.1038/nmat3722.
- [11] L.H. Jimison, M.F. Toney, I. McCulloch, M. Heeney, A. Salleo, Charge-Transport Anisotropy Due to Grain Boundaries in Directionally Crystallized Thin Films of Regioregular Poly(3-hexylthiophene), *Adv. Mater.* 21 (2009) 1568–1572. doi:10.1002/adma.200802722.
- [12] E.G. Bittle, J.I. Basham, T.N. Jackson, O.D. Jurchescu, D.J. Gundlach, Mobility overestimation due to gated contacts in organic field-effect transistors, *Nat. Commun.* 7 (2016) 1–7. doi:10.1038/ncomms10908.
- [13] D. Venkateshvaran, M. Nikolka, A. Sadhanala, V. Lemaire, M. Zelazny, M. Kepa, M. Hurhangee, A.J. Kronemeijer, V. Pecunia, I. Nasrallah, I. Romanov, K. Broch, I. McCulloch, D. Emin, Y. Olivier, J. Cornil, D. Beljonne, H. Sirringhaus, Approaching disorder-free transport in high-mobility conjugated polymers, *Nature.* 515 (2014) 384–388. doi:10.1038/nature13854.

- [14] M. Caironi, M. Bird, D. Fazzi, Z. Chen, R. Di Pietro, C. Newman, A. Facchetti, H. Sirringhaus, Very low degree of energetic disorder as the origin of high mobility in an n-channel polymer semiconductor, *Adv. Funct. Mater.* 21 (2011) 3371–3381. doi:10.1002/adfm.201100592.
- [15] H. Sirringhaus, 25th anniversary article: Organic field-effect transistors: The path beyond amorphous silicon, *Adv. Mater.* 26 (2014) 1319–1335. doi:10.1002/adma.201304346.
- [16] F.C. Krebs, M. Hösel, M. Corazza, B. Roth, M. V. Madsen, S.A. Gevorgyan, R.R. Søndergaard, D. Karg, M. Jørgensen, Freely available OPV—The fast way to progress, *Energy Technol.* 1 (2013) 378–381. doi:10.1002/ente.201300057.
- [17] M. Brinkmann, L. Hartmann, L. Biniek, K. Tremel, N. Kayunkid, Orienting semi-conducting pi-conjugated polymers, *Macromol. Rapid Commun.* 35 (2014) 9–26. doi:10.1002/marc.201300712.
- [18] S. Nagamatsu, W. Takashima, K. Kaneto, Y. Yoshida, N. Tanigaki, K. Yase, K. Omote, Backbone arrangement in “friction-transferred” regioregular poly(3-alkylthiophene)s, *Macromolecules.* 36 (2003) 5252–5257. doi:10.1021/ma025887t.
- [19] L. Biniek, N. Leclerc, T. Heiser, R. Bechara, M. Brinkmann, Large scale alignment and charge transport anisotropy of pBTTT films oriented by high temperature rubbing, *Macromolecules.* 46 (2013) 4014–4023. doi:10.1021/ma400516d.
- [20] N. Yamasaki, Y. Miyake, H. Yoshida, A. Fujii, M. Ozaki, Solution flow assisted fabrication method of oriented  $\pi$ -conjugated polymer films by using geometrically-asymmetric sandwich structures, *Jpn. J. Appl. Phys.* 50 (2011). doi:10.1143/JJAP.50.020205.
- [21] S. Nagamatsu, W. Takashima, K. Kaneto, Y. Yoshida, N. Tanigaki, K. Yase, Polymer field-effect transistors by a drawing method, *Appl. Phys. Lett.* 84 (2004) 4608–4610. doi:10.1063/1.1751222.
- [22] T. Morita, V. Singh, S. Nagamatsu, S. Oku, W. Takashima, K. Kaneto, Enhancement of transport characteristics in poly(3-hexylthiophene) films deposited with floating film transfer method, *Appl. Phys. Express.* 2 (2009) 1–4. doi:10.1143/APEX.2.111502.
- [23] A. Dauendorffer, S. Nagamatsu, W. Takashima, K. Kaneto, Optical and transport anisotropy in poly(9,9-dioctyl-fluorene-alt-bithiophene) films prepared by floating film transfer method, *Jpn. J. Appl. Phys.* 51 (2012). doi:10.1143/JJAP.51.055802.
- [24] A. Tripathi, M. Pandey, S. Nagamatsu, S.S. Pandey, S. Hayase, W. Takashima, Casting Control of Floating-films into Ribbon-shape Structure by modified Dynamic FTM, *J. Phys. Conf. Ser.* 924 (2017). doi:10.1088/1742-6596/924/1/012014.
- [25] A.S.M. Tripathi, M. Pandey, S. Sadakata, S. Nagamatsu, Anisotropic charge transport in highly oriented films of semiconducting polymer prepared by ribbon-shaped floating film, (n.d.). doi:10.1063/1.5000566.
- [26] R.H. Lohwasser, M. Thelakkat, Toward perfect control of end groups and polydispersity in poly(3-hexylthiophene) via catalyst transfer polymerization, *Macromolecules.* 44 (2011) 3388–3397. doi:10.1021/ma200119s.

- [27] W. Takashima, S.S. Pandey, T. Endo, M. Rikukawa, N. Tanigaki, Y. Yoshida, K. Yase, K. Kaneto, Photocarrier transports related to the morphology of regioregular poly(3-hexylthiophene) films, *Thin Solid Films*. 393 (2001) 334–342. doi:10.1016/S0040-6090(01)01109-9.
- [28] H. Sirringhaus, P.J. Brown, R.H. Friend, M.M. Nielsen, K. Bechgaard, A.J.H. Spiering, Two-dimensional charge transport in conjugated polymers, (1999) 685–688.
- [29] J.R. Tumbleston, B.A. Collins, L. Yang, A.C. Stuart, E. Gann, W. Ma, W. You, H. Ade, The influence of molecular orientation on organic bulk heterojunction solar cells, *Nat. Photonics*. 8 (2014) 385–391. doi:10.1038/nphoton.2014.55.
- [30] J. Noh, S. Jeong, J.Y. Lee, Ultrafast formation of air-processable and high-quality polymer films on an aqueous substrate, *Nat. Commun.* 7 (2016) 1–9. doi:10.1038/ncomms12374.
- [31] R.K. Pandey, A.K. Singh, R. Prakash, Directed self-assembly of poly(3,3'-dialkylquaterthiophene) polymer thin film: Effect of annealing temperature, *J. Phys. Chem. C*. 118 (2014) 22943–22951. doi:10.1021/jp507321z.
- [32] F.C. Spano, Modeling disorder in polymer aggregates: The optical spectroscopy of regioregular poly(3-hexylthiophene) thin films, *J. Chem. Phys.* 122 (2005). doi:10.1063/1.1914768.
- [33] A. Babel, S.A. Jenekhe, Alkyl chain length dependence of the field-effect carrier mobility in regioregular poly(3-alkylthiophene)s, *Synth. Met.* 148 (2005) 169–173. doi:10.1016/j.synthmet.2004.09.033.
- [34] K. Kaneto, W.Y. Lim, W. Takashima, T. Endo, M. Rikukawa, Alkyl Chain Length Dependence of Field-Effect Mobilities in Regioregular Poly ( 3-Alkylthiophene ) Films I ' D (  $\mu A$  ) I D (  $\mu A$  ), *Jpn. J. Appl. Phys.* 39 (2000) L872–L874. doi:10.1063/1.1891301.
- [35] M. Pandey, S.S. Pandey, S. Nagamatsu, S. Hayase, W. Takashima, Influence of backbone structure on orientation of conjugated polymers in the dynamic casting of thin floating-films, *Thin Solid Films*. 619 (2016) 125–130. doi:10.1016/j.tsf.2016.11.015.



## ***Chapter: 7 General conclusion and future work***

Fabrication of large area, uniform and oriented thin films or organic semiconductor is highly desired for the practical implementation and large-scale application of organic electronic devices. Research work in this thesis revolves around application of FTM for the fabrication of large area oriented thin films on desired substrate, their characterization and application as active semiconductor element for the investigation of anisotropic charge transport after OFET fabrication. Implementation of newly designed PTFE slider led to fabrication of large area and oriented ribbon-shaped films and a number of conjugated polymers have been successfully oriented.

In the first chapter, we have discussed the basic introduction of inorganic and organic semiconductor technology and focused on organic semiconductor materials especially organic conjugated polymers. Role of the molecular orientation in conjugated polymers for OFETs have been critically reviewed taking different exiting orientation control method in combination with conventional FTM reported previously. Apart from this, related discussion have also been made pertaining to the various OFET device architectures, working principle and their electrical characterization parameters.

Second chapter deals with materials, processes and characterization techniques used for the present research. Details about the conjugated polymer utilized, thin film fabrication techniques, characterization methods for molecular orientation of the fabricated thin film along with fabrication and characterization of the OFETs have been discussed.

In the third chapter, a new method named as ribbon-shaped FTM has been utilized in order to fabricate large area oriented thin films by improvising conventional FTM using a newly designed

PTFE slider. Utilizing NR-P3HT as a representative conjugated polymer, parametric optimization in terms of concentration of polymer solution, casting temperature and viscosity of the liquid substrate have been amicably made in order to control the molecular anisotropy while maintaining the large area and film uniformity.

Fourth chapter deals with fabrication and optoelectronic characterization anisotropic large area thin films conjugated polymer PQT-C12. Implication of casting temperature upon the extent of molecular orientation has been clearly demonstrated along with observation of very high optical anisotropy ( $DR > 22$ ) under optimized casting condition. In plane GIXD, measurement clarified the edge-on orientation, which is highly desired for high performance planner device. By controlling the synthetic parameters PQT-C12 with different in molecular weight and polydispersity index (PDI) were synthesized and subjected to investigation pertaining to the implication of molecular weight and PDI upon the extent of molecular orientation and anisotropic charge transport. These four extract showing the variation in molecular orientation and in charge carrier transport.

In the fifth chapter, five different conjugated polymers such as PQT-C12, F8T2, NR-P3HT, PBTTT-C14 and PTB7 were utilized for the fabrication of large area oriented thin films by ribbon-shape FTM. It has been shown that all of the polymers provide large area oriented thin films with dimensions 20 cm in length  $\times$  2 cm in width with only 20  $\mu$ l polymer solution. Under similar casting conditions, polymers exhibited differential molecular orientation, which was explained considering the nature and rigidity of polymeric chains in the light of reported values of persistent length. Amongst used CPs, PQT-C12 not only exhibits highest optical anisotropy but also highest anisotropic charge transport with best device performance and a charge carrier mobility  $5 \times 10^{-2}$   $\text{Cm}^2/\text{Vs}$  in parallel orientation.

In the chapter six, regioregular poly(3-alkylthiophene) with varying alkyl chain length were utilized for the fabrication of large area oriented thin films and investigation of anisotropic charge transport. Extent of molecular orientation was found to decrease as a function of increasing alkyl chain length because of enhanced interdigitation as evidenced by XRD measurements. Problem of drastically hampered charge mobility in long chain regioregular P3ATs has been amicably solved by utilizing FTM processed oriented films, where there was only a slight decrease in the mobility even for longest alkyl chain (C18) substituted P3AT. This was attributed to the attainment of edge-on orientation, whether hindrance in in-plane transport is minimized since alkyl chains are out-of-plane as probed by in-plane GIXD observations.

In future point of view more development could be envisioned for the further improvisation in the ribbon shape FTM by implementing novel slider designs leading to very large area oriented thin films. At the same time, new donor-acceptor p-type conjugated polymers with high mobility ( $1-10 \text{ cm}^2/\text{Vs}$ ) have already been reported but lacks for the report of their orientation characteristics. Utilization of FTM for their orientation and optimization of casting parameters may lead to further enhancement in the charge carrier mobility. Currently ambipolar organic semiconductors are being used for organic CMOS inverters but their poor performance is still a major obstacle for practical applications in the area of organic electronics. Apart from p-type polymer, orientation n-type high mobility conjugated polymers by ribbon-shape FTM may lead to fabrication of high performance and low cost CMOS inverter and logic circuits in very cost effective solution based approaches.

## *Achievements*

### **Publications**

1. Atul S. M. Tripathi, Manish Pandey, Shifumi Sadakata, Wataru Takashima, Shuichi Nagamatsu, Shuzi Hayase, Shyam S. Pandey "Anisotropic charge transport in highly oriented films of semiconducting polymer prepared by ribbon-shaped floating film"**Applied Physics Letters** **112**, (2018)
2. Atul S. M. Tripathi, M. Pandey, S. Nagamatsu, S. S. Pandey, S. Hayase and W. Takashima "Casting Control of Floating-films into Ribbon-shape Structure by modified Dynamic FTM" **Journal of Physics: Conference Series** **924** (2017) **012014**.
3. Atul S. M. Tripathi, Nikita Kumari , Shuichi Nagamatsu, Shuzi Hayase and Shyam S. Pandey, "Large area molecular orientation of conjugated polymers by ribbon-shaped FTM and its implication on anisotropic carrier transport" **Organic Electronics** **65** (2019) **1–7**.
4. ZHEN WANG Zhaosheng Hu, MS; Muhammad A Kamarudin, Gaurav Kapil, Atul S Tripathi, MS; Qing Shen, Kenji Yoshino, Takashi Minemoto, Shyam S Pandey, Shuzi Hayase, "Enhancement of charge transport in quantum dots solar cells by N-butylamine-assisted sulfur-necking of PbS quantum dots" **Solar Energy** **174** (2018) **399–408**.
5. Nikita Kumari, **Atul S. M. Tripathi**, Manish Pandey, Shuichi Nagamatsu, Shuzi Hayase and Shyam S. Pandey<sup>1</sup> "2D Positional profiling of molecular orientation and thickness uniformity in the semiconducting polymers thin films" **Organic Electronics**, **68** (2019) **221-229**.
6. **Atul S. M. Tripathi**, Shuichi Nagamatsu, Shuzi Hayase and Shyam S. Pandey "Molecular weight dependence of aligned film prepared by dynamic FTM: Implication of optical and carrier transport anisotropy" **to be submitted Macromolecule ACS**.
7. **Rajiv Pandey, Atul Mani Tripathi**, Shyam S. Pandey, and Rajiv Prakash "2D nanosheets strengthened optical and electrical anisotropic film of polythiophene fabricated over high surface free energy mobile substrate" **Carbon**, **147** (2019) **252-261**.
8. ZHEN WANG, Anusha Pradhan, Zhaosheng Hu, MS; Muhammad A Kamarudin, **Atul S Tripathi**, MS; Qing Shen, Kenji Yoshino, Takashi Minemoto, Shyam S Pandey, Shuzi Hayase, "Passivation of grain boundary by squaraine for defect passivation and efficient perovskite solar cells" submitted **ACS Applied Material Interface**, **11** (10) (2019) **10012–10020**

## ***Presentations***

### **International Conferences (\*presenting Author)**

- 1. Atul S M, Tripathi**, Nikita, Kumari, Shuichi, Nagamatsu, Shuzi, Hayase, Shyam S, Pandey, "Utilization of Oriented Conjugated Polymer Film Prepared by ribbon shaped FTM Towards Its Application for Flexible Organic Field Effect Transistor" **6<sup>th</sup> International Symposium on Applied Engineering and Sciences (SAES2018)** KIT Japan, December 15-16, 2018.
- 2. Shyam S. Pandey**, Manish Pandey, Nikita Kumari, **Atul SM Tripathi**, Shuichi Nagamatsu and Shuzi Hayase "Correlating Molecular Orientation and Device Performance in Organic Electronic Devices based on Oriented Thin Films of Conjugated Polymers" **6<sup>th</sup> International Symposium on Applied Engineering and Sciences (SAES-2018) Kyushu Institute of Technology**, 15<sup>th</sup> – 16<sup>th</sup> Dec 2018.
- 3. Nikita Kumari**, Manish Pandey, **Atul SM Tripathi**, Shuichi Nagamatsu, Shuzi Hayase, Shyam S. Pandey, "**Two-Dimensional Positional Mapping of Macroscopically Oriented Thin Films of Organic Semiconducting Polymers**" 6<sup>th</sup> International Symposium on Applied Engineering and Sciences (SAES-2018) Kyushu Institute of Technology, 15<sup>th</sup> – 16<sup>th</sup> Dec 2018 15 Dec 2018
- 4. Shyam S. Pandey**, Manish Pandey, Nikita Kumari, **Atul SM Tripathi**, Shuichi Nagamatsu and Shuzi Hayase, "**Orientating Thin Films of Conjugated Polymers by FTM and Its Visualization by 2D Positional Mapping for Organic Electronics**" India-Japan Workshop on Biomolecular Electronics and Organic Nanotechnology for Environment Preservation (IJWBME-2018), National Physical Laboratory, New Delhi, India December 6-9, 2018 6 Dec 2018.
- 5. ASM Tripathi\***, Shifumi Sadakata, Shuichi Nagamatsu, Shuzi Hayase, Shyam Pandey, "Orientation and alkyl chain length dependence of carrier transport in regioregular Poly (3-alkylthiophenes) fabricated by ribbon shaped FTM" **International Conference on the Science and Technology of Synthetic Metals (ICSM-2018)**, July 1-6 Busan, South Korea.
- 6. Shyam Pandey\***, Manish Pandey, **ASM Tripathi**, Shifumi Sadakata, Nikita Kumari, Shuichi Nagamatsu, Shuzi Hayase "FTM as A Highly Facile Method towards Fabrication of Macroscopically Oriented Thin Films for Anisotropic Electronic Devices" **International Conference on the Science and Technology of Synthetic Metals (ICSM-2018)**, July 1-6 Busan, South Korea.
- 7. Atul S.M. Tripathi\***, Shuichi Nagamatsu, Shuzi Hayase and Shyam S Pandey "Large area orientation dependent charge transport in conjugated polymers prepared by ribbon shaped FTM Method " **55<sup>th</sup> Kyushu Branch Chemical Society Meeting**, Kitakyushu International Conference Center, Kokura, June 30, 2018.
- 8. S. S. Pandey\***, **ASM Tripathi**, S. Sadakata, M. Pandey, S. Nagamatsu, S. Hayase "Floating Film Transfer as an Unique and Cost-Effective Method for Fabrication of Macroscopically Oriented Thin Films of Conducting Polymers" **75<sup>th</sup> International Symposium on Applied Engineering and Sciences (SAES-2017)**, **University Putra Malaysia, Malaysia**, 14<sup>th</sup> – 15<sup>th</sup> Nov 2017, 15 Nov 2017.
- 9. Atul S.M. Tripathi\***, Shifumi Sadakata, Manish Pandey, Shuichi Nagamatsu, Shuzi Hayase and Shyam S Pandey "Optoelectronic Characterization of Highly Oriented Conjugated Polymers Prepared by Ribbon-Shaped Dynamic FTM" **54<sup>th</sup> Kyushu Branch Chemical Society Meeting**, Kitakyushu International Conference Center, Kokura, July 1, 2017.
- 10. Shifumi Sadakata\***, **Atul S. M. Tripathi**, Manish Pandey, Shyam S. Pandey, Shuichi Nagamatsu, Shuzi Hayase and Wataru Takashima "Mapping of molecular alignment of conducting polymer using

FTM "**54th Kyushu Branch Chemical Society Meeting**, Kitakyushu International Conference Center, Kokura, July 1, 2017.

**11. Atul S. M. Tripathi\***, Shifumi Sadakata, Manish Pandey, Shyam S. Pandey, Shuichi Nagamatsu, Shuzi Hayase and Wataru Takashima "Facile Fabrication and Orientation Analysis of Ribbon-Shaped Floating Thin Films " to be held in **9th International Conference on Materials for Advanced Technologies (ICMAT-2017)** 18 - 23 June (2017) at Suntec Singapore.

**12. Atul S. M. Tripathi\***, Manish Pandey, Shuichi Nagamatsu, Shyam Pandey, Shuzi Hayase and Wataru Takashima "Orientation Characteristics in Ribbon Shaped Floating Thin-Films of Conjugated Polymers Prepared by Dynamic FTM" **12th International Conference on Nano-Molecular Electronics** 14-16 December, 2016 (Poster : P1-35) (Selected as ICNME **2016 Best Poster Award**).

**13. A. S. M. Tripathi\***, M. Pandey, S.Sadakata, S. Nagamatsu, S. S. Pandey, S. Hayase and W. Takashima "Orientation Parameters of NR-P3HT macromolecules in a Ribbon-shape Floating-film by Dynamic FTM" **4th International Symposium on Applied Engineering and Sciences (SAES 2016)**, KIT Japan, December 17-18. (M-19) Dec 18.

**14. M. Pandey\***, **A. S. M. Tripathi**, S. Nagamatsu, S. Hayase, S. S. Pandey and W. Takashima "Solvent Driven Performance in Thin Floating Films of Conjugated Polymers for Organic Field Effect Transistor: Role of Macroscopic Orientation" **4th International Symposium on Applied Engineering and Sciences (SAES 2016)**, KIT Japan, December 17-18, 2016.

### **Domestic Conferences (\*presenting Author)**

**1. Atul S.M.Tripathi**, Rajiv K. Pandey, and Rajiv Prakash, Shuzi Hayase<sup>1)</sup>, Shyam S. Pandey "Anisotropic Optoelectrical Characterization of Oriented Conjugated Polymer-Graphene Oxide Nanocomposite Thin Films Fabricated by FTM" **28<sup>th</sup> MRS Annual meeting**, Japan, December 18-19, 2018.

**2. ASM Tripathi\***, S. Sadakata, M. Pandey, S. Nagamatsu, S. Hayase S S Pandey " Large area molecular orientation of conjugated polymers by ribbon-shaped FTM and its implication on anisotropic carrier transport" **65th Spring meeting of Japan Society Applied Physics (JSAP)**, March 17-20 (2018), March 19.

**3. Manish Pandey\***, **Atul S. M. Tripathi**, Shyam S. Pandey, Shuichi Nagamatsu, Shuzi Hayase, Wataru Takashima "Static vs. Dynamic FTM: Implication of the Solvent Evaporation on Casting Thin Floating-Films of Polymer Semiconductor" **64th Spring meeting of Japan Society Applied Physics (JSAP)**, **March 14-17 (2017)**, March 14, [14p-313-6].

**4. Shifumi Sadakata\***, **Atul S. M. Tripathi**, Manish Pandey, Shyam S. Pandey, Shuichi Nagamatsu, Shuzi Hayase and Wataru Takashima "Topical mapping of orientation distribution in floating-thin films of conjugated polymers prepared by dynamic FTM" **64th Spring meeting of Japan Society Applied Physics (JSAP)**, March 14-17 (2017), March 14, [14p-313-8].

**5. Atul S. M. Tripathi\***, Manish Pandey, Shifumi Sadakata, Shyam S. Pandey, Shuichi Nagamatsu, Shuzi Hayase and Wataru Takashima "Ribbon-shaped floating-film of polythiophene-based conjugated

polymers for orientation analysis" **64th Spring meeting of Japan Society Applied Physics (JSAP)**, March 14-17 (2017), March 14, [14p-313-7]

**6. Atul S.M. Tripathi\*** , Shifumi Sadakata , Manish Pandey , Shuichi Nagamatsu, Shuzi Hayase and Shyam S Pandey"Orientation of Conjugated Polymers by Ribbon Shaped Floating Film Transfer Method: Implication of Nature Polymeric Backbone" **78th Autumn meeting of Japan Society Applied Physics (JSAP)**, Fukuoka International Conference Center, Fukuoka, Sept 5-8 (2017), Sept 6 [6p-A413-15].

**7.** Shifumi Sadakata\* , **Atul S. M. Tripathi**, Manish Pandey, Shyam S. Pandey, Shuichi Nagamatsu, Shuzi Hayase and Wataru Takashima "Two-dimensional mapping of orientation PQT film by FTM" **78th Autumn meeting of Japan Society Applied Physics (JSAP)**, Fukuoka International Conference Center, Fukuoka, Sept 5-8 (2017), Sept 6 [6p-A413-16].

## *Acknowledgement*

I am extremely grateful to my research supervisor Prof. **Shyam S. Pandey** for his valuable advice throughout the research duration. His continuous support of my Ph.D study and related research, for his patience, motivation, and immense knowledge. His guidance helped me in all the time of research and writing of this thesis. I could not have imagined having a better advisor and mentor for my Ph.D study. Apart from research he is always there take care of us I all means

I am also special thanks **(Late) Prof. Wataru Takashima** whose contribution in these last one year is so much that it is cover the basic of my fundamental research, I wish his soul to rest in peace. I am very thankful to **Prof. Shuzi Hayase** for providing all required research facilities needed to carry out this research. I am thankful to **Prof. Shuichi Nagamatsu** for his valuable discussions and comments on my work. I am also thankful to Prof. **Rajeev Prakash IIT BHU Varanasi** for his consistent help in research.

I am also very grateful to my M.Tech supervisor **Prof. V.N Mishra** from IIT BHU who suggested and give the recommendation for doctoral studies and suggested me time to time.

I am very grateful to my father **G. M. Tripathi** and my mother **Gyan Prabha Tripathi** for their belief, patience, support and understanding throughout these 3 years when I was thousands of miles away from them. I am very thankful to my wife **Pratibha Tripathi** give me confidence for higher studies and take care of my loving daughters **Vaishnavi** and **Shanvi** in all means. I am also thankful to my younger brother **Navneet Mani tripathi** and all my sisters for support and motivation time to time. I am very thankful to all my lab colleagues for helping me research as well as personal.

I am especially thanks to my research institute KIT Japan for providing me all three years sufficient fund for research conferences as well as living expenses.